



Pacific Northwest
NATIONAL LABORATORY

Proudly Operated by Battelle Since 1965



The Salem Smart Power Center

An Assessment of Battery Performance and Economic Potential

September 2017

P Balducci, PNNL
V Viswanathan, PNNL
D Wu, PNNL
M Weimar, PNNL
K Mongird, PNNL

J Alam, PNNL
A Crawford, PNNL
A Somani, PNNL
K Whitener, PGE

DISCLAIMER

This report was prepared as an account of work sponsored by an agency of the United States Government. Neither the United States Government nor any agency thereof, nor Battelle Memorial Institute, nor any of their employees, makes **any warranty, express or implied, or assumes any legal liability or responsibility for the accuracy, completeness, or usefulness of any information, apparatus, product, or process disclosed, or represents that its use would not infringe privately owned rights.** Reference herein to any specific commercial product, process, or service by trade name, trademark, manufacturer, or otherwise does not necessarily constitute or imply its endorsement, recommendation, or favoring by the United States Government or any agency thereof, or Battelle Memorial Institute. The views and opinions of authors expressed herein do not necessarily state or reflect those of the United States Government or any agency thereof.

PACIFIC NORTHWEST NATIONAL LABORATORY

operated by

BATTELLE

for the

UNITED STATES DEPARTMENT OF ENERGY

under Contract DE-AC05-76RL01830

Printed in the United States of America

Available to DOE and DOE contractors from the
Office of Scientific and Technical Information,

P.O. Box 62, Oak Ridge, TN 37831-0062;

ph: (865) 576-8401

fax: (865) 576-5728

email: reports@adonis.osti.gov

Available to the public from the National Technical Information Service

5301 Shawnee Rd., Alexandria, VA 22312

ph: (800) 553-NTIS (6847)

email: orders@ntis.gov <<http://www.ntis.gov/about/form.aspx>>

Online ordering: <http://www.ntis.gov>



This document was printed on recycled paper.

(8/2010)

The Salem Smart Power Center

An Assessment of Battery Performance and Economic Potential

P Balducci, PNNL

V Viswanathan, PNNL

D Wu, PNNL

M Weimar, PNNL

K Mongird, PNNL

J Alam, PNNL

A Crawford, PNNL

A Somani, PNNL

K Whitener, PGE

September 2017

Prepared for
the U.S. Department of Energy
under Contract DE-AC05-76RL01830

Pacific Northwest National Laboratory
Richland, Washington 99352

Executive Summary

With a vision to drive the nation towards a more efficient, sustainable, and resilient power system, the Pacific Northwest Smart Grid Demonstration Project, or Smart Grid Demo, was launched in 2010 as a five-year \$178 million program co-funded by the U.S. Department of Energy (DOE) through the American Recovery and Reinvestment Act of 2009. The Smart Grid Demo was led by the Battelle Memorial Institute, which operates the Pacific Northwest National Laboratory (PNNL), with other program participants including the Bonneville Power Administration, 11 utilities from five states throughout the Pacific Northwest (Washington, Oregon, Idaho, Montana, and Wyoming), and six technology partners.

Portland General Electric (PGE), an investor-owned utility serving approximately 830,000 customers in 52 Oregon cities, participated in the Smart Grid Demo and co-sponsored the development of the Salem Smart Power Center (SSPC) project, an 8,000 square foot test and demonstration facility near PGE's Oxford substation in Salem, Oregon. The SSPC includes a 5 MW, 1.25 MWh EnerDel lithium-ion battery energy storage system (BESS).

While the Smart Grid Demo was completed by the end of January 2015, PGE has continued using this facility in a manner consistent with the original purpose of the program. PNNL was engaged by DOE and PGE to review SSPC operations and to evaluate its technical performance and financial potential. This report presents the results of the PNNL performance tests and the efforts to co-optimize a bundle of SSPC energy storage use cases to enhance its economic value to PGE and the customers it serves. The following key lessons and implications can be drawn from the analysis.

1 – The SSPC is Currently Underutilized and Optimal Operation Could Generate an Additional \$170,000 in Value Annually

In terms of economic operation, the SSPC is currently underutilized, operating an average of 14 hours per month, or 1.9 percent of available hours. With that noted, PGE is using the BESS for the highest value application (primary frequency response), the value of which we have estimated at \$264,000 annually or \$3.6 million in present value (PV) terms over 20 years. Modeling completed for this study indicates that optimal operation of the BESS could generate an additional \$170,000 in value annually or \$2.3 million over 20 years in PV terms. Details on the additional value streams are provided under Point 2 below. Note that the 20-year economic life of the SSPC assumes battery replacement after 10 years.

2 – Based on its Initial Design and Cost, the SSPC Does Not Generate Positive Net Benefits; However, a Modified Design and Operation Could Yield Positive Returns on Investment with Costs Based on Current-Day Prices

The SSPC was originally conceived as a groundbreaking research and development (R&D) project that would advance PGE's understanding of, and technical capacity around, integration of energy storage, smart grid technologies, and microgrid resources. As a result of the R&D focus of the SSPC and the more nascent stage of development the technology was in when the facility was originally conceived, system costs were high at \$20.4 million. Based on current-day prices present in energy storage deals being completed across the U.S., a 5 MW/1.25 MWh BESS could be designed and built today for approximately \$5.4 million (Lahiri 2017). Revenue requirements for the SSPC under these two scenarios are \$28.4 million and \$7.9 million, respectively. Revenue requirements include tax, debt, operations and maintenance costs, and other elements commonly built into utility rate structures.

SSPC benefits for the base case (\$5.9 million) fall far short of the revenue requirements for the SSPC as originally designed and built. However, results indicate that co-optimized benefits roughly equal revenue requirements when current prices are used. As mentioned previously, primary frequency response was deemed the highest value benefit. All other use cases or services yielded an additional \$2.3 million in currently unrealized benefits over 20 years. Of those services, arbitrage when also bidding into the Western Energy Imbalance Market (EIM) held the most revenue potential at \$0.7 million, followed by regulation down (\$0.7 million), demand response (\$0.4 million), and Volt-VAR/conservation voltage reduction (CVR) (\$0.4 million). Results are presented in Table ES.1 and Figure ES.1. Detailed methods are presented later in this report. Note that PNNL relied on its own production cost model in developing all ancillary service values.

The energy capacity of the SSPC (1.25 MWh) is quite limited in relation to its power capacity of 5 MW. With an energy to power ratio of only 0.25, it is not well suited to engage in most energy-intensive applications, such as arbitrage or ancillary services. While increasing the energy capacity would increase costs, modeling results indicate that doing so would generate much more value. By upsizing the energy storage capacity to 5 MWh and 10MWh while retaining the 5 MW rated power, modeled benefits grow to \$13.3 million and \$20.3 million, respectively, and exceed revenue requirements (\$11.5 and \$16.4 million, respectively). The return on investment ratios under these scenarios reach up to 1.24. The value would be much higher yet if the BESS was sited in a manner that generated locational benefits associated with outage mitigation, distribution deferral, or solar integration.

PNNL evaluated the impact of adjusting upward the energy to power ratio of the SSPC from 0.25 (1.25 MWh) to 4.0 (20 MWh). It is observed, with an energy to power ratio less than approximately 0.5, the cost is higher than total benefits and the ROI is thus less than 1. As the ratio increases, benefits increase at a higher rate than the costs, and therefore ROI continues to increase until the energy to power ratio reaches a value of 2. Once the ratio surpasses 2, benefits increase at a lower rate than costs, causing the ROI ratio to decrease. At an energy to power ratio of approximately 3.5, costs surpass benefits, and therefore the ROI ratio falls below 1.0.

Table ES.1. Co-Optimized 20-Year Benefits vs. Revenue Requirements (Base Case-Lahiri 2017 Costs)

Service	Individual	Revenue Requirements
Charging Costs	\$(449,115)	
Arbitrage (Mid-Columbia)	\$746,299	
Energy Imbalance Market		
Demand Response	\$428,155	
Regulation Up	\$374,609	
Regulation Down	\$656,706	
Primary Frequency Response	\$3,568,826	
Spin Reserve	\$100,622	
Non-Spin Reserve	\$46,124	
Volt-VAR / CVR	\$393,619	
Total	\$5,865,846	\$7,893,775

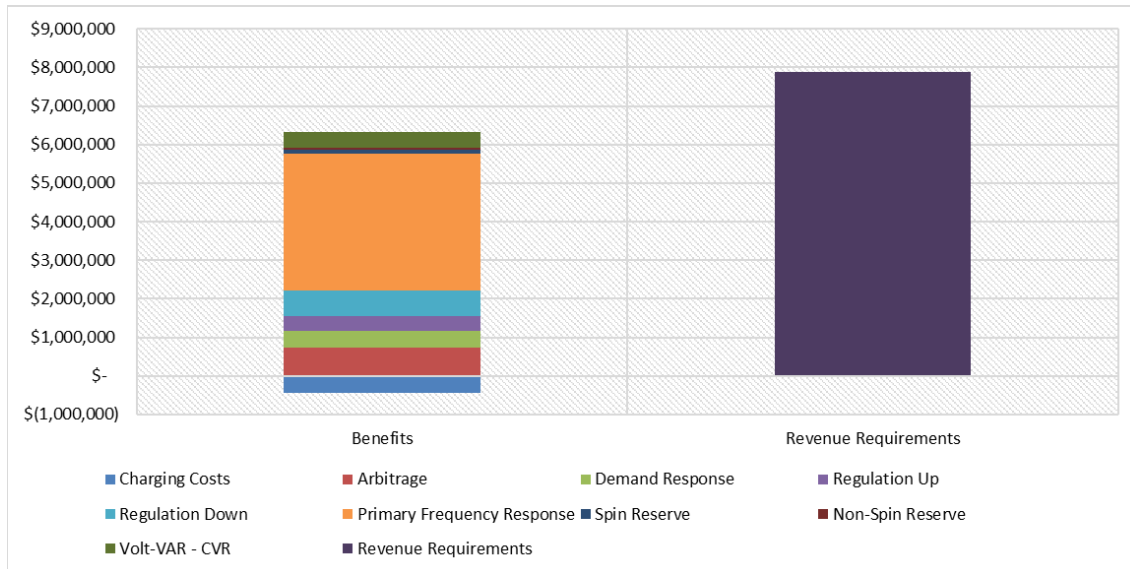


Figure ES.1. Benefits and Revenue Requirements, Using Current-Day Pricing, for the SSPC BESS under the Base Case

3 – A Small Number of Power-Intensive Applications Generate Significant Value over a Small Number of Hours of Operation

Primary frequency response and demand response provide tremendous value despite the fact that those services are concentrated in a very small number of hours each year—17 and 19, respectively. While the SSPC would be optimally engaged in arbitrage and ancillary services 78 percent of the time, those services only generate 27 percent of the total value. Note that Volt-VAR/CVR services are provided at least partially during every hour of the year, varied as necessary based on the available VAR capacity of SSPC inverters.

4 – The Western Energy Imbalance Market Represents an Interesting Opportunity for PGE

PGE will be joining the Western EIM operated by the California Independent System Operator (CAISO) in 2017. Under the EIM, CAISO performs 5- and 15-minute dispatch of least-cost electricity to balance generation and load in its wholesale energy market. A scenario was run in which PGE would bid the SSPC into the EIM on an hourly basis but it would be dispatched by CAISO subject to 5-minute real-time market (RTM) prices. This scenario takes advantage of BESS flexibility in providing energy at a fast ramp rate throughout each hour. When bid into the 5-minute RTM, EIM benefits for the SSPC were \$152,619 annually or \$2.1 million in PV terms over 20 years. EIM benefits expand to \$214,109 annually or \$2.9 million in PV terms over 20 years if the BESS energy capacity expands to 5 MWh.

5 – Extensive Testing Suggests the BESS is Performing Well and Capable of Meeting the Performance-Related Demands Placed upon It in Providing the Services Defined in this Study

The research team completed extensive testing of the BESS, and has drawn the following conclusions.

1. Energy capacity tests indicate that the round trip efficiency (RTE), without counting auxiliary power for the BESS, ranges from 78–85 percent, the RTE peaked at a 3,000 kW discharge, and the RTE decreased with increasing charge power demonstrating that the lithium-ion BESS performs better under moderate (C/2 to C rate, where C is the rated energy capacity of BESS) charging conditions.

2. The alternating current (AC) power delivered by all BESS blocks was quite uniform. This was supported by uniform per cell internal resistance among the BESS vaults, racks, and blocks. Interesting linear relationships with R^2 of >0.98 were found for deviations in state-of-charge (SOC) versus deviations in voltage for vaults with racks, vaults within blocks, and vaults across all blocks. Weaker relationships were found for the deviations in Δ SOC versus Δ current, Δ voltage versus Δ current, Δ SOC versus Δ temperature, Δ voltage versus Δ temperature, and Δ current versus Δ temperature pairs, with some demonstrating negative slope. This provided insight into the inner workings of the BESS.
3. When operated in a normal manner, the BESS took 12–13 seconds to reach rated power. Three blocks had similar ramp rates, while the other blocks had 68 and 50 percent of the rate measured for the first three blocks. During discharge, the ramp rates for the blocks with lower rates decrease with decreasing SOC, while the stronger blocks have a stable ramp rate across the SOC range investigated. The charge ramp rate is stable for all blocks across all SOCs.
4. The BESS ramp rate was in the range of 67 to 100 percent of rated power in one second when the BESS was set in the special ramp mode. This indicates that the ramp rate limitation is not due to the BESS hardware but rather due to the nature of the commands it receives.

Acknowledgments

We are grateful to Dr. Imre Gyuk, the Energy Storage Program Manager in the Office of Electricity Delivery and Energy Reliability at the U.S. Department of Energy. Without his office's financial support and his leadership, this project would not be possible. We wish to acknowledge the other members of the Grid Modernization Laboratory Consortium team: Dan Borneo, Ben Schenkman, and Ray Byrne of Sandia National Laboratories; Michael Starke of Oak Ridge National Laboratory; and Todd Olinsky-Paul of the Clean Energy States Alliance. We want to acknowledge the useful cost information provided by Sudipta Lahiri of DNV GL. Finally, we would also like to acknowledge the technical assistance provided by other members of the Portland General Electric team not acknowledged as authors, including Wayne Lei, Elaine Hart, and Pam Sporborg.

Acronyms and Abbreviations

AC	alternating current
ADR	automated demand response
AGC	automatic generation control
BESS	battery energy storage system(s)
BMS	battery management system
BPA	Bonneville Power Administration
CVR	conservation voltage regulation
DAS	data acquisition system
DC	direct current
DOE	U.S. Department of Energy
DOD	depth of discharge
DSG	dispatchable standby generation
FR	frequency regulation
GMLC	Grid Modernization Laboratory Consortium
HVAC	heating, ventilation, and air conditioning
I	current
IEEE	Institute of Electrical and Electronics Engineers
kVAr	kilovolt-ampere reactive
kW	kilowatt(s)
ms	millisecond
MW	megawatt(s)
MWh	megawatt hour(s)
NWPP	Northwest Power Pool
OCV	open circuit voltage
OE	Office of Energy
PCC	point of common coupling
PCS	power conversion system
PGE	Portland General Electric
PLC	programmable logic controller
PNNL	Pacific Northwest National Laboratory
PS	peak shaving
PGE	Portland General Electric
PV	present value
RMS	root mean square
RMSE	root mean square error
RTE	round trip efficiency

RTM	real-time market
SCL	Seattle City Light
SOC	state-of-charge
SSPC	Salem Smart Power Center
T	temperature
V	voltage
W	watt
WECC	Western Electricity Coordinating Council
Wh	watt hour(s)

Contents

Executive Summary	iii
Acknowledgments.....	vii
Acronyms and Abbreviations	ix
1.0 Introduction	1.1
1.1 Project Synopsis	1.1
1.2 The Salem Smart Power Center	1.2
2.0 Battery Performance Test Plan.....	2.1
2.1 Introduction.....	2.1
2.1.1 Data Requirements.....	2.1
2.1.2 Battery Testing.....	2.2
2.1.3 Comprehensive Data Recording.....	2.4
2.2 Expected Timeline.....	2.4
2.3 Test Protocols.....	2.4
2.4 Stored Energy Capacity Test.....	2.5
2.4.1 Test Overview	2.5
2.4.2 Response Time and Ramp Rate Test.....	2.7
2.5 Duty Cycles for Peak Shaving and Frequency Regulation	2.14
2.5.1 System Ratings.....	2.14
2.5.2 PNNL Frequency Regulation	2.14
2.5.3 Performance Metrics	2.16
2.6 Reporting Performance Results.....	2.17
2.6.1 System Stored Energy Capacity and Roundtrip Efficiency.....	2.17
2.6.2 Response Time and Ramp Rate.....	2.18
2.6.3 Internal Resistance Test	2.19
2.6.4 Frequency Regulation Applications.....	2.19
3.0 Battery Performance Test Results	3.1
3.1 Battery System Layout.....	3.1
3.2 BESS Details.....	3.4
3.3 Data Tags	3.7
3.4 Performance Test Results and Discussion.....	3.8
3.4.1 Discharge at Various Rates	3.8
3.4.2 Variation of Parameters within a Rack.....	3.15
3.4.3 Variation of Parameters within a Block	3.19
3.4.4 Variation of Parameters across Blocks.....	3.25
3.4.5 Charge at Various Rates.....	3.29
3.4.6 Variation of Parameters within a Rack.....	3.37

3.4.7	Variation within a Block	3.41
3.4.8	Deviation Across all Blocks in the BESS	3.43
3.5	Response Time/Ramp Rate Test	3.45
3.6	Internal Resistance Test Results.....	3.51
3.7	Frequency Regulation	3.60
4.0	Energy Storage Valuation Methodology and Cost Estimates.....	4.1
4.1	Use Cases	4.1
4.1.1	Energy Arbitrage	4.2
4.1.2	Western Energy Imbalance Market.....	4.2
4.1.3	Demand Response Benefit	4.3
4.1.4	Regulation Up/Down.....	4.4
4.1.5	Primary Frequency Response.....	4.5
4.1.6	Spin and Non-Spin Reserves.....	4.6
4.1.7	Volt/VAR and Conservation Voltage Reduction	4.7
4.2	Valuation Modeling Approach.....	4.13
4.3	Estimating Energy Storage Costs and Revenue Requirements	4.14
5.0	Economic Results	5.1
5.1	Evaluation of SSPC Benefits and Revenue Requirements.....	5.1
5.2	Application Hours and Values	5.5
5.3	Participation in the Western EIM.....	5.7
5.4	Evaluation of Alternative Scenarios and Sensitivity Analysis	5.8
6.0	Conclusions	6.1
7.0	References	7.1
	Appendix A – Supplemental Data Tables.....	A.1

Figures

1.1	Task Flow Diagram	1.2
1.2	Organization of Cells, Modules, Vaults, and Racks in a BESS Block	1.3
1.3	Connection of Battery Racks to Inverters and Step-Up Transformers, Bank of 2x125 kVA Inverters, and PLC-Based Control System for SSPC	1.3
2.1	Response Time Test.....	2.8
2.2	The Pulse Discharge Profile for BESS	2.10
2.3	One Way DC System and PCS Efficiency during Charge and Discharge.....	2.14
2.4	Frequency Regulation Duty Cycle.....	2.15
3.1	One-Line Diagram of the SSPC BESS	3.2
3.2	Three-Line Diagram of the SSPC BESS	3.3
3.3	Layout of One 590.4 Volt DC, 250 kW, 62.5 kWh Rack.....	3.4
3.4	Drawer Internal Components.....	3.5
3.5	Battery Block Layout.....	3.6
3.6	BESS Panels	3.6
3.7	BESS Control Station	3.7
3.8	Discharge Energy at Various Power Levels	3.9
3.9	Discharge Energy at Various Power Levels Varied by Order of Experiment	3.10
3.10	Difference in Power Flow between the 12.47 kV and 480 V AC Level of the BESS	3.11
3.11	Discharge Energy and RTE as a Function Power for the First Two Test Cycles	3.13
3.12	AC Power Flow through Each Value during Various Power Discharge Test	3.14
3.13	Standard Deviation for SOC, Temperature, and Voltage within Each Block.....	3.15
3.14	RMS Difference between Vault Pair Values	3.16
3.15	RMS of Δ SOC between Vaults in a Rack.....	3.17
3.16	Correlation Coefficients for RMS of Differences between Vaults in a Rack for Various Parameter Pairs	3.18
3.17	Correlation between the Median and RMS of Current Difference between Vaults in a Rack	3.19
3.18	Deviations of Various Vault Parameters within Each Block RMS and Mean.....	3.20
3.19	Linear Regression for Deviation of Vault SOC and Deviation of Vault Unit Cell Voltage within a Block for All Blocks RMS, Mean.....	3.21
3.20	Correlation for Deviation of Vault Δ SOC as a Function of Time within a Block for All Five Blocks RMS, Mean.....	3.22
3.21	Correlation of Deviation of Vault Δ Current as a Function of Time within a Block for All Five Blocks RMS, Mean.....	3.23
3.22	Correlation of Deviations of Current as a Function of Voltage within a Block for All Five Blocks RMS, Mean.....	3.24
3.23	Correlation Coefficient R^2 for Various Parameter Pairs for Vaults within a Block for All Five Blocks RMS, Mean.....	3.25
3.24	Deviation of Parameters for Vaults across all Blocks within the BESS RMS, Mean	3.26

3.25 Correlation of Δ SOC versus Δ Voltage in Vaults across all Blocks RMS, Mean	3.27
3.26 Correlation Coefficient for Deviation of Various Parameter Pairs across all Blocks.....	3.28
3.27 Correlation Coefficient R^2 for Deviations of Various Parameter Pairs for Vaults within Racks, Blocks, and across all Blocks.....	3.29
3.28 Difference between Power at the 12.47 kV and 430 V AC Level during Charge at Various Rates	3.30
3.29 Discharge and Charge Energy for Various Charge Powers and 1,000 kW Discharge	3.33
3.30 Average Discharge and Charge Energy as a Function of Charge Power.....	3.34
3.31 Cumulative RTE for Various Charge Powers and Discharge at 1,000 kW	3.34
3.32 Effect of Order of Experiment on BESS Discharge Energy for Discharge at 1,000 kW and Various Rates of Charge.....	3.35
3.33 Effect of Order of Experiment in BESS Performance for 1,000 kW Charge and Various Rate Charge.....	3.36
3.34 Standard Deviation for SOC, Temperature, and Voltage for Vaults within the BESS for Testing at Various Charge Powers	3.36
3.35 Standard Deviation of SOC versus Voltage for all BESS Vaults	3.37
3.36 RMS of Difference between Vault Pair Values across the Time Range Normalized with Respect to Largest RMS Value for Various Charge Power Levels.....	3.38
3.37 Linear Fit for SOC Deviation versus Voltage Deviation for Vault Pairs Compared to Other Pairs in the BESS.....	3.39
3.38 Correlation between the Median and RMS of Current Difference between Vaults in a Rack	3.40
3.39 Deviation of Parameters for Vaults within Each Block.....	3.41
3.40 Correlation for Various Deviation Pairs within Each Block.....	3.42
3.41 Deviation of Parameters for Vaults across All Blocks	3.43
3.42 Correlation for Deviation Pairs across All Blocks.....	3.44
3.43 Correlation Coefficient for Deviation of Various Pairs within a Rack, a Block, and Across Blocks for Various Charge Rates	3.45
3.44 BESS Power, Average Cell Voltage, and Current through Each Rack during Ramp Up and Down to 5,000 kW Discharge	3.48
3.45 Plot of Average Cell Voltage versus Current through Vaults.....	3.49
3.46 Ramp Rate of BESS for Charge and Discharge.....	3.50
3.47 Ramp Rate for Blocks during Charge and Discharge.....	3.51
3.48 Per Cell Resistance on the BESS Level for Charge and Discharge at Various SOC's	3.53
3.49 Per Cell Resistance on Vault Basis for All SOC's Based on Slope of V versus I Plot, and Based on Voltage and Current at Δ SOC of 0.2%.....	3.54
3.50 Per Cell Resistance on Vault Basis for Charge and Discharge Pulses Across all Tested SOC's.....	3.55
3.51 Median per Cell Resistance on a Rack and Block Basis for Charge and Discharge across All SOC's on a Rack Basis, and Block Basis.....	3.56
3.52 Per Cell Resistance on a Rack Basis for Charge and Discharge across All SOC's Tested.....	3.57
3.53 Per Cell Resistance on a Block Basis for Charge and Discharge across SOC's.....	3.58
3.54 Frequency Regulation Tracking – Signal (Red) and Response (Black)	3.60
3.55 Histogram of the Frequency Regulation Error.....	3.61

3.56 Tracking Error as a Function of Power.....	3.62
3.57 Percent Signal Tracking for Frequency Regulation at Various Percentages of Signal and Rated Power.....	3.64
4.1 Hourly Mid-Columbia Price Index Values for 2015	4.2
4.2 Western Energy Imbalance Market	4.3
4.3 Frequency Response Event.....	4.6
4.4 A Fictitious System Showing a BESS Meeting Local VAR Demand.....	4.10
4.5 Release of Upstream Network Capacity in Terms of Synchronous Generator Capability	4.11
4.6 Illustration of a BESS Performing CVR in a Distribution Network.....	4.12
4.7 24-hour Energy Storage Schedule	4.14
5.1 Individual Benefits Estimates by Use Case vs. Co-Optimized Benefits.....	5.2
5.2 Base Case Benefits and Revenue Requirements for SSPC.....	5.3
5.3. Benefits and Revenue Requirements, Using Current-Day Pricing, for a 5 MW/1.25MWh Energy Storage System	5.4
5.4 Impacts of Energy to Power Ratio on Costs, Benefits, and ROI	5.5
5.5 Annual Application Hours of the Energy Storage System under Base Case.....	5.6
5.6 20-year PV Benefits Derived from Each Service under Base Case.....	5.7
5.7 Energy Imbalance Market Operations	5.7
5.8 Sensitivity Analysis Results.....	5.9
5.9 Return on Investment Ratios for Alternative Scenarios.....	5.10

Tables

2.1 Data Requested from PGE.....	2.2
2.2 List of Tests and Duration.....	2.4
2.3 Stored Energy Capacity and Roundtrip Efficiency at Various Discharge Power Levels	2.18
2.4 Response Time and Ramp Rate.....	2.19
2.5 Internal Resistance of the BESS	2.19
2.6 Frequency Regulation Metrics.....	2.20
3.1 Number of Various Components.....	3.5
3.2 Results for 1 MW Charge and Various Discharge Rates.....	3.8
3.3 Energy Obtained at Various Power Levels with Order of Experiment Shown.....	3.10
3.4 Value of Parameters for Vaults in Block 1 during Various Rate Discharge Testing.....	3.12
3.5 Correlation Coefficient R^2 for Deviations of Various Parameter Pairs for Vaults within Rack, Block, and across All Blocks.....	3.28
3.6 Parameter Values for Vaults in Block 1 during Variable-Rate Charge Testing	3.31
3.7 Parameter Values Results for 1 MW Discharge and Variable-Rate Charge.....	3.31
3.8 Discharge Energy Obtained at Various Charge Power Levels with Order of Experiment Shown..	3.35
3.9 Charge Energy Obtained at Various Charge Power Levels with Order of Experiment Shown.....	3.35

3.10 Response Time and Ramp Rate Test Procedure	3.46
3.11 Results for Response Time/Ramp Rate Test during 5 MW Charge	3.49
3.12 Results for Response Time/Ramp Rate Test during 5 MW Discharge.....	3.50
3.13 Results for Response Time/Ramp Rate Test - Charge.....	3.52
3.14 Results for Response Time/Ramp Rate Test - Discharge.....	3.53
3.15 Fast Ramp Rate Results	3.59
3.16 Frequency Regulation Metrics.....	3.63
4.1 2016 ADR Events	4.4
4.2 Previous Field Studies on CVR	4.7
4.3 PGE Estimated Costs for SSPC	4.14
4.4 Lahiri 2017 Estimated Costs.....	4.15
4.5 Major Parameters Used in Estimating BESS Revenue Requirements.....	4.15
4.6 BESS Revenue Requirements.....	4.16
5.1 Individual vs. Co-Optimized Benefits	5.2
5.2 Co-Optimized 20-Year Benefits vs. Revenue Requirements.....	5.3

1.0 Introduction

With a vision to drive the nation towards a more efficient, sustainable, and resilient power system, the Pacific Northwest Smart Grid Demonstration Project, or Smart Grid Demo, was launched in 2010 as a five-year \$178 million program co-funded by the U.S. Department of Energy (DOE) through the American Recovery and Reinvestment Act of 2009. The Smart Grid Demo was led by the Battelle Memorial Institute, which operates the Pacific Northwest National Laboratory (PNNL), with other program participants including the Bonneville Power Administration (BPA), 11 utilities from five states throughout the Pacific Northwest (Washington, Oregon, Idaho, Montana, and Wyoming), and six technology partners.

Portland General Electric (PGE), an investor-owned utility serving approximately 830,000 customers in 52 Oregon cities, participated in the Smart Grid Demo and co-sponsored development of the Salem Smart Power Center (SSPC) project, an 8,000 square foot test and demonstration facility near PGE's Oxford substation in Salem, Oregon.

The SSPC developed a smart grid-based platform to integrate residential and commercial demand response assets, grid-connected commercial dispatchable standby generation (DSG), grid-connected battery storage, and distributed switching into a commercial microgrid. DOE funding in 2010 covered 50 percent of the \$20 million cost for the SSPC, with the remaining 50 percent shared by PGE and its principal technology partners: EnerDel, Eaton, and Alstom.

While the Smart Grid Demo was completed by the end of January 2015, PGE has continued using this facility in a manner consistent with the original purpose of the program, while attempting to optimize its value to PGE customers as a grid-integrated asset. As reported in the SSPC project advisory committee briefing paper, a pool of 15 use cases involving the SSPC were created by PGE focusing on transactive energy, energy shifting, demand response, ancillary services, distribution automation, and emergency/back up/reliability services (Whitener et al. 2014).

PNNL was engaged by DOE and PGE to review and modify these use cases and to evaluate the technical performance and financial opportunity associated with the SSPC. This report presents the results of the PNNL performance tests and the efforts to co-optimize a bundle of SSPC energy storage use cases to enhance its economic value to PGE and the customers it serves.

1.1 Project Synopsis

This analysis presented in this report is a component of a multi-year effort under the Grid Modernization Laboratory Consortium (GMLC) titled "Energy Storage Demonstrations—Validation and Operational Optimization." The overarching project is led by Sandia National Laboratories, with PNNL, the Oak Ridge National Laboratory, Clean Energy States Alliance, and UniEnergy Technologies participating as technology and research partners. The goal of this GMLC project is to collaborate with states, utilities, and storage providers to help elucidate storage benefits and integration challenges. Analyses will be conducted on four demonstration projects: Green Mountain Power (Vermont), PGE's SSPC (Oregon), Electric Power Board of Chattanooga (Tennessee), and Los Alamos County (New Mexico). The outcome of this effort will be an analysis that identifies the value streams for each potential application, as well as methods to operate the device to maximize the value derived from the services it provides.

PNNL has been working closely with PGE staff for the past year to evaluate the technical performance and economic potential of the SSPC. Tasks performed by PNNL in Phase 1 of this project are shown in a task flow diagram in Figure 1.1. Phase 2 focuses on the development of control strategies and algorithms.

Following kickoff and scoping, PNNL developed a test plan for evaluating the technical performance of the SSPC (section 2.0). PNNL developed all the necessary methods and input information to perform the use case analyses and, as appropriate, provide input for the development of optimal control strategies (section 4.0).

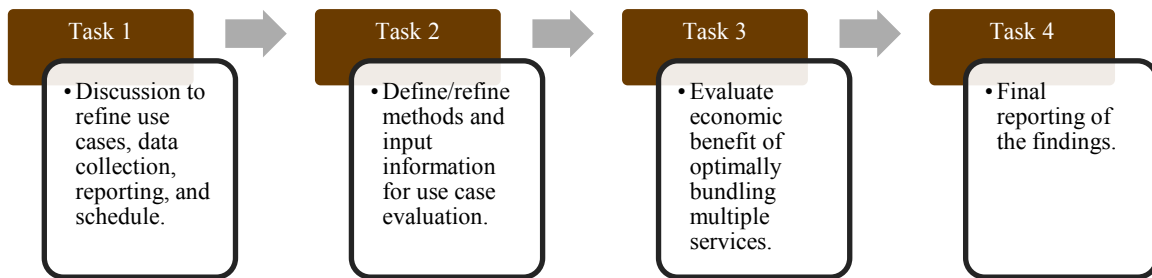


Figure 1.1. Task Flow Diagram

This final report documents the use cases and the individual performance of the SSPC battery energy storage system (BESS) when engaged in single or bundled use cases. It defines the approaches used in monetizing the economic benefits associated with BESS services and documents the modeling techniques used to optimize BESS values. It identifies which of the use cases are the most economically viable for the BESS and under what circumstances or market conditions the value of BESS can be maximized.

Understanding of the technical features and limitations is essential to performing economic evaluation of the use cases. General information on the SSPC is provided in the following section.

1.2 The Salem Smart Power Center

The SSPC BESS is comprised of a 5 MW, 1.25 MWh lithium-ion battery system installed at PGE's Oxford substation. The SSPC BESS is composed of 20 EnerDel-manufactured SP90-590 modular energy storage racks organized into five blocks with each block containing four racks (EnerDel 2013). Each of the racks consist of 18 small drawer type units, each containing four battery modules; there are a total of 1,440 modules in the system. Each battery module contains 12 series-connected lithium-ion cells, which leads to a total of 48 series-connected cells in a drawer unit. Organization of the cells, modules, and racks in a battery block is shown in Figure 1.2.

A battery string is composed of three drawers in series and operates at approximately 600 direct current (DC) voltage (Osborne et al. 2013). The lithium-ion cells in the battery modules are rated at 3,000 charge-discharge cycles. EnerDel supplied a programmable logic controller (PLC) based battery management system (BMS), which performs battery monitoring functions only; control is accomplished by Eaton's PLC-based control system, which is described later.

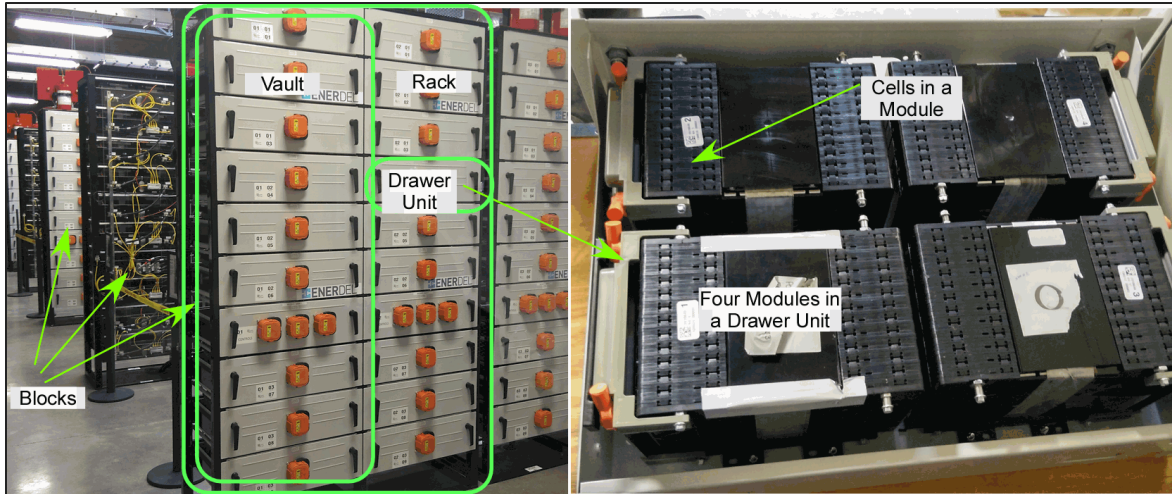


Figure 1.2. Organization of Cells, Modules, Vaults, and Racks in a BESS Block

Each rack of battery modules feeds a bank of 2x125 kVA Eaton Power Xpert inverters, which makes the output of a single block consisting of four racks equivalent to 1 MVA. Hence, five blocks of battery modules feeding 20 banks of 2x125 kVA inverters result in a system output of 5 MVA. The inverters provide full four-quadrant operation with the capability to import and export real and reactive power, providing the opportunity to deploy the BESS for various ancillary services. Each inverter bank is connected to a 208/480 V 260 kVA step-up transformer, and 480 V outputs of four inverter banks in a battery block are stepped up through a 480 V/12.47 kV 1 MVA step-up transformer. Inverter banks and transformer connections for a block of the BESS are shown in Figure 1.3(a), and a bank of 2x125 kVA inverters is shown in Figure 1.3(b).

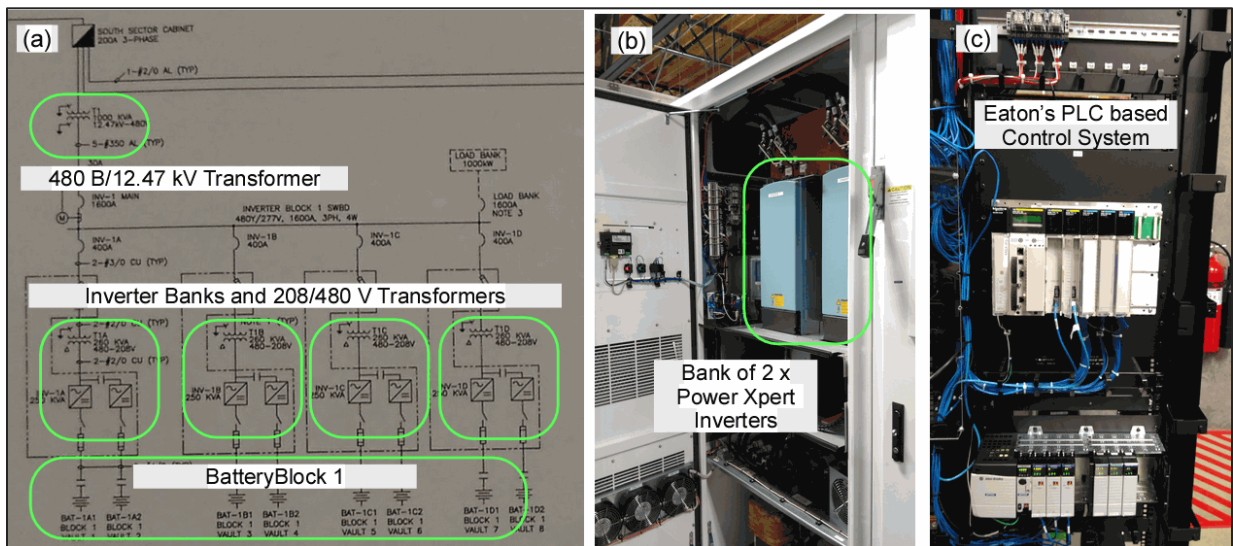


Figure 1.3. (a) Connection of Battery Racks to Inverters and Step-Up Transformers, (b) Bank of 2x125 kVA Inverters, and (c) PLC-Based Control System for SSPC

The BESS is connected to the 12.47 kV Oxford-Rural feeder at the Oxford substation. There are two more 12.47 kV feeders (Oxford-Lee and Oxford-Shelton) connected to the same location where the Oxford-Rural feeder is connected; both are considered in the economic benefit calculations for relevant use cases (e.g., Volt/VAR and conservation voltage reduction (CVR)).

Eaton, in collaboration with PGE and EnerDel, designed and deployed a PLC-based control system, as shown in Figure 1.3(c), for the SSPC BESS. The control system creates an interface among the inverters, power meters, the EnerDel, BMS, and PGE's upstream system to operate the BESS in a variety of modes according to PGE specifications while intelligently coordinating the operation of the inverters to distribute demands among the battery blocks. The control system, combined with custom inverter programming, provides seamless support for loads in the event of an upstream outage—keeping the power on for commercial and residential customers served by the rural feeder. System modes allow the operator to request that the battery cells be equalized in charge and enable the storage system to respond to real and reactive power commands from PGE. Eaton also customized the Power Xpert inverters, originally designed to maximize energy harvest from renewable resources, for use in the site's energy storage system. Control modifications allowed the inverters to operate bi-directionally to perform charging and discharging operations.

2.0 Battery Performance Test Plan

2.1 Introduction

Battery energy storage systems have the potential to improve the operating capabilities of the electricity grid. Their ability to store energy and deliver power can increase the flexibility of grid operations while providing the reliability and robustness that will be necessary in the grid of the future—one that will be able to provide for projected increases in demand and the integration of clean energy sources while being economically viable and environmentally sustainable. Energy storage has received a great deal of attention in recent years. Entrepreneurs are working enthusiastically to commercialize a myriad of promising technologies and venture capitalists and the U.S. government are investing in this space. The technologies show promise but it remains difficult to quantify the benefits that BESS may provide.

This study is designed to add to the resources targeting this issue by providing a generalizable approach and tool for estimating the value of BESS services, as applied to a BESS deployed by PGE with batteries procured from EnerDel. The PGE BESS, which is part of the Salem Smart Power Center in Salem, Oregon is rated at 5 MW/1.25 MWh.

Since the system is rated at 5 MW, it is assumed it can provide and absorb energy at a maximum rate of 5 MW. No assumptions are made about system peak power being higher than 5 MW for short durations up to 10 seconds. The system will be charged and discharged at 5 MW for determination of internal resistance.

As part of this study, PNNL will monitor the performance of the storage systems using battery-specific and grid-specific measurements outlined in this test plan. The test plan will be executed as defined in this document. The performance evaluation will focus on assessing the unit purely as a power and energy device (e.g., charge–discharge rates, effects of the depth of discharge (DOD), efficiencies, transient response, and accuracy of following signals).

Note that throughout this section the writing is in the future tense, reflecting the fact that the test plan was written prior to the performance of any testing procedures. The authors of this study have left it as such in order to reflect the nature of the test plan, which describes future actions.

2.1.1 Data Requirements

The following data are requested from PGE during testing.

Alternating Current (AC) Side:

- The control signal to the BESS, which would simply be a power signal—charge or discharge at certain power.
- Actual power and energy delivered or absorbed by the BESS—both in and out of the transformer and in and out of the power conversion system (PCS).
- BESS state-of-charge—this may be communicated to the PCS by the direct current battery management system (BMS) or be available from the direct current (DC) BMS.
- Efficiency information from the inverter at various power levels.

DC Side:

- Power and energy
- Voltage
- Current
- SOC

Optional Data, DC Side:

When the BESS powers the auxiliary loads, it is not necessary to have the auxiliary load data. However, access to this data would be useful to estimate round trip efficiency (RTE) with and without including auxiliary power consumption.

When the BESS does not power auxiliary loads, the electricity required to power auxiliary loads should be measured separately. Auxiliary power is a catch-all for multiple items: heating, ventilation and air conditioning (HVAC) for the battery container, lighting, communications, battery heating with heater blankets, or active cooling with circulating coolant. In either case, it would be useful to have auxiliary power data.

It would be useful to have data at the point of common coupling (PCC) in terms of power in and out of the transformer connecting the BESS to the grid. This allows calculation of system efficiency at the PCC. If this is not available, the transformer efficiency could be provided as a function of power in and out to allow determination of system efficiency inclusive of the transformer. Requested data are summarized in Table 2.1.

Table 2.1. Data Requested from PGE

Test	Data Frequency	Critical Data	Optional
Stored Energy Capacity Test	Every second	Watt (W), watt hour (Wh), current, volts (AC and DC), SOC, and DC battery temperature, auxiliary power consumption (if powered by a separate line), transformer power in and out	Auxiliary power (if BESS supplies it)
Response Time and Ramp Test	Every second	Same as above	Same as above
Internal Resistance Test	Every second	Same as above	Same as above
Frequency Regulation (FR)	Every second	Same as above	Same as above

2.1.2 Battery Testing

The BESS will be subjected to performance tests to determine the beginning of life reference performance. These test will allow the research team to determine BESS degradation during operation by repeating these performance tests. Tests developed by the U.S. DOE Office of Energy (OE) sponsored working groups will be used with modifications as appropriate. The DOE-OE published document will be

referred to as the protocol in this work (Viswanathan et al. 2014). Language that describes baseline testing steps are taken directly from Viswanathan et al. (2014) without modification.

Baseline testing consists of performance or reference performance tests to determine the initial performance of the BESS. This reference performance test can be repeated at any time to assess the state of health of the BESS. Duty cycle testing will involve subjecting the BESS to peak shaving (PS) and frequency regulation (FR) duty cycles to determine the performance of the BESS for these two extreme use cases. Peak shaving (PS) is an energy-intensive application while FR involves exercising the BESS around a narrow SOC range using an energy neutral signal of 1-4s frequency, with the ability of the BESS to follow the signal being of great importance. It should be noted that while the FR duty cycle is energy neutral, the RTE of the BESS will result in a deviation of the ending SOC from the starting SOC.

The following general performance metrics were identified in the DOE-OE sponsored Protocol development effort:

- RTE
- Response time & ramp rate (this was considered to be an application-specific metric in the Protocol but has been moved up to general metrics)
- Energy capacity stability (this can be performed at any time during BESS operation)
- Internal resistance during charge and discharge
- Stability of internal resistance over time.

The following application duty cycle-related performance metrics were identified, with the application that these metrics are relevant to within brackets:

- Duty cycle round trip efficiency (FR)
- Reference signal tracking (FR)
- SOC excursion (FR).

The following performance tests will be conducted:

- Capacity test
- Response time and ramp rate test and internal resistance test performed at 10%, 20%, 30%, 40%, 50%, 60%, 70%, 80%, and 90% SOC.

This will be followed by applying FR duty cycles as described in the Protocol. Table 2.2 lists the tests, the start and end SOC, and the anticipated test duration.

Table 2.2. List of Tests and Duration

Test	Begin SOC	End SOC	Duration (Days)
Stored Energy Capacity, 0.5 MW charge, various rates discharge at 0.5, 1, 3, 5 MW	80%	20%	3
Stored Energy Capacity, 0.5 MW discharge, various rates charge at 0.5, 1, 3, 5 MW	80%	20%	3
Response time & ramp test; internal resistance test	80%	20%	2
FR duty cycle	60%	Estimated to be ~ 50%	2
Total days			10

2.1.3 Comprehensive Data Recording

All measurements of charge rate, input current and voltage, output current and voltage, thermal output, system temperatures, ambient conditions, and other parameters that must be measured shall be collected simultaneously at a temporal resolution applicable to the function of the BESS application and BESS metrics to which they are being applied in accordance with recognized standards applicable to the measurements being taken. All parameters measured and recorded shall be used for determination and reporting of BESS performance.

2.2 Expected Timeline

The performance testing is expected to take 10 days after all relevant issues have been resolved.

2.3 Test Protocols

This section outlines the tests that will be performed as part of the technical performance testing of this research program. PNNL will coordinate with PGE in the implementation of the data acquisition for the evaluation. PNNL will summarize the performance evaluation for each of the control strategies defined in this section of the report. To acquire the needed data, the following tests will be conducted on the BESS.

1. Preliminary tests to determine rated power, energy content, RTE, and internal resistance.
2. Tests per PNNL/DOE protocol for PS and FR.

The remainder of this section is organized around these tests.

A reference performance test, also known as baseline performance test, shall be conducted in accordance with this section, and the results shall be used to determine baseline BESS performance that can be subsequently used to assess any changes in the condition of the BESS and rate of performance over time and use. This test shall be repeated at regular intervals as specified in this document during cycle testing for same-system comparison purposes. Such intervals shall be selected to identify how the testing or operation affects the performance of the BESS and shall be in units of time, number of cycles, or energy throughput.

2.4 Stored Energy Capacity Test

A stored energy capacity test shall be performed in accordance with this section and is intended to be used to determine the stored energy capacity at the rated electrical or thermal power for the intended application as specified by the manufacturer.

2.4.1 Test Overview

The BESS energy capacity shall be measured at various discharge and charge power levels in the 80 percent to 20 percent SOC range. Energy storage system AC and DC power during charge and discharge shall be recorded every second. The associated energy input and output of the BESS shall be calculated from the recorded power.

2.4.1.1 Stored Energy Capacity Test Routine

Charge at fixed rate, discharge at various rates, starting with lowest rate.

The BESS shall be tested for its stored energy capacity at selected power in accordance with the procedure listed below. The measurements shall be collected in accordance with all test steps, listed below. Any auxiliary power consumed that is not powered by the BESS shall also be monitored and recorded. Based on how PGE defines its BESS boundary, the power in and out of the transformer shall also be recorded to get the RTE inclusive of the transformer. If this data is not available, the total system efficiency will be calculated by multiplying the BESS RTE with the transformer RTE, where BESS ends at the PCS (and not transformer).

1. The BESS shall be discharged to its lower SOC limit (or minimum SOC) at 0.5 MW. Steps 2-6 shall be repeated for each discharge power in the following sequence:
 - a. 0.5 MW
 - b. 1 MW
 - c. 3 MW
 - d. 5 MW.
2. The BESS shall be charged to its upper SOC limit of 80% SOC (or maximum SOC) at the AC power of 1 MW. The AC energy input, WhC_i , into the BESS during BESS charging, including all auxiliary power consumption, shall be measured directly during charging and recorded as the charge energy capacity of the BESS. Here C corresponds to charge, and i corresponds to cycle number.
3. The system shall be left at rest in an active state in accordance with the BESS manufacturer's operating instructions for 60 minutes.
4. The system shall be discharged at the desired power (starting with 0.5 MW for the first test) to the lower SOC limit specified by the manufacturer, at the discharge time prescribed by the duty cycle. That lower SOC shall be measured and recorded as V_{min} (voltage). The AC energy output, WhD_i , from the BESS during BESS discharging shall be calculated from the power measurements during discharge and recorded, where D corresponds to discharge.
5. The BESS shall be left at rest in an active standby state for the same period of time selected under Step 3 above (60 minutes).

6. Steps 2 through 5 above shall be repeated at least twice (total of three cycles). The reference performance test value shall be calculated as the mean of the values of WhCi and WhDi as measured under Steps 2 and 4 above associated with each test and the standard deviation shall also be calculated and reported.
7. Steps 2–6 shall be repeated at the next higher discharge power level listed in Step 1.

Charge at various rates, starting with the lowest rate, discharge at fixed rate.

1. The BESS shall be discharged to its lower SOC limit of 20 percent SOC (or minimum SOC) at 1 MW. Steps 2–6 shall be repeated for each charge power in the following sequence:
 - a. 0.5 MW
 - b. 1 MW
 - c. 3 MW
 - d. 5 MW.
2. The BESS shall be charged to its upper SOC limit (or maximum SOC) at the desired AC power. The AC energy input WhCi, into the BESS during BESS charging, including all auxiliary power consumption, shall be measured directly during charging and recorded as the charge energy capacity of the BESS. Here C corresponds to charge, and i corresponds to cycle number.
3. The system shall be left at rest in an active state in accordance with the BESS manufacturer’s operating instructions for 60 minutes.
4. The system shall be discharged at the 1 MW (or the standard discharge rate for this BESS) to the lower SOC limit specified by the manufacturer, at the discharge time prescribed by the duty cycle. That lower SOC shall be measured and recorded as Vmin (voltage). The AC energy output, WhDi, from the BESS during BESS discharging shall be calculated from the power measurements during discharge and recorded, where D corresponds to discharge.
5. The BESS shall be left at rest in an active standby state for the same period of time selected under Step 3 above (60 minutes).
6. Steps 2 through 5 above shall be repeated at least twice (total of three cycles). The reference performance test value shall be calculated as the mean of the values of WhCi and WDi as measured under Steps 2 and 4 above associated with each test and the standard deviation shall also be calculated and reported.
7. Steps 2–6 shall be repeated at the next higher charge power level listed in Step 1.

2.4.1.2 Roundtrip Energy Efficiency Calculation

An RTE calculation shall be conducted to determine the amount of energy that a BESS can deliver relative to the amount of energy injected into the BESS during the preceding charge for a cycle. A cumulative RTE is also calculated for a set of cycles by determining the total discharge and charge energy for those cycles. This calculation, with minor changes, shall also be used for the applicable duty cycle for the intended application of the system.

2.4.1.3 Roundtrip Energy Efficiency from Stored Energy Capacity Test Routine

The RTE of the BESS is the efficiency for each cycle, cumulative efficiency for two and three cycles, and shall be determined in accordance with Equations (2.1) through (2.3) based on the data obtained from the tests conducted in accordance with the provisions in section 2.4.1.1.

$$\text{Round trip efficiency for cycle } i = \left(\frac{Wh_{D_i}}{Wh_{C_i}} \right) \quad (2.1)$$

$$\text{Cumulative Round trip efficiency for all 3 cycles} = \left(\frac{\sum_1^3 Wh_{D_i}}{\sum_1^3 Wh_{C_i}} \right) \quad (2.2)$$

$$\text{Cumulative Round trip efficiency for cycles 2 and 3} = \left(\frac{\sum_2^3 Wh_{D_i}}{\sum_2^3 Wh_{C_i}} \right) \quad (2.3)$$

where 3 is the total number of cycles; WhDi is the BESS electrical energy discharge output (AC) in watt-hours for cycle number i; and WhCi is the Watt hour charge input (AC) into the BESS, including all auxiliary power consumption for cycle number i. If the auxiliary power system is powered by the BESS, no adjustment to the above equations is needed. If the auxiliary load is powered by another line, the RTE will be calculated by subtracting the auxiliary load during discharge from the numerator and adding it to the denominator during charge.

2.4.2 Response Time and Ramp Rate Test

The BESS shall have a response time and ramp rate test performed in accordance with this section to determine the amount of time required for the BESS output to transition from no discharge to full discharge rate and from no charge to full charge rate. The ramp rate of the BESS shall be determined by dividing the BESS rated power by the response time in accordance with the provisions in this section. This test is done in conjunction with the internal resistance test. The starting SOC is the maximum allowable SOC, which is 80 percent. The end SOC is the minimum allowable SOC, which is 20 percent.

2.4.2.1 Test Overview

The method for measuring ramp rate shall be the same for all BESSs regardless of application. PGE shall provide information about rated power as required by the provisions in section 2.1.

The response time shall be measured in accordance with Figure 2.1 starting when the signal (command) is received at the BESS boundary as established in section 4.2 of the DOE protocol (Viswanathan et al. 2014) and continuing until the BESS discharge power output (electrical or thermal) reaches $100 \pm 2\%$ of its rated power.

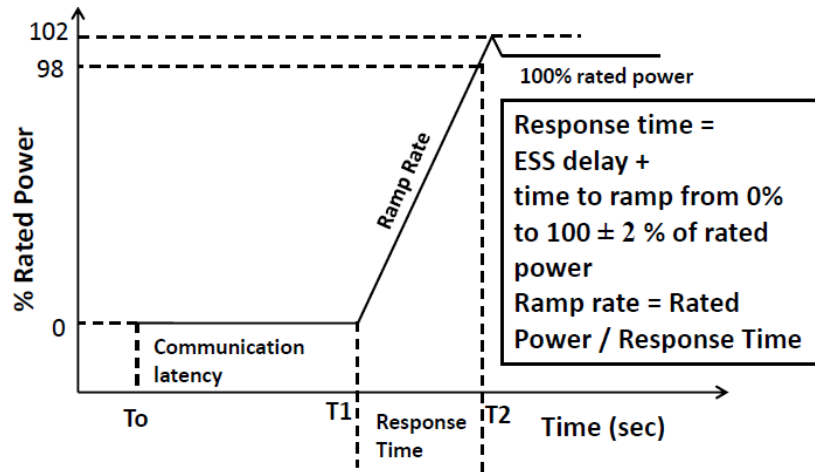


Figure 2.1. Response Time Test

2.4.2.1.1 Discharge Test Routine

The discharge response time test shall be conducted in accordance with the following procedure and the discharge response time calculated in accordance with Equation (2.4).

1. Take BESS to 80% SOC by charging at the standard charge rate of 1 MW used for this BESS. Keep at rest for 30 minutes. Measure open circuit voltage (OCV) at the end of the rest time. Go to Step 6.
2. The data acquisition system (DAQS) shall be configured to record a time stamp T_0 when a change in set point from rest to a discharge output command is sent to the BESS. Data is collected every second.
3. The DAQS shall be configured to record a time stamp T_1 when the BESS starts responding to the discharge command signal.
4. The DAQS shall be configured to record a time stamp T_2 when the output of the BESS reaches $100 \pm 2\%$ of its rated power capacity. The acquisition rate of data shall be at least twice as fast as the rated power capacity divided by the discharge ramp rate of the BESS, as determined in accordance with Equation (2.4) and at least one intermediate data point shall be acquired as the BESS transitions from rest to full discharge.
5. The BESS shall be configured to respond to a step change in power output set point according to the BESS manufacturer's specifications.
6. The DAQS shall be started and shall command to change the power output of the BESS to full rated discharge power output of 5 MW, and T_1 and T_2 shall be measured and recorded. The BESS is maintained at rated power for 30 seconds. This is followed by 15 minutes of rest.
7. The DAQS shall be reset to a state to begin recording data and the BESS placed in a state of active standby.

$$RTD = T_2 - T_1 \quad (2.4)$$

where RTD is the discharge response time in seconds; T_1 is the beginning time stamp, in seconds, when the BESS starts responding to the discharge signal; and T_2 is the end time stamp, in seconds, when the output of the BESS reaches $100 \pm 2\%$ of its rated power output.

The discharge ramp rate RR_D shall be calculated in accordance with Equation (2.5) and expressed in megawatts per minute.

$$RR_D = [PT_2]/[T_2 - T_1] \times 60 \quad (2.5)$$

where P_{T_2} is the power output of the BESS recorded at time T_2 ($100 \pm 2\%$ of rated power capacity); T_1 is the beginning time stamp, in seconds, when the BESS starts responding to the discharge signal; and T_2 is the end time stamp, in seconds, when the output of the BESS reaches $100 \pm 2\%$ of its rated power output.

The discharge ramp rate shall also be expressed as percent rated power per minute (RR_{pct}) in accordance with Equation (2.6).

$$RR_{pct} = RR_D / PR \times 100 \quad (2.6)$$

where P_R is the rated power of the BESS.

The response time and ramp rate will be reported in accordance with the provisions in section 2.6. After the discharge ramp rate is measured, the BESS is kept at rest for 15 minutes and a similar measurement is done for charge ramp rate as described later in this section

The internal resistance measurement procedure is measured as described below.

Procedure to determine the internal resistance during the ramp test:

Figure 2.2 presents the pulse discharge profile for the BESS. Chart (a) shows the OCV before pulse and the full pulse. Chart (b) shows the first 50 milliseconds (ms) of the discharge pulse.

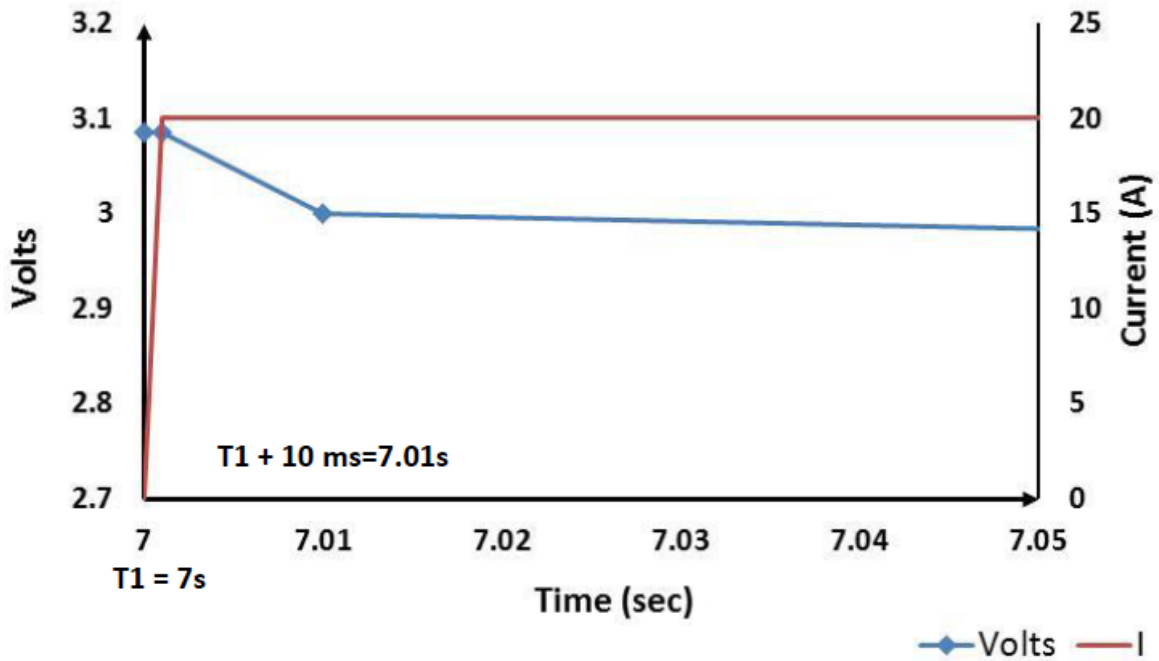
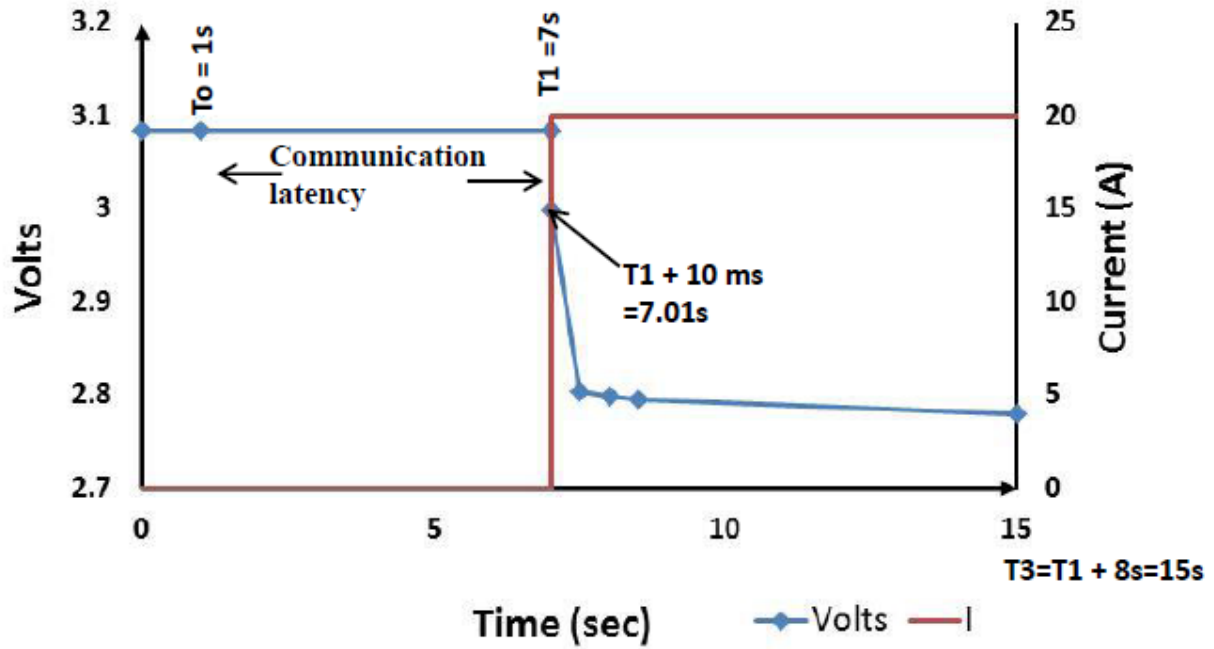


Figure 2.2. The Pulse Discharge Profile for BESS

The total resistances are calculated by the following equation:

$$R_{\text{total-discharge}} = \{V(T_0) - V(T_1 + 2 \text{ sec})\} / I_{\text{discharge}} \quad (2.7)$$

where $T_1 + 8s$ is T_3 .

If 10 ms resolution data are available, the ohmic resistance is calculated by using the voltage at 10 ms in Equation (2.7).

From the OCV data after discharge, total resistance is calculated by the following equations:

$$R_{\text{total-discharge}} = \{V(T_3+15 \text{ minutes})-V(T_3)\}/I_{\text{discharge}} \quad (2.8)$$

One way DC discharge efficiency, $\eta_{\text{dc_dischg}}$, is given by

$$\eta_{\text{dc_discharge}} = V(T_1+8 \text{ sec}) / V(T_0) \quad (2.9)$$

$$\eta_{\text{dc_discharge}} = V(T_3)/V(T_3+15 \text{ minutes}) \quad (2.10)$$

Equation (2.9) gives the efficiency based on the voltage decrease during discharge, while Equation (2.10) provides the efficiency based on voltage relaxation after discharge. Ideally, these two values should be equal if the charge times and relaxation times have been chosen appropriately.

One way PCS efficiency during discharge, $\eta_{\text{PCS_discharge}}$ is given by

$$\eta_{\text{PCS_discharge}} = \text{AC power from PCS} / \text{DC power from battery to PCS} \quad (2.11)$$

where

$$\text{DC power from battery to PCS} = \text{DC voltage} \times I_{\text{discharge}} \text{ at } 8 \text{ sec} \quad (2.12)$$

The one way BESS discharge efficiency, $\eta_{\text{BESS_dis}}$ is given by:

$$\eta_{\text{BESS_discharge}} = \eta_{\text{dc_dischg}} \times \eta_{\text{PCS_discharge}} \quad (2.13)$$

2.4.2.1.2 Charge Test Routine

The charge response time test shall be conducted in accordance with the following procedure and the charge response time calculated in accordance with Equation (2.14).

1. The BESS shall be at the 80% SOC and in an active standby state.
2. The DAQS shall be configured to record a time stamp T_0 when a change in set point from rest to a charge output command is sent to the BESS. Data is collected every second.
3. The DAQS shall be configured to record a time stamp T_1 when the BESS starts responding to the charge command signal.
4. The DAQS shall be configured to record a time stamp T_2 when the input to the system reaches a $100 \pm 2\%$ of its rated power capacity. The acquisition rate of data shall be at least twice as fast as the rated power capacity divided by the ramp rate of the BESS, as determined in accordance with Equation (2.15), and at least one intermediate data point shall be acquired as the BESS transitions from rest to full charge.
5. The BESS shall be configured to respond to a step change in power input set point according to the BESS specifications provided by the manufacturer.

6. The DAQS shall be started and shall command to change the power input to the BESS to full rated charge power input, and T_1 and T_2 shall be measured and recorded. The BESS is maintained at rated power for 30 seconds. This is followed by 15 minutes of rest.
7. The DAQS shall be reset to a state to begin recording data and the BESS placed in a state of active standby.

$$RT_C = T_2 - T_1 \quad (2.14)$$

where RT_C is the charge response time in seconds; T_1 is the beginning time stamp, in seconds, when the BESS starts responding to the charge signal; and T_2 is the end time stamp, in seconds, when the input to the BESS reaches $100 \pm 2\%$ of its rated power output.

The charge ramp rate (RR) shall be calculated in accordance with Equation (2.15) and expressed in megawatts per minute.

$$RR_C = [P_{T_2}] / [T_2 - T_1] \times 60 \quad (2.15)$$

where P_{T_2} is the power input to the BESS recorded at time T_2 ($100 \pm 2\%$ of rated power capacity).

The charge ramp rate shall also be expressed as percent rated power per minute (RRC_{pct}) in accordance with Equation (2.16).

$$RRC_{pct} = RRC / PR \times 100 \quad (2.16)$$

where PR is the rated power of the BESS.

The total resistances is calculated by the following equation:

$$R_{total\text{-}charge} = \{V(T_1+8 \text{ sec}) - V(T_0)\} / I_{charge} \quad (2.17)$$

where T_1+8s is T_3

If 10 ms resolution data is available, the ohmic resistance is calculated by using the voltage at 10 ms in Equation (2.17).

From the OCV data after charge, the total resistance is calculated by the following equations:

$$R_{total\text{-}charge} = \{V(T_3) - V(T_3+15 \text{ minutes})\} / I_{charge} \quad (2.18)$$

The DC efficiency and the PCS efficiency is calculated using Figure 2.3 as guide for power flow between the DC and AC side.

One way DC charge efficiency, η_{d_chg} , is given by the following equations:

$$\eta_{dc_chg} = V(T_0) / V(T_1+8sec) \quad (2.19)$$

$$\eta_{dc_chg} = V(T_3+15 \text{ minutes}) / V(T_3) \quad (2.20)$$

Equation (2.19) gives the efficiency based on the voltage increase during charge, while Equation (2.20) provides the efficiency based on voltage relaxation after charge. Ideally, these two values should be equal if the charge times and relaxation times have been chosen appropriately.

One way PCS efficiency during charge, η_{PCS_charge} is given by

$$\eta_{PCS_charge} = \text{DC power in to battery} / \text{AC power in to PCS} \quad (2.21)$$

where

$$\text{DC power in to battery from PCS} = \text{DC voltage} \times I_{\text{charge}} \text{ at 8 sec} \quad (2.22)$$

The one way BESS charge efficiency, η_{BESS_chg} is given by:

$$\eta_{BESS_charge} = \eta_{dc_charge} \times \eta_{PCS_charge} \quad (2.23)$$

The BESS RTE during the internal resistance measurement at each SOC is calculated as follows:¹

$$\eta_{ESS_RTE} = \text{One way BESS charge efficiency} \times \text{one way BESS discharge efficiency} \quad (2.24)$$

$$\text{DC RTE} = \text{One way DC charge efficiency} \times \text{one way DC discharge efficiency} \quad (2.25)$$

$$\text{PCS RTE} = \text{one way PCS efficiency during charge} \times \text{one way PCS efficiency during discharge.} \quad (2.26)$$

Figure 2.3 shows power flow in and out of the BESS (with PCS as the boundary).

¹ This can be cross-checked versus the measured RTE from the reference performance test. Note that for the latter, the charge and discharge power are the same, resulting in different currents.

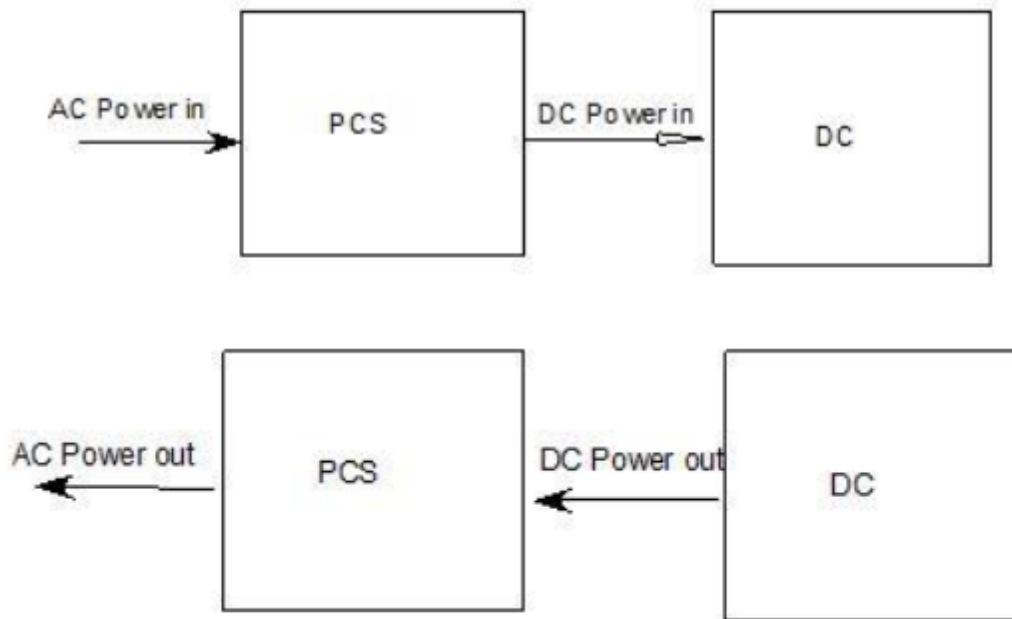


Figure 2.3. One Way DC System and PCS Efficiency during Charge and Discharge

If the BESS SOC is \geq to 30%, discharge the BESS at rated power to decrease its SOC by 10%. Then go to Step 2 in section 2.4.2.1.1. If the BESS SOC = 20 percent, go to Step 2 in section 2.4.2.1.1. Go through the discharge and charge ramp rate/internal resistance steps, and then stop.

2.5 Duty Cycles for Peak Shaving and Frequency Regulation

2.5.1 System Ratings

Ratings for BESSs covering rated power and energy available at rated power and the performance of the BESS associated with response time, ramp rate, and RTE at the beginning of life shall be based on a set of ambient operating conditions specified by the manufacturer of the BESS. PGE shall also provide an indication of how the performance of the BESS is expected to change over time to account for time and use of the system.

2.5.2 PNNL Frequency Regulation

2.5.2.1 Frequency Regulation Performance

Energy storage systems intended for use in FR shall have their performance determined in accordance with section 2.5.2. Frequency regulation shall be permitted to represent area regulation as used by a balancing authority to meet North American Electric Reliability Corporation Balancing Authority Performance Control Standards.

2.5.2.2 System Ratings

The determination and reporting of ratings for a BESS to be applied for frequency regulation shall be in accordance with the provisions of section 2.5.2 using the duty cycle in section 2.5.2.3 and metrics in section 2.5.3

2.5.2.3 Duty Cycle

The duty cycle to be applied in determining the performance of a BESS for an FR application is shown in Figure 2.4 as power normalized with respect to the rated power of the BESS of 5 MW over a 24-hour time period, where positive represents discharge from the BESS and negative represents charge into the BESS as a function of time in hours. The raw data upon which Figure 2.4 is based on is the regulation duty cycle developed in Balducci et al. (2013). Note that due to the operator having to enter each signal value manually, testing was restricted to the first 20 minutes of Figure 2.4.

PGE shall be permitted to conduct additional testing using another duty cycle. Where this is done, PGE shall provide a description of and rationale for the duty cycle chosen, shall conduct all tests required herein while subjecting the BESS to the additional duty cycle chosen, and shall report all performance measures as required in section 2.6 under the designation “alternative duty cycle.”

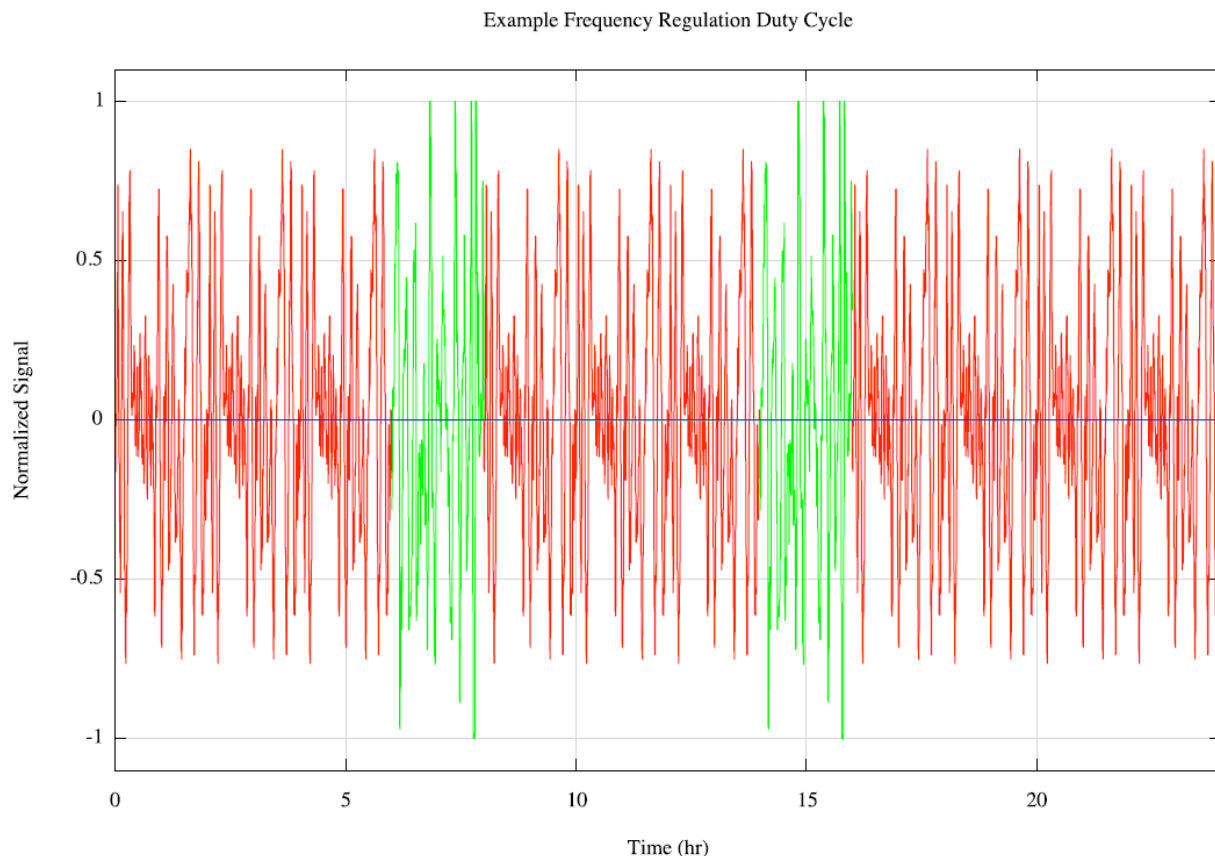


Figure 2.4. Frequency Regulation Duty Cycle

In conducting the tests required in section 2.5.2, the charge and discharge of the BESS shall be in accordance with the duty cycle described in this section.

1. The system shall be brought to the initial desired SOC of 60 percent as dictated by a given V_{initial} by adding or removing the necessary amount of charge at the rated power of the BESS as provided by the manufacturer's specifications. Alternatively, the system shall be permitted to be brought directly to the desired initial SOC by charging or discharging the BESS to the desired V_{initial} at rated power and held at that V or T for at least 10 minutes, but no more than 30 minutes.
2. The BESS shall then be subjected to the duty cycle as described in this section and shown in Figure 2.4.
3. At the end of the duty cycle, the BESS shall be returned to the initial SOC as dictated by a given V_{initial} by charging or discharging at rated power.
4. At the end of this test, the BESS shall be brought to the required SOC to prepare for the next test using a procedure as recommended by the manufacturer's specifications and operating instructions.

2.5.3 Performance Metrics

The performance of the BESS shall be expressed in accordance with the provisions of sections 2.5.1 to 2.5.2 based on the application of the duty cycle regimen provided in section 2.5.2.

2.5.3.1 Roundtrip Energy Efficiency

The RTE of the BESS shall be determined in accordance with the provisions in section 2.4.1.3.

2.5.3.2 Duty Cycle Roundtrip Efficiency

The duty cycle RTE of the BESS shall be determined by dividing the energy removed (output) from the BESS by the energy required to recharge (input) the BESS.

2.5.3.3 Reference Signal Tracking

The ability of the BESS to respond to signal for the 24-hour duty cycle described in section 2.5.2 shall be defined and determined by PGE in accordance with the provisions in this section. The balancing signal shall be changed every 4 seconds during the duty cycle.

In addition, PGE shall also determine and report separately the total percentage tracking and the times when the BESS stops tracking and restarts tracking as an indication of whether the BESS is capable of tracking high peaks and/or high energy half cycles. PGE shall also determine if the BESS can go through a 24-hour period without reaching the lower or upper SOC limits. Any time during that period when the BESS indicates an ability or inability to follow the signal shall be reported. An inability to follow the signal shall be considered a situation where the BESS cannot deliver or absorb required signal power during the 4-second duration and cannot deliver or absorb the required signal energy during the duration when the signal remains above or below the x-axis. The total time the BESS cannot follow the signal and percentage tracked shall be determined in accordance with the provisions in this section.

The ability of the BESS to respond to a reference signal shall be recorded during the RTE test. The sum of the square of errors between the balancing signal (P_{signal}) and the power delivered or absorbed by the BESS (P_{bess}) shall be calculated in accordance with Equation (2.27) and used to estimate the inability of the BESS to track the signal.

$$\Sigma (P_{\text{signal}} - P_{\text{bess}})^2 \quad (2.27)$$

where P_{signal} is the balancing signal and P_{bess} is BESS power (watts).

The measurements shall be taken at every point in time that the BESS receives a change in the balancing signal. The sum of the absolute magnitude of the difference between the balancing signal and BESS power shall be calculated in accordance with Equation (2.28).

$$\Sigma |P_{\text{signal}} - P_{\text{bess}}| \quad (2.28)$$

where P_{signal} is the balancing signal and P_{bess} is BESS power (watts).

The sum of the absolute magnitude of the difference between the balancing signal energy and BESS energy shall be calculated in accordance with Equation (2.29) and reported by PGE to account for the inability for the BESS to follow the signal due to the BESS reaching the SOC limits provided in the manufacturer's specifications and operating instructions.

$$\Sigma |E_{\text{signal}} - E_{\text{bess}}| \quad (2.29)$$

where E_{signal} is the signal energy for a half-cycle, with half-cycle being the signal of the same sign (above or below the x-axis), and E_{bess} is the energy supplied to or absorbed by the BESS for each half-cycle.

When $|(P_{\text{signal}} - P_{\text{bess}})/P_{\text{signal}}|$ is less than 0.02, the BESS shall be considered to track the signal. The total time the BESS cannot follow the signal and percentage tracked where $(P_{\text{signal}} - P_{\text{bess}})/P_{\text{signal}}$ is less than 0.02 shall be determined in accordance with Equation (2.30).

$$\% \text{ of time signal is tracked} = [\text{Time signal is tracked (h)} / 24 \text{ h}] \times 100. \quad (2.30)$$

2.5.3.4 State-of-Charge Excursions

The SOC of the BESS during testing required under the protocol shall be monitored and continuously updated by integrating the current with respect to time for each half-cycle. For the purpose of this requirement, a half-cycle shall be considered the amount of time when the current or power is of the same sign. The integrated area shall be added to the SOC as the charge half-cycle is started or subtracted from the prior SOC as the discharge cycle is started. The SOC excursion shall be reported in accordance with the provisions in section 2.6.4.2.

2.6 Reporting Performance Results

The performance of a BESS shall be reported by PGE in accordance with the provisions in section 2.6 as determined in accordance with the applicable provisions of section 2.5. PNNL will oversee all BESS testing operation and will be responsible for capturing and filling out all report documentation with support from PGE.

2.6.1 System Stored Energy Capacity and Roundtrip Efficiency.

The stored energy capacity of the BESS determined in accordance with the provisions in section 2.4.1.1 and the RTE determined in accordance with the provisions in section 2.4.1.2 shall be reported as provided in Table 2.3. Where additional testing is performed beyond the minimum required two cycles, an

additional row shall be added for each cycle and the total charge and discharge energy shall be the sum of all values reported and the RTE based on those totals.

Table 2.3. Stored Energy Capacity and Roundtrip Efficiency at Various Discharge Power Levels – One Table for Each Discharge Power Level

Date					
Ambient Temperature °C					
Barometric Pressure, psia					
	Charge Energy (Wh)	Discharge Energy (Wh)	Cycle RTE	Cumulative RTE	Capacity stability (% of initial energy capacity)
Cycle 1	_____	_____	_____		_____
Cycle 2	_____	_____	_____		_____
Cycle 3	_____	_____	_____		_____
Sum cycle 1-3				_____	
Sum cycle 2-3				_____	

This calculation is done with and without auxiliary power, and with and without rest time. When auxiliary power is excluded, the results for with and without rest time are the same. Note that PGE has not provided auxiliary power data.

2.6.2 Response Time and Ramp Rate

The response times in seconds and ramp rates in megawatts per minute of the BESS shall be reported as determined in accordance with the provisions in section 2.4.2 as shown in Table 2.4.

Table 2.4. Response Time and Ramp Rate

Date			
Ambient Temperature °C			
Barometric Pressure, psia			
Mode	Response time (T ₂ -T ₁) (s)	Ramp rate	
		MW/min	% rated power/min
Discharge			
Change with respect to baseline (Present – baseline)			
Charge			
Change with respect to baseline (Present – baseline)			

2.6.3 Internal Resistance Test

The internal resistance shall be reported in accordance with the provisions in section 2.4.2 and as shown in Table 2.5. This test is done as part of baseline testing, as well as after use case tests.

Table 2.5. Internal Resistance of the BESS

Date:		
Ambient Temperature °C		
Barometric Pressure, psia		
	Internal Resistance Charge	Internal Resistance Discharge
SOC, %		
80		
70		
60		
50		
40		
30		
20		

2.6.4 Frequency Regulation Applications

The performance of a BESS intended for an FR application shall be reported by PGE in accordance with the provisions in section 2.5.3 as determined in accordance with the applicable provisions of section 2.5.1.

2.6.4.1 Duty Cycle Roundtrip Efficiency

The duty cycle RTE shall be reported in Table 2.6.

2.6.4.2 Reference Signal Tracking and SOC Excursion

The reference signal tracking of the BESS shall be reported in accordance with the provisions in section 2.4.2. The SOC excursion shall be reported as determined in accordance with the provisions in section 2.5.3.4. These results will be reported in Table 2.6.

Table 2.6. Frequency Regulation Metrics

Date
Ambient Temperature °C
Barometric pressure, psia
Duty cycle RTE
$\Sigma (P_{\text{signal}} - P_{\text{bess}})^2$
$\Sigma P_{\text{signal}} - P_{\text{bess}} $
$\Sigma E_{\text{signal}} - E_{\text{bess}} $
$\Sigma E_{\text{signal}} - E_{\text{ess}} $
% of time signal is tracked
State-of-charge excursion
Lowest SOC, %
Highest SOC, %

3.0 Battery Performance Test Results

The PGE SSPC, which was developed as part of the Smart Grid Demo, deployed an EnerDel 5 MW 1.25 MWh lithium-ion BESS in March of 2013. To date, the primary service provided by the SSPC has been primary frequency response. See section 4.1.5 for a detailed overview of this service. The purpose of this project is to evaluate the technical performance of the BESS, and given those technical constraints, explore the landscape of economic opportunities for PGE in order to expand the impact of the SSPC and inform industry on the lessons learned in the process.

During the first phase of tests, the BESS was subjected to baseline testing as described in the DOE-OE Performance Protocol (Viswanathan 2014), with discharge at various C rates for a constant C rate charge.² Response time and ramp rate were measured at various SOCs, along with charge and discharge resistance. The BESS was also subjected to the FR duty cycle outlined in section 2.5.2. The results of these tests are presented in this section of the report.

3.1 Battery System Layout

The BESS is located on the 480 volt (V) AC side of five 1,000 kVA 12.47 to 480 V AC transformers in the Oxford-Rural Feeder. Each transformer feeds one out of five battery blocks, with Blocks 1–3 being connected to the South Sector Cabinet (200A, 3-Phase) and Blocks 4 and 5 connected to the North Sector Cabinet.

A separate 300 kVA 12.47/480 V AC transformer provides power to an auxiliary system through a 37.5 kVA 480 V-120V/240V AC transformer. The auxiliary power consists of heating and cooling of the building in which the BESS is housed. There are no heaters or coolers for the BESS other than the building HVAC. Figure 3.1 shows a one-line diagram of the SSPC BESS, while Figure 3.2 shows the three-line diagram of a 1 MW block. The three-line diagram shows details up to the string level within a vault; three strings in parallel form a vault. The diagram also shows that each vault is connected to a 125 kW inverter. However, the AC data is available only for each 250 kW rack, which is essentially the parallel connection of the two 125 kW inverters.

² For batteries, if the nominal capacity (typically measured at the 10-hour rate, also known as C_{10}) is 100Ah, then 1/2C rate is $C_{10}*(1/2)$, and 2C is $C_{10}*(2)$. For a BESS, if the rated energy content is 100 Wh, measured at a power specified by the BESS manufacturer or integrator, then the C rate is 100 watts, 1/2C rate is $100*(1/2)$ watts, and 2C is $100*2$ watts.

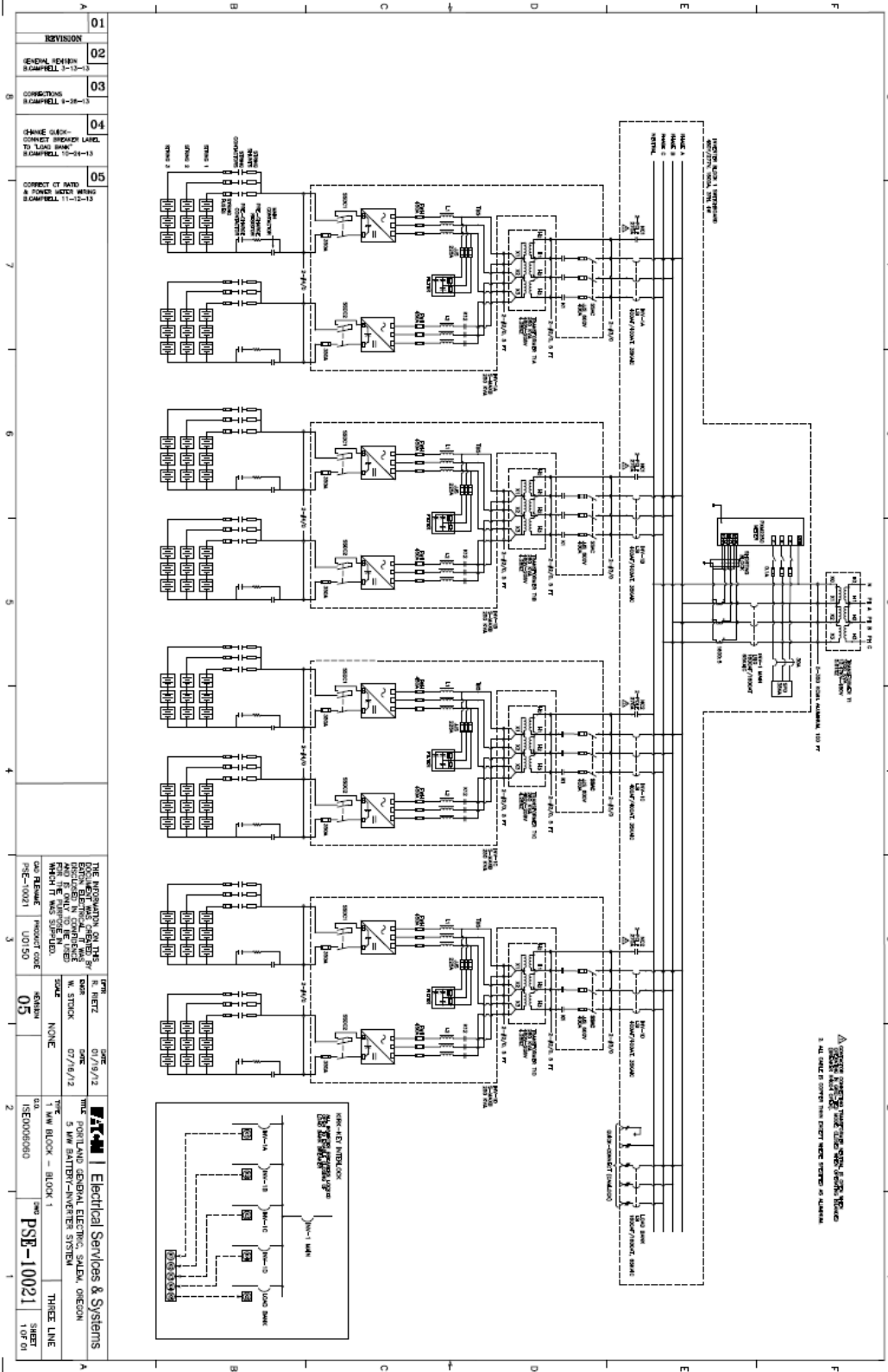


Figure 3.2. Three-Line Diagram of the SSPC BESS

3.2 BESS Details

This BESS consists of five blocks, with power capacities of 1 MW per block. Each block consists of four racks connected in parallel with 250 kW inverters at the 480 V AC level. Each rack has two vaults connected in parallel by 125 kW inverters at the 480 V AC level. Each vault consists of three parallel strings, with each string comprised of three drawers in series. Figure 3.3 presents a detailed overview of Block 1 up to the string level within each vault.

Each string comprises of three drawers connected in series. Each drawer has four modules in series, and each module has 24 cells (two parallel strings of 12 cells in series). There are a total of 1,440 rack-mounted modules, with 36 modules per vault, two vaults per rack and four racks per block. Each of the 20 racks is a channel rated at 250 kW/62.5 kWh and 600 V DC. Each channel has an independent BMS.

The maximum voltage for each cell is 4.1 V. There are 24 cells in a module, with two parallel strings of 12 cells connected in series. This corresponds to a module voltage of 49.2 V at 4.1 V/cell. Four modules connected in series form a 196.8 volt drawer. Three drawers connected in series form a 590.4 V string. Three such strings connected in parallel form a vault. The layout for one rack is shown in Figure 3.3, while the BESS layout for the whole battery is shown in Table 3.1. Note that Figure 3.3 provides information only up to the drawer level. Figure 3.4 shows four modules connected in series within a drawer. Each module has 24 cells (two parallel strings of 12 cells in series). Individual cell voltage and temperature within each module are monitored. These resulted in interference, causing the measurement accuracy to be compromised. A patch fix was incorporated, which appeared to resolve the issue.

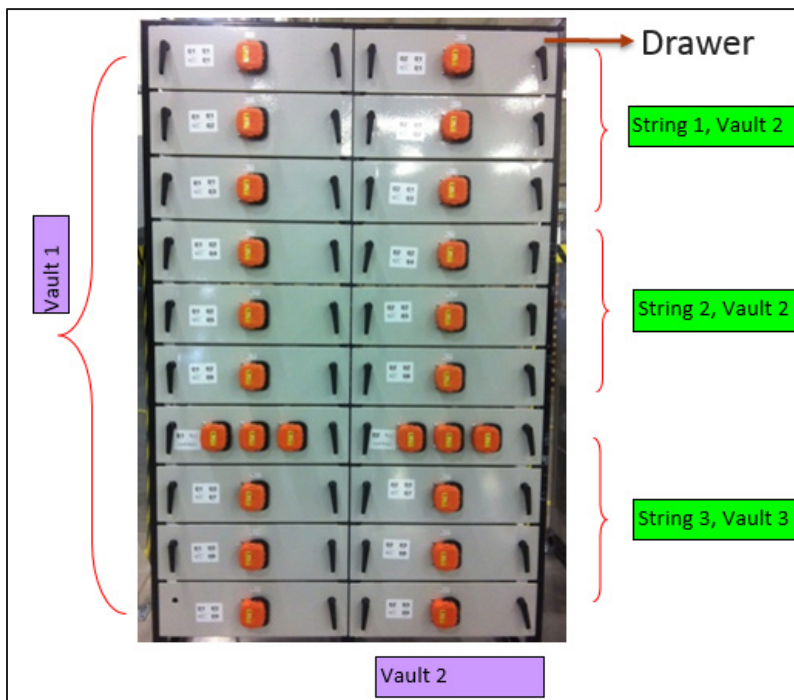


Figure 3.3. Layout of One 590.4 Volt DC, 250 kW, 62.5 kWh Rack

Table 3.1. Number of Various Components

Components	#	# cells	Max Voltage	Average V	Energy (kWh)
Series-connected cells in module	12	12	49.2	45.60	0.44
Parallel strings in a module	2	24	49.2		0.88
Series-connected modules per drawer	4	96	196.8		3.50
Series-connected drawers per string	3	288	590.4		10.50
Parallel strings per vault	3	864	590.4		31.50
Parallel vaults per rack	2	1,728	590.4		63.00
Racks per block	4	6,912	590.4		252.00
Blocks in the BESS	5	34,560	590.4		1260.00



Figure 3.4. Drawer Internal Components

Figure 3.5 shows the layout of the five battery blocks. The front of each block faces the front of the next, while the back of each block faces the back of the adjacent block. Fire extinguishers are available at the top of each block. The fire extinguishers spray cooling fluid through a system of tubes that surrounds each drawer. The tubing is continuous, and is designed such that if the temperature exceeds an upper limit, the tubing will melt and the fire suppressant is forced from the reservoir at the top of each vault through small holes in the tubing. Because the heat from the fire would melt the tubing at the point nearest to the fire's hottest point, the fluid is automatically directed towards the flame. As shown, each vault has its own independent fire extinguishing system. The image shows the face of six vaults.



Figure 3.5. Battery Block Layout

Figure 3.6 shows the south sector cabinet (200A, 3-Phase) to which Blocks 1-3 are connected through 250 kW inverters. There are four 250 kW inverters per block. The panel on the extreme right represents the set up to connect battery block 5 with an electronic load for preliminary commissioning testing and to test the block 5 periodically as appropriate.



Figure 3.6. BESS Panels

Figure 3.7 shows the monitor that is used to control the BESS. The set point for SOC and the required power can be specified. If any inverters are known to not be operational, they can be de-selected. If a vault goes beyond its operating range during operation, it is automatically taken out of service and the corresponding inverter is shown to be out of service. Each rack has two vaults, which are connected in parallel at the AC side of their 125 kW inverters. Thus, if one of the vaults goes out of the specified operating range, the rack consisting of that vault is taken out of service and the corresponding 250 kW inverter is shown as not operating.

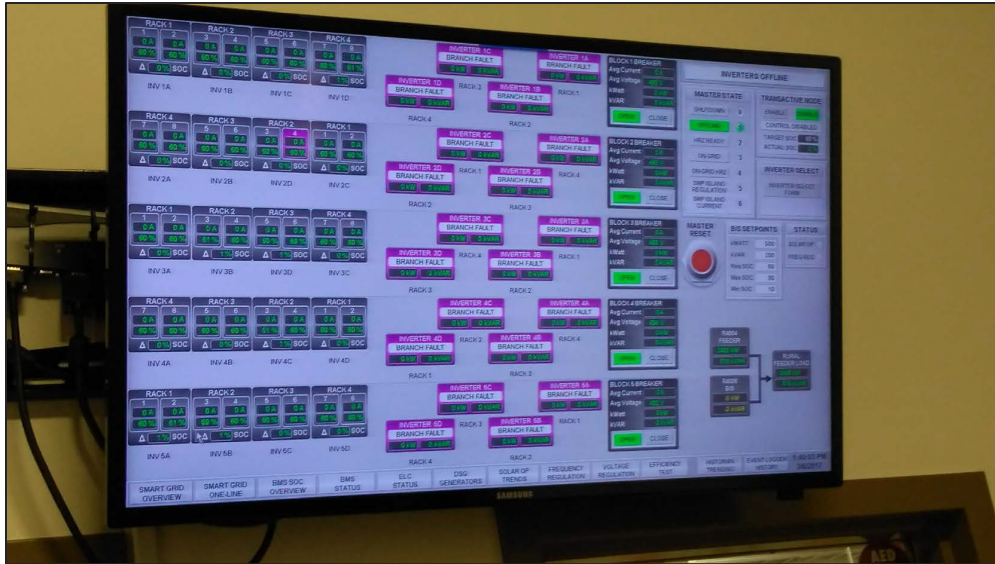


Figure 3.7. BESS Control Station

It is worth noting that the 250 kW inverter does not physically exist. Rather, two 125 kW inverters connected in parallel at the AC end are represented as a 250 kW inverter in the line diagram as seen in Figure 3.7. When one vault goes out of commission, its paired vault is also forced into an inactive state. Since there are four racks in a block and five blocks in the BESS, that means 5 percent (one out of 20 racks) of the BESS is inactive when one vault goes out of commission.

If the SOC of that vault is low (or high), that value is included in the estimation of BESS SOC. Hence, while the actual SOC of the remaining vaults may be 30 percent, the reported SOC value during discharge could be 27 percent if the SOC of the inactive vaults is lower. The charge or discharge power is now distributed, thus increasing the power through each of the remaining racks. Hence, when discharge is terminated at a 20 percent end of discharge SOC condition, the actual SOC of the active vaults may be higher than 20 percent, leading to premature termination. Increasing the discharge power per rack also results in higher temperatures, which could lead to improved performance and hence higher energy during discharge.

If the inactive vaults were terminated at a high SOC condition, the situation is reversed. The active vaults would be discharged to < 20 percent SOC, since the inactive vaults drive the average SOC upward. The only time this would not happen is if the end of discharge condition is 0 percent SOC, assuming 0 percent SOC is the lower limit at which the hard stop for discharge is initiated. In this case, the discharge would terminate as soon as any vault reaches 0 percent SOC, even if the average SOC of all vaults is > 0. This, in combination with the higher cell temperature associated with higher discharge power for the remaining racks, can lead to higher energy obtained when a rack is taken out of service.

3.3 Data Tags

The PNNL battery testing team was given broad access to data flowing from the BESS during testing. All available data tags from vaults, racks, and blocks were collected. The data tags provided to PNNL, along with descriptions of these tags, are provided in Table A.1 in Appendix A.

Data sampling was completed every second. There were multiple objectives.

- Determine round trip efficiency (RTE) across multiple discharge rates at fixed charge rate.
- Determine RTE across multiple charge rates at fixed discharge rate.
- Determine signal tracking for frequency regulation.
- Determine uniformity for the following between vaults in a rack, vaults in a block, and vaults among all the blocks in the BESS:
 - Voltage
 - State-of-Charge (SOC)
 - Temperature
 - Power flow.
- Bookkeeping of power flow at the 12.5 kV level and the sum of power flow through all blocks at 480 V AC.

The extensive data collected at various levels allows a deep understanding of the BESS performance and reliability across various levels, which translates into a greater understanding of system reliability.

3.4 Performance Test Results and Discussion

Baseline capacity tests were performed per the DOE-OE Performance Protocol (Viswanathan 2014). The system rating is 5MW/1.25 MWh. The Protocol recommends determining the energy capacity of the BESS using a fixed charge and discharge rate. Additional capacity tests are recommended by varying the discharge rate. The system energy at rated discharge power is defined as the energy delivered from the high end of the SOC to when the discharge power drops by one percent. In this testing process, in addition to various rate discharges, the BESS was discharged at constant power following various rate charges. This allows estimation of the BESS performance across a range of charge and discharge powers.

3.4.1 Discharge at Various Rates

The BESS was discharged at various power levels after a charge at 1,000 kW to 80 percent SOC, followed by a rest period of one hour. The results of this test are presented in Table 3.2. The available discharge energy is also shown in Figure 3.8. At 500 kW, the energy available is the lowest, possibly due to higher internal resistance at lower cell temperature at this low discharge rate ($< C/2$). The highest discharge energy appears to be at 3,000 kW. For some of the charge or discharge half cycles, some inverters were not working properly. Note that the discharge energy falls short of the rates 1.25MWh because the BESS was operated during the tests between a 20 percent and 80 percent SOC.

Table 3.2. Results for 1 MW Charge and Various Discharge Rates

Cycle #	Charge Power (kW)	Discharge Power (kW)	Charge Energy (kWh)	Discharge Energy (kWh)	RTE	Cum RTE	Notes
1	1,085	498	937	737	0.79		All inverters working
2	1,084	508	952	731	0.77		All inverters working
3	1,088	500	940	717	0.76	0.77	All inverters working
1	1,088	1,022	947	738	0.78		Three inverters not working during discharge– 1A, 2D, 3D
2	1,085	1,011	892	754	0.85		

Cycle #	Charge Power (kW)	Discharge Power (kW)	Charge Energy (kWh)	Discharge Energy (kWh)	RTE	Cum RTE	Notes
3	1,089	1,011	991	789	0.80	0.81	3 rd cycle started after next day morning, so start is cold. 3D and 1A inverters down during discharge, so possibly high temperature results in better performance. On cycle one, two inverters did not work but gave lower energy
1	1,081	3,006	945	757	0.80		3D and 1A not working (only during charge)
2	1,042	3,005	898	796	0.89		3D and 5B not working (only during charge)
3	1,086	2,999	943	784	0.83	0.84	3 rd cycle started after next day morning, so it started cold. All inverters working
1	1,085	4,547	933	724	0.78		5C and 5A not working during discharge
2	1,086	4,829	941	772	0.82	0.80	5B not working (only during charge)

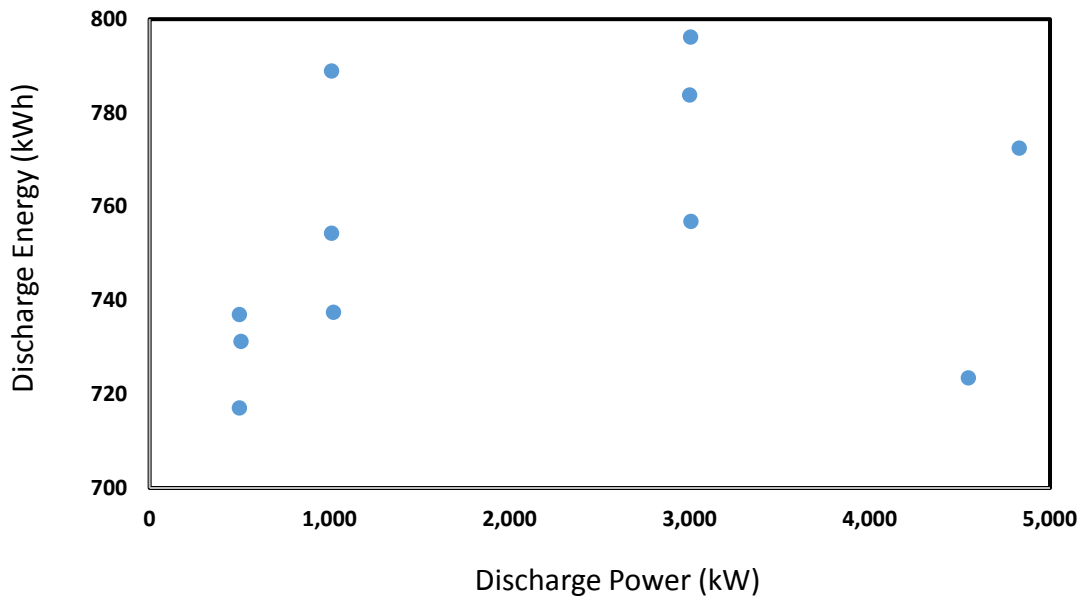


Figure 3.8. Discharge Energy at Various Power Levels

The available energy at various discharge powers as a function of order in which the experiments were conducted are shown in Table 3.3 and Figure 3.9. For 1,000 kW and 3,000 kW discharge, the third run was completed after an overnight rest. Hence, the initial temperature was lower, leading to a lower available energy for the 3,000 kW discharge. However, for the 1,000 kW discharge, two inverters (out of 20) were not working during the third run. This issue likely led to a rise in average BESS temperature, resulting in higher energy during the third discharge.

Table 3.3. Energy Obtained at Various Power Levels with Order of Experiment Shown

Order	500 kW	1,000 kW	3,000 kW	5,000 kW
1	737	738	757	724
2	731	754	796	772
3	717	789	784	

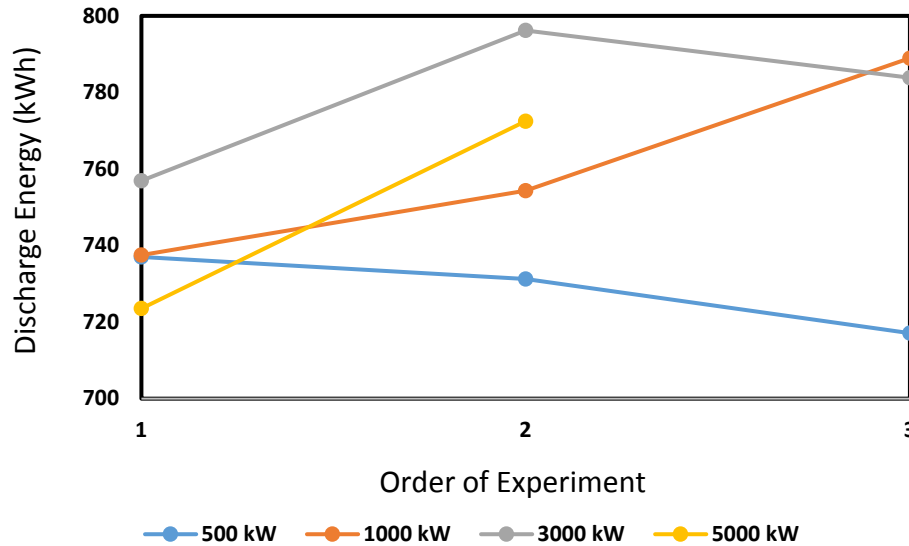


Figure 3.9. Discharge Energy at Various Power Levels Varied by Order of Experiment

The power flow was measured at various levels:

- At the 12.47 kV side (BESS meter)
- At the 480 V AC side (LV1 to LV5 meters)
- At the DC side of the 125 kW inverter.³

Figure 3.10 shows the difference between the power flow at the 12.47 kV line and the sum of the low voltage meters for blocks 1–5 at the 420 V AC level. The difference is very small for the most part, and reflects the 1,000 KVA 12.47-480 V AC transformer T1–T5 losses. Spikes in this difference occur at the start of each charge or discharge, possibly related to time lags in the meter on either side of the transformers.

³ This measurement only took place during the internal resistance test.

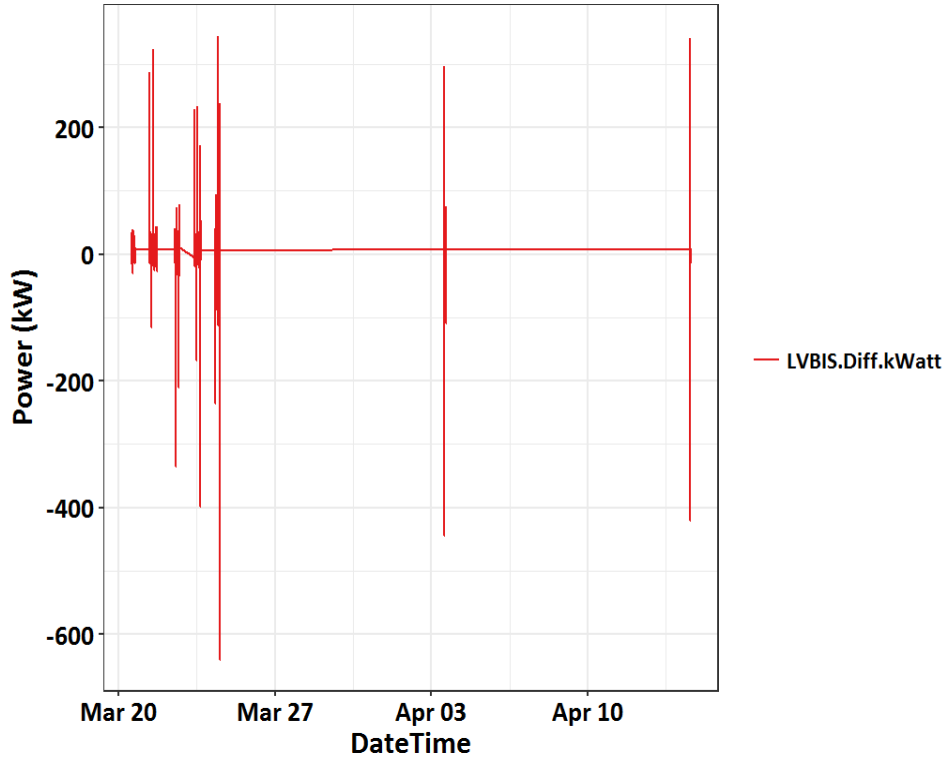


Figure 3.10. Difference in Power Flow between the 12.47 kV and 480 V AC Level of the BESS

Within each block, the maximum, minimum, and average values of cell temperature was recorded, along with the difference between maximum and minimum cell temperature. The average cell voltage in each vault, the difference between maximum and minimum cell voltage in each vault, current flow, and average SOC for each vault was also recorded. Under normal operation with all inverters working, the current through each vault is nearly equal. For each vault pair, the median current difference is <0.04 amperes, except during start of charge or discharge, when the difference shoots up to nearly 10 amperes. The average SOC for all vaults fall within a tight range. The difference between maximum and minimum cell voltage in each vault is in the 0.01 V to 0.06 V range, except at the start of charge or discharge when it shoots up to 0.08 V to 0.15 V. Table 3.4 summarizes these observations for Block 1. Similar observations were made for the other blocks.

Table 3.4. Value of Parameters for Vaults in Block 1 during Various Rate Discharge Testing

What is being compared?	Parameter	Range at Max T		Range at Mid T		Range at Min T	
		Low T, deg C	High T, deg C	Low T, deg C	High T, deg C	Low T, deg C	High T, deg C
All 8 vaults in Block 1	Cell T Max.	41.5	46	32	35	25	28
All 8 vaults in Block 1	Cell T Min.	28	39	22	30	18	24
All 8 vaults in Block 1	Cell T Avg.	38	43	24	32	24	27
All 8 vaults in Block 1	Cell T Difference	Highest for vaults 1 at 30°C March 21-25. Inverter 1A was not working. That appears to indicate 1A was not working from March 21 st through March 25 th					
All 8 vaults in Block 1	Cell V Delta	Delta V is 0.01 to 0.06V, except at start of charge or discharge when it shoots up to 0.08 to 0.15V					
All 8 vaults in Block 1	Adj. SOC	Pretty tight range – within 1%.					
All 8 vaults in Block 1	Current (I) Difference for Vault Pairs	0 to 0.04A median. Very tight range, except during start of charge or discharge where the difference is as high as 10 A.					

Figure 3.11a presents the discharge energy by discharge power available for Cycles 1 and 2. For Cycle 1, the discharge energy is nearly the same for 500 kW and 1,000 kW power discharge, while it peaks at 3,000 kW followed by a steep fall at 5,000 kW. This demonstrates that up to 3,000 kW, the higher temperature associated with higher discharge rates provide higher discharge energies. At 5,000 kW, however, the increase in temperature is not sufficient to overcome the higher polarization associated with the higher discharge rate. For Cycle 2, the 500 kW discharge provides the smallest energy, followed by a 1,000 kW discharge. The maximum energy is obtained at 3,000 kW, about 9 percent higher than at 500 kW, while a 5,000 kW discharge provides 6 percent higher energy than at 500 kW. This shows the effect of temperature on BESS performance. Figure 3.11b shows the RTE as a function of discharge power. The RTE peaks at 84 percent for 3,000 kW, where the temperature effect overcomes polarization related to higher current.

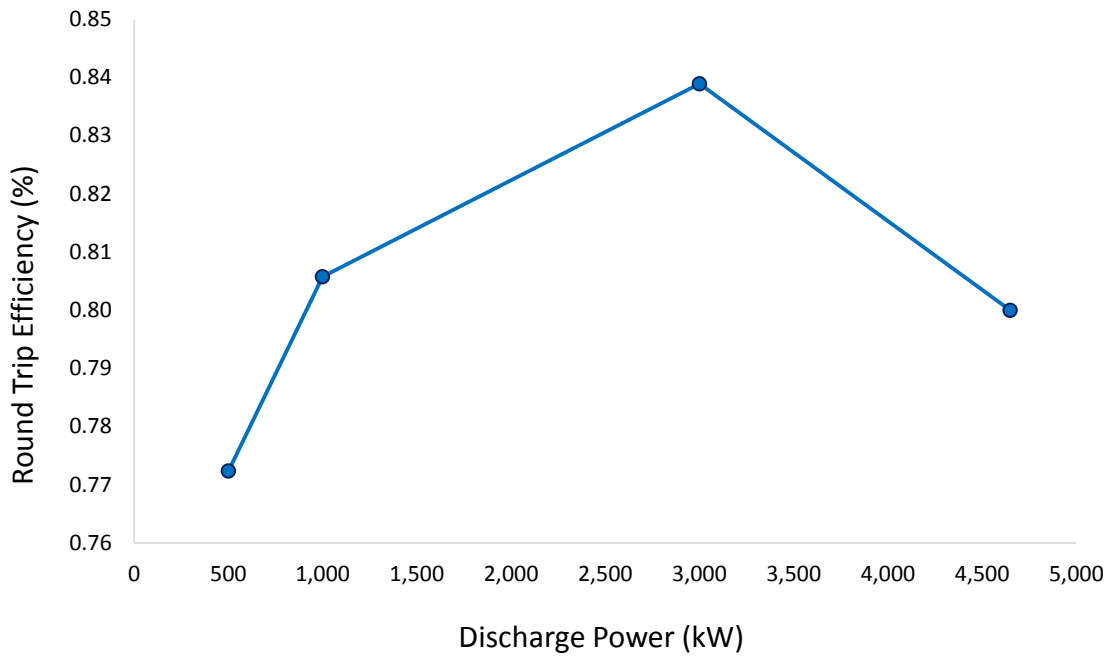
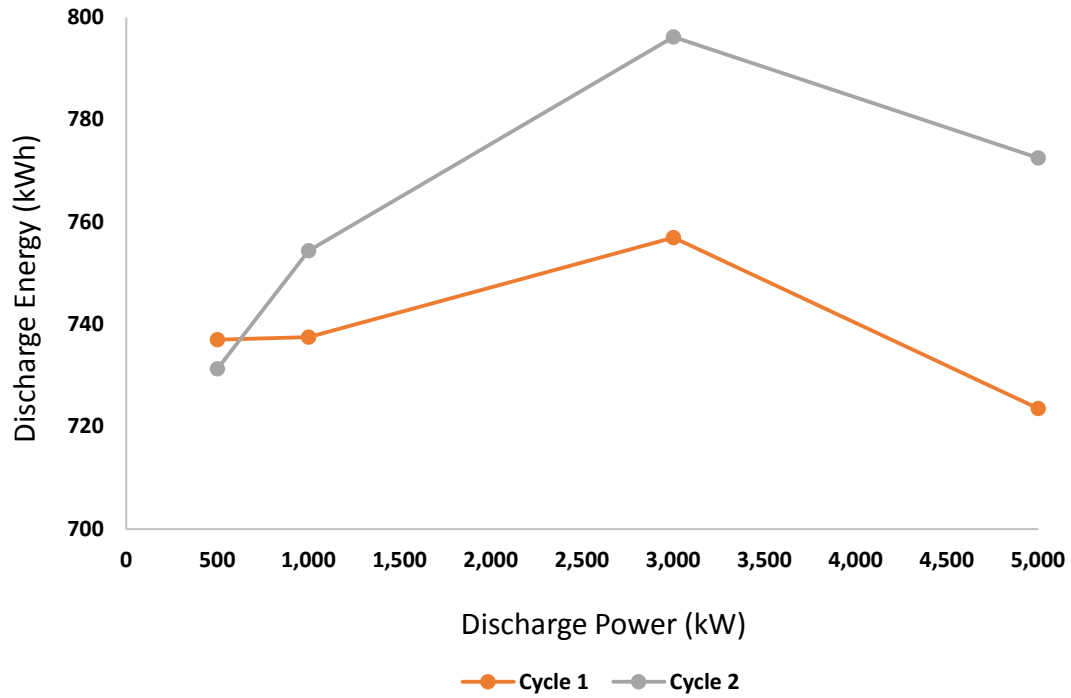


Figure 3.11. Discharge Energy (a) and RTE (b) as a Function Power for the First Two Test Cycles

The AC power flow through each block is shown in Figure 3.12. This figure demonstrates the uniformity of power flow in each block.

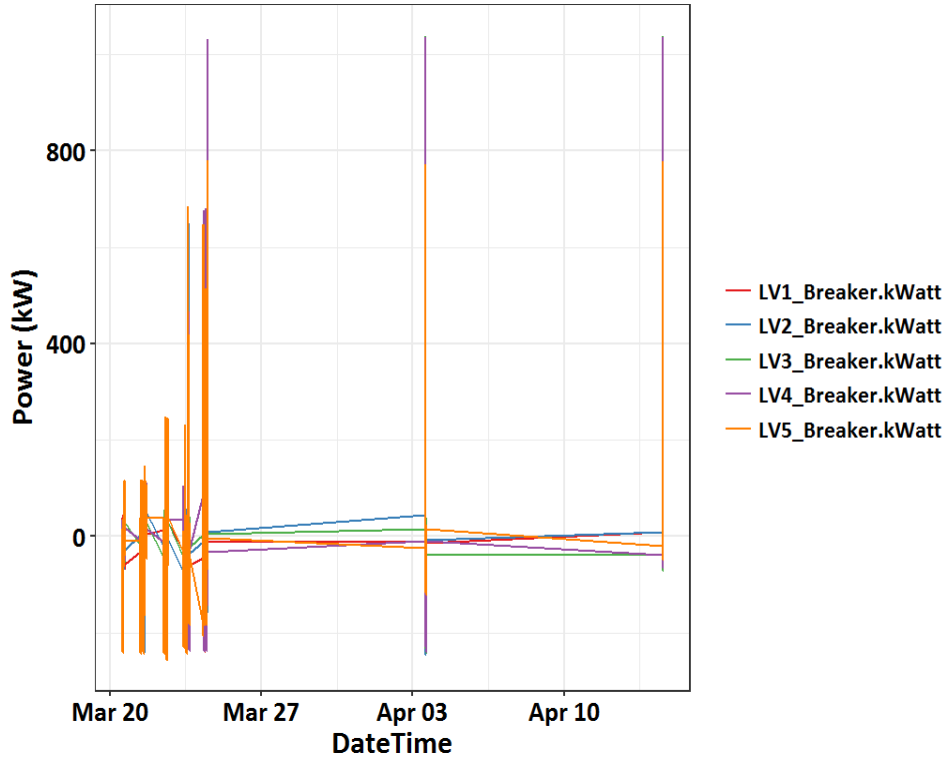


Figure 3.12. AC Power Flow through Each Value during Various Power Discharge Test

The inverter efficiency was calculated using AC and DC power flow. The DC power flow was calculated using average voltage, average SOC, average temperature, and current for all vaults in each block for various discharge power levels. The inverter efficiency was measured in the 96 to 99 percent range.

The RMS of the deviation for the March 22–April 14 test period for SOC, temperature, and voltage for vaults with respect to all the vaults in the BESS and with respect to vaults within each block are shown in Figure 3.13. The RMS of the deviation for the temperature of the vaults is 2°C. The RMS for the SOC deviation is high at 10 percent, while the RMS for the voltage deviation is around 0.14 V.

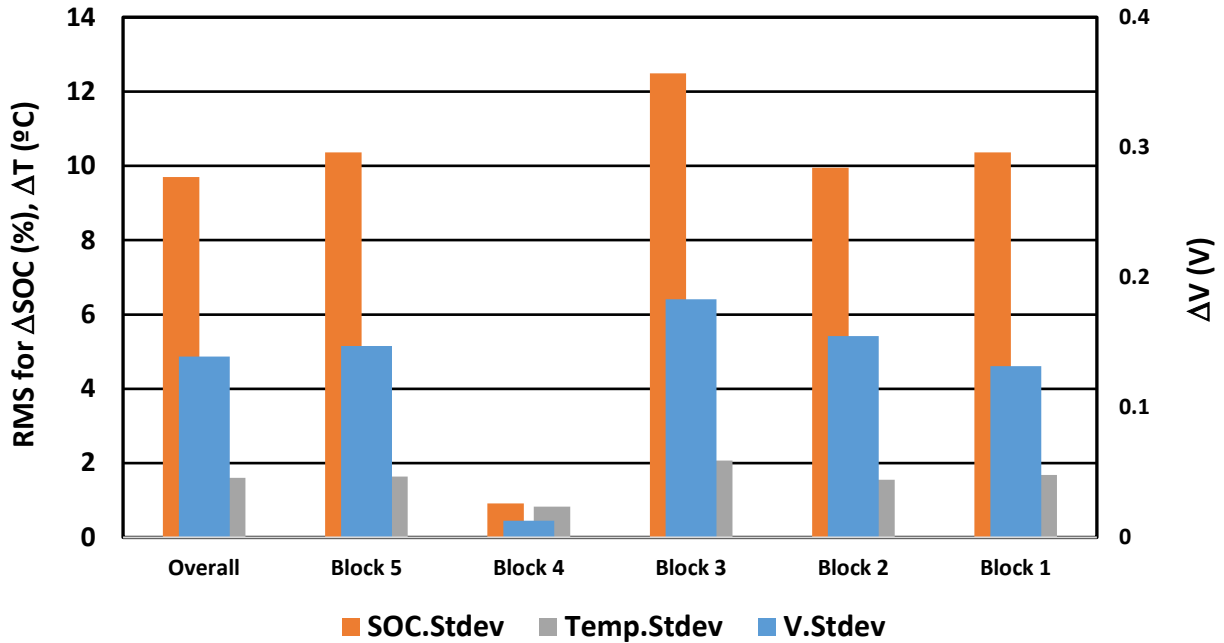


Figure 3.13. Standard Deviation for SOC, Temperature, and Voltage within Each Block

While the SOC deviation appears much higher than the deviation in voltage, it may be more useful to normalize with respect to the average value of the parameter. The SOC deviation is 20 percent of the average SOC of 50 percent. The voltage deviation is 4 percent of the estimated average voltage of 3.5 V, while the temperature deviation is 4.8 percent of the average temperature of 42°C. The lower value of voltage deviation is understandable since voltage as a function of SOC has a plateau over a large SOC range. Hence, it would not be expected to change rapidly with respect to SOC.

3.4.2 Variation of Parameters within a Rack

The next level of analysis involves comparing vault pairs in each rack. The difference in the vault pair values of various parameters measured were computed as a function of time. The root mean square (RMS) value of this difference across the time range was plotted for each parameter, normalized with respect to the higher RMS value, for all vaults in the BESS (Figure 3.14). As shown, the largest SOC difference occurs for Rack 2c, which also has the largest differences for average temperature, average voltage, and average current.

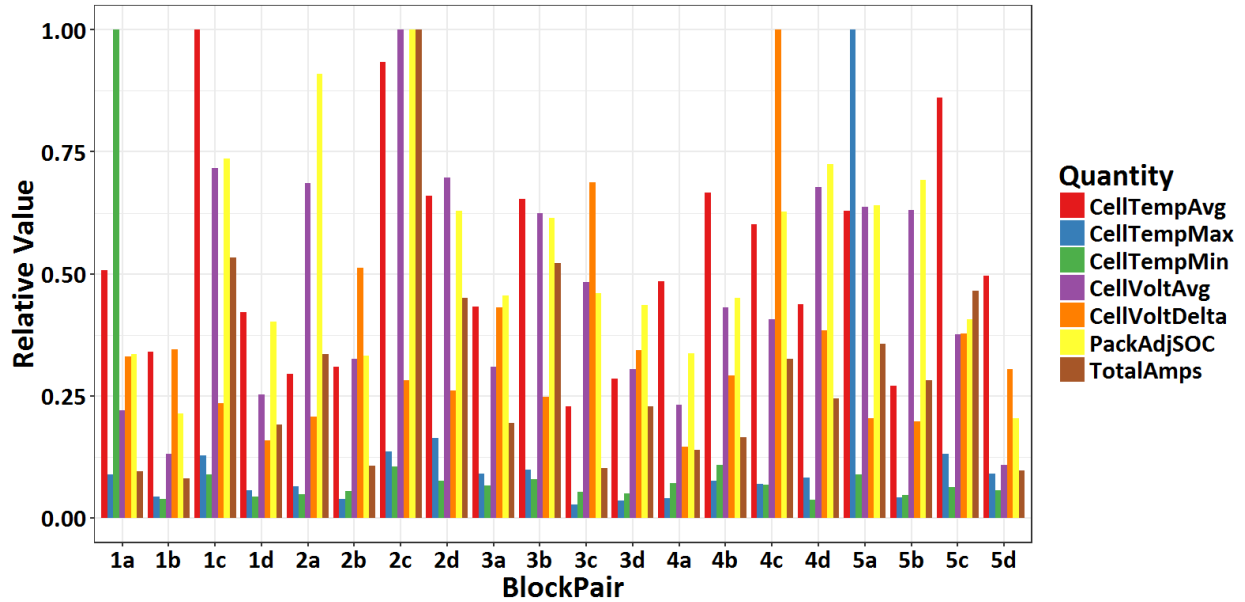


Figure 3.14. RMS Difference between Vault Pair Values

Plotting the RMS for Δ SOC as a function of the RMS for differences in T, V, and I shows a linear relationship for Δ V with an R^2 of 0.89, while the corresponding fits for Δ I and Δ T had R^2 of 0.59 and 0.12, respectively (Figure 3.15). This indicated that the differences in operating voltage was more correlated with differences in SOC than current and temperature. A possible reason is that over a period of time, the differences in current may cancel each other out, as low current in one vault may be followed by high current in the same vault (compared to its partner in the pair). It may be more instructive to plot the magnitude of the differences in current to verify this is indeed happening. When one vault has higher current, its temperature also rises but the voltage may rise faster due to increases in SOC and higher polarization. As voltage and SOC increases, this could reduce current flow through this vault, thus directing more current through the other vault; whereas, the SOC moves in line with the vault voltage.

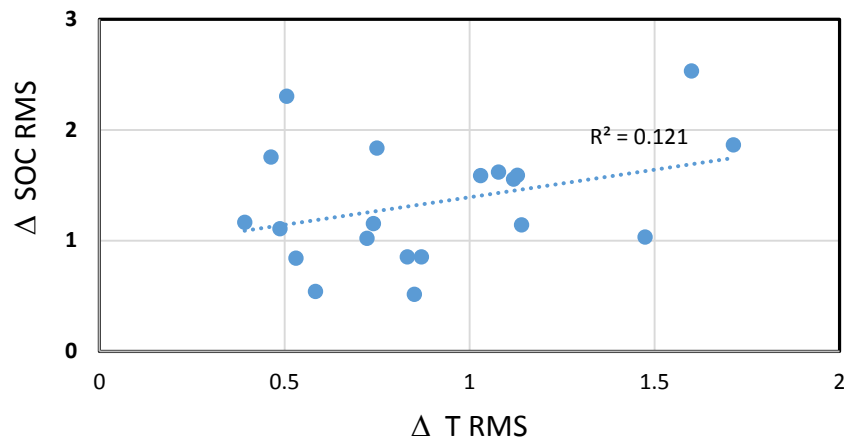
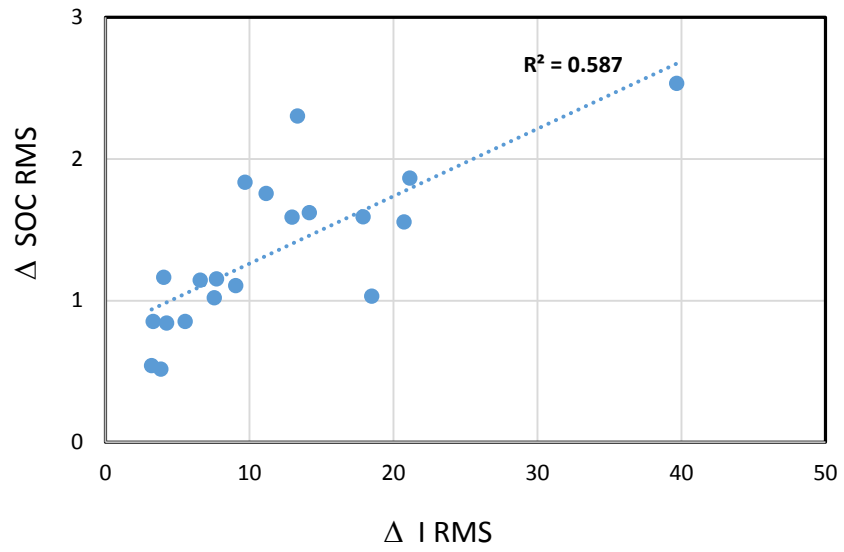
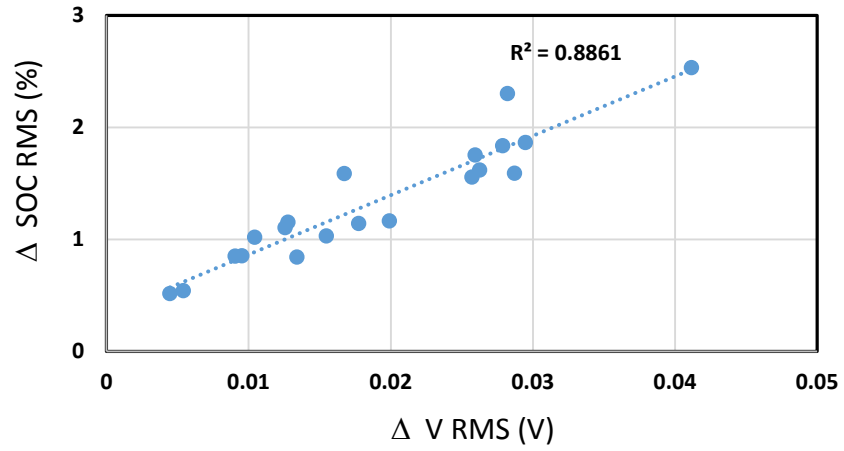


Figure 3.15. RMS of ΔSOC between Vaults in a Rack

Figure 3.16 shows the R^2 for the RMS of differences for various parameter pairs for vaults in a rack. The R^2 decreases from left to right, with SOC and voltage differences having the highest correlation, and SOC and temperature differences having the least correlation.

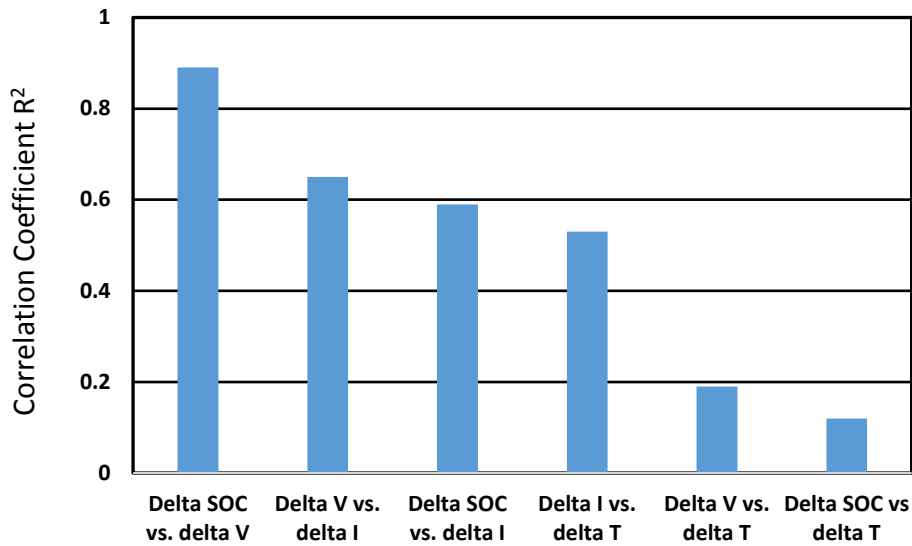


Figure 3.16. Correlation Coefficients for RMS of Differences between Vaults in a Rack for Various Parameter Pairs

The median of the difference in current and the RMS of the difference in current between vault pairs is plotted in Figure 3.17. The high RMS also correlates with a high bias (median value is high) as seen for vaults in Rack 2c. The positive value of the median shows that during discharge, the current is higher in one vault, while during charge the current may be higher in the other vault in the rack pair. This is because the sign for charge current is different than the sign for discharge current. Also, the RMS is two orders of magnitude higher than the median values. This could be due to the high effect of the data points during the transition from zero current to charge or discharge, where there are spikes observed.

By taking the absolute value of the current, the confusion related to the sign of current affecting the interpretation of results can be removed. The RMS for Rack 2c is high for cell temperature, voltage, SOC, and current. Hence, the high median current difference for 2c is related to the high RMS of the difference of cell temperature, voltage, SOC, and current between vaults in a rack.

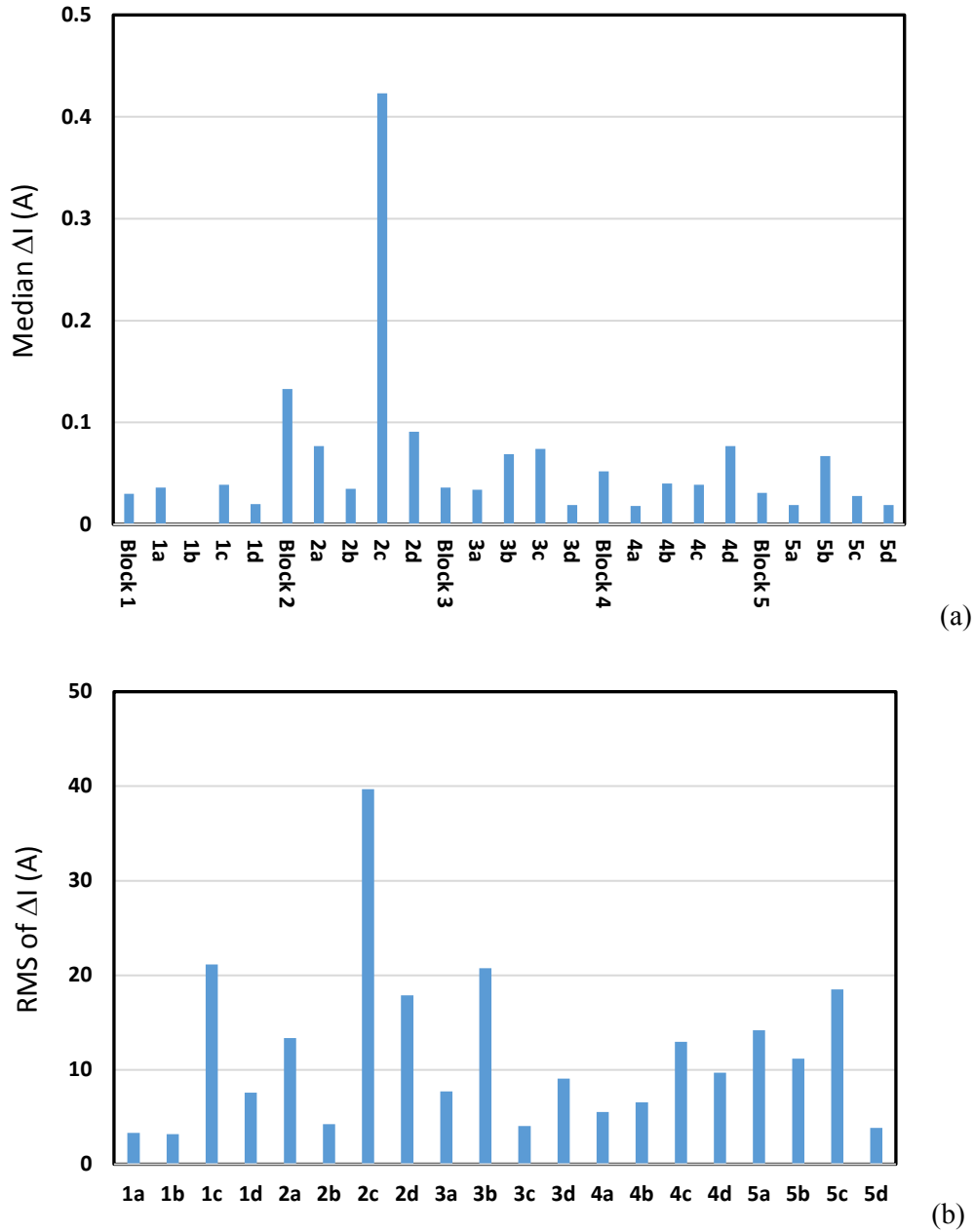


Figure 3.17. Correlation between the Median (a) and RMS (b) of Current Difference between Vaults in a Rack

3.4.3 Variation of Parameters within a Block

The various parameters for each vault were also compared with the remaining vaults in the same block (Figure 3.18). The top graph (a) is the RMS value of the difference, while the bottom graph (b) is the mean of the difference across the time investigated. One important note is that the voltage and SOC deviation go hand-in-hand. For vaults 3-5 and 3-6, all parameters deviate significantly (except T_{min}). This could give insight on whether this particular inverter (3C) was not working for some of the time during testing. Vault 1-2 also has high deviation for all parameters, but this may not be related to inverter 1A, since vault 1-1 does not deviate as much. Vaults 1-2, 3-5, and 3-6 all have negative deviations from the

mean for all parameters. For almost all vaults, the direction of deviation for related parameters is the same in that if SOC deviation is negative so too is the voltage deviation.

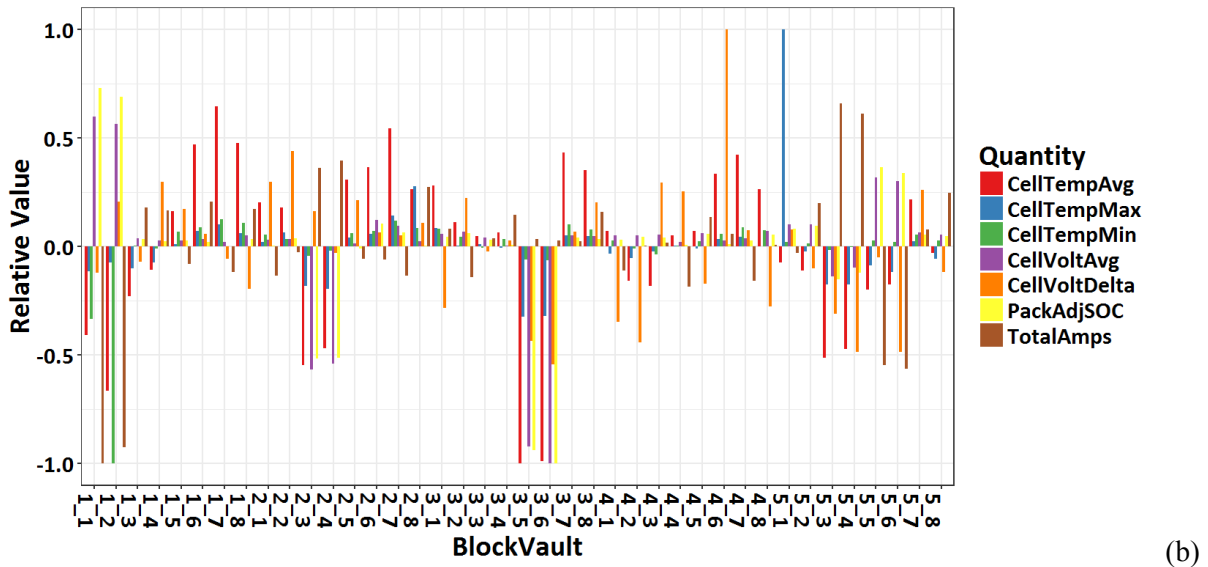
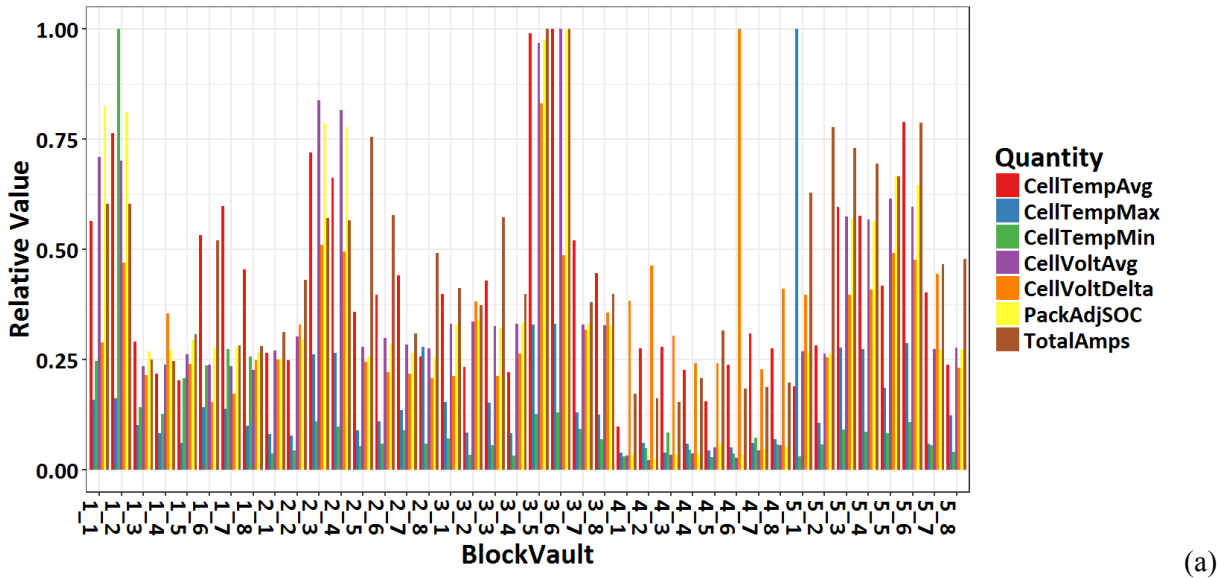


Figure 3.18. Deviations of Various Vault Parameters within Each Block (a) RMS and (b) Mean

The RMS deviation of vault SOC as a function of the deviation of vault unit cell voltage within a block for all five blocks is shown in Figure 3.19a, while Figure 3.19b shows the equivalent data for the mean of the deviations. The R^2 is 0.99 for both plots, thus showing a direct correlation between the deviation in SOC and the deviation in unit cell voltage for each vault with respect to other vaults in a block. The higher the deviation in voltage, the higher the Δ SOC. The greater the vault voltage, the greater the SOC with respect to the other vault. Note that the Δ SOC RMS normalized with respect to average SOC of 50 percent is one order of magnitude higher than Δ V normalized with respect to average voltage of 3.5V for differences between vault pairs within a rack. This may be due to the vault pairs being connected in parallel, albeit on the AC side.

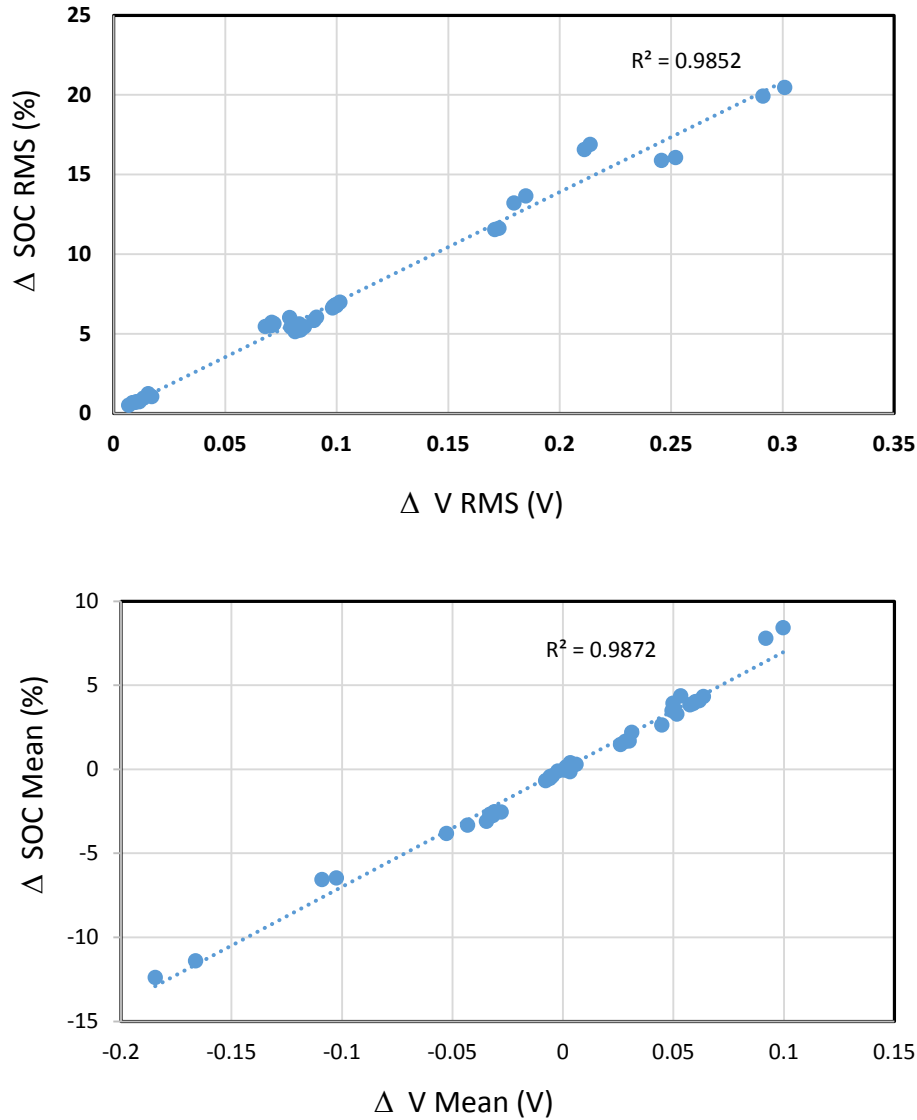


Figure 3.19. Linear Regression for Deviation of Vault SOC and Deviation of Vault Unit Cell Voltage within a Block for All Blocks (a) RMS, (b) Mean

A plot of SOC deviation versus the deviation in temperature registered an R^2 of 0.73 (Figure 3.20a). The corresponding plot using mean has a weaker correlation with respect to temperature with an R^2 of 0.20 (Figure 3.20b). As the ΔT increases, the ΔSOC also increases. This measure was registered for a constant charge rate of 1,000 kW and various C rate discharges. Discharge is exothermic, so it is possible that at a high power output level of 3,000 and 5,000 kW all vaults are hot, thus reducing the temperature difference. During charge, vaults with a lower temperature have a lower charge acceptance. Charging is endothermic, hence at 1,000 kW there may be some cooling taking place. This may lead to a lower SOC for these colder vaults at the end of charge.

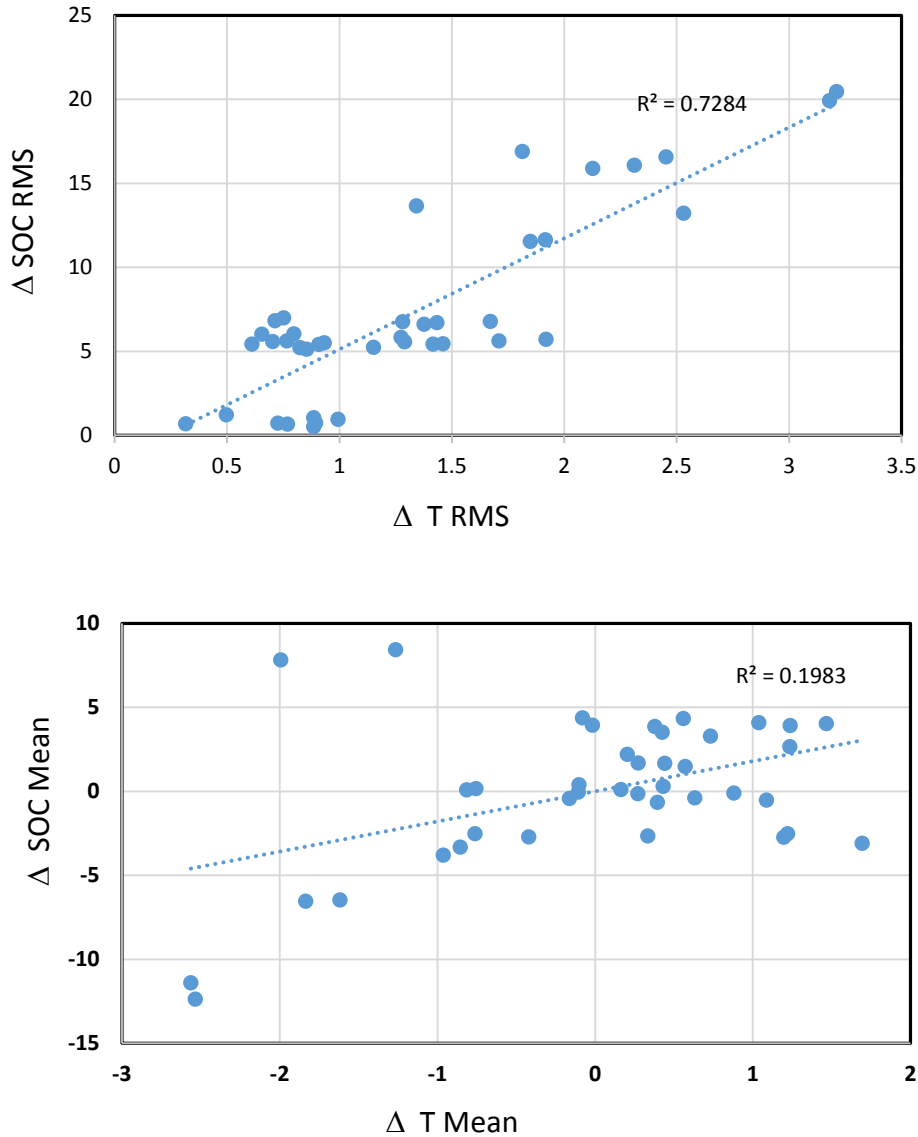


Figure 3.20. Correlation for Deviation of Vault Δ SOC as a Function of Time within a Block for All Five Blocks (a) RMS, (b) Mean

A plot of I versus T deviation showed a weak linear correlation for the RMS values with $R^2 = 0.483$ (Figure 3.21). When the plot used the mean values, the correlation disappeared, thus indicating the deviation in current did not depend on the value of the temperature. That is, high temperature differences did not necessarily imply high (or low) current differences. However, the fact that larger differences in temperature (RMS) led to larger differences in current (RMS) is still instructive, thus indicating that there is a weak correlation of these parameters, which is exaggerated when RMS is taken into account and virtually disappears when the mean is considered. This appears to indicate that high temperature differences lead to high current differences. Eventually, the SOC of the vault being subjected to high current decreases more rapidly, which lowers the current through the vault thus lowering its temperature.

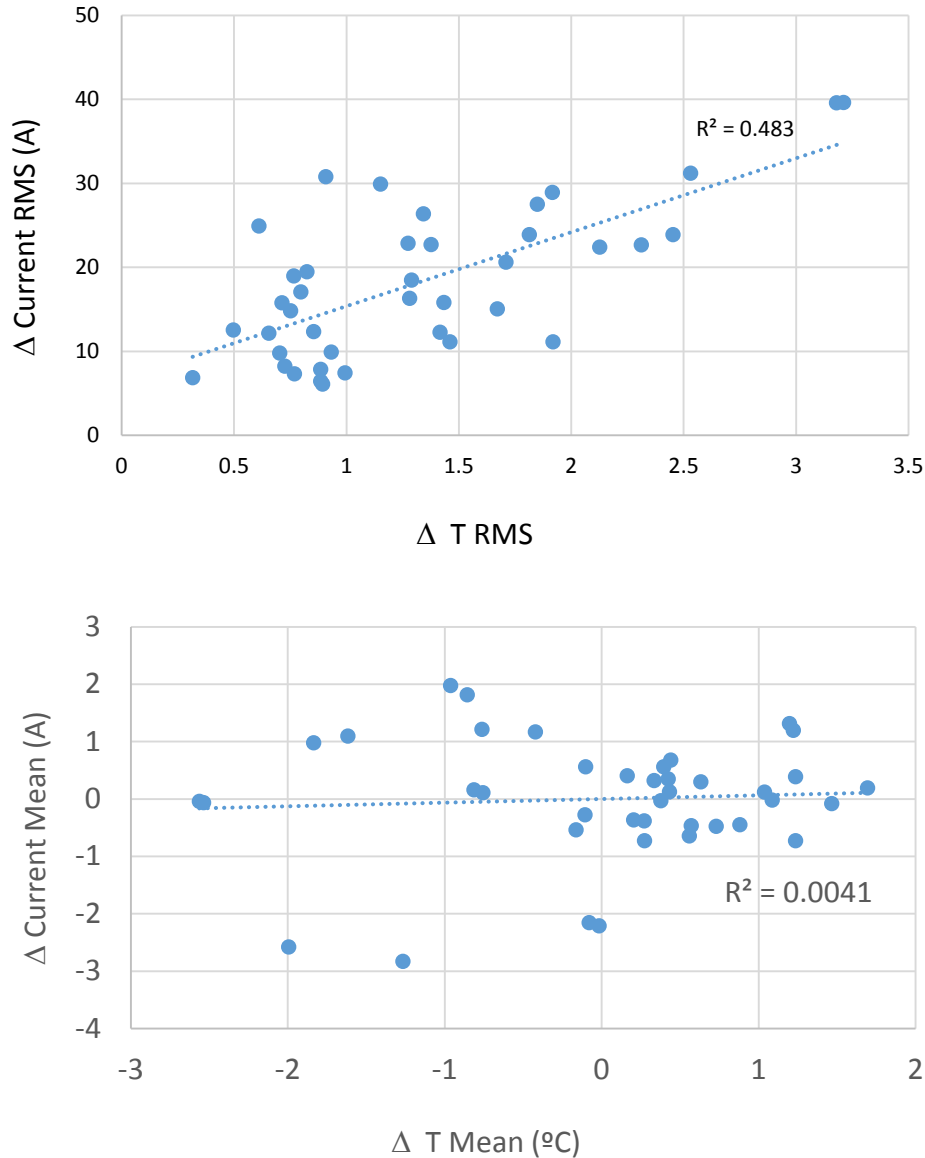


Figure 3.21. Correlation of Deviation of Vault Δ Current as a Function of Time within a Block for All Five Blocks (a) RMS, (b) Mean

The ΔI versus ΔV plot (Figure 3.22) is more correlated than ΔI versus ΔT (Figure 3.21). The plot with the mean values still exhibits poorer correlation, possibly due to the greater impact of values during rest. Similar results were obtained for SOC versus I (both RMS and mean). SOC and voltage have a negative correlation with I, which has a poor correlation with T mean. This shows that as SOC or voltage increases, current decreases. This result was expected during charge mode, but not during discharge. It appears that the trend in deviations is mainly supported by what is occurring during the 1,000 kW charge.

As shown in Figure 3.23, SOC correlates with voltage and temperature, and current (negative correlation with current mean) amperes correlates with V (negative correlation with V mean) and slightly with RMS of temperature; amperes does not correlate with T (mean).

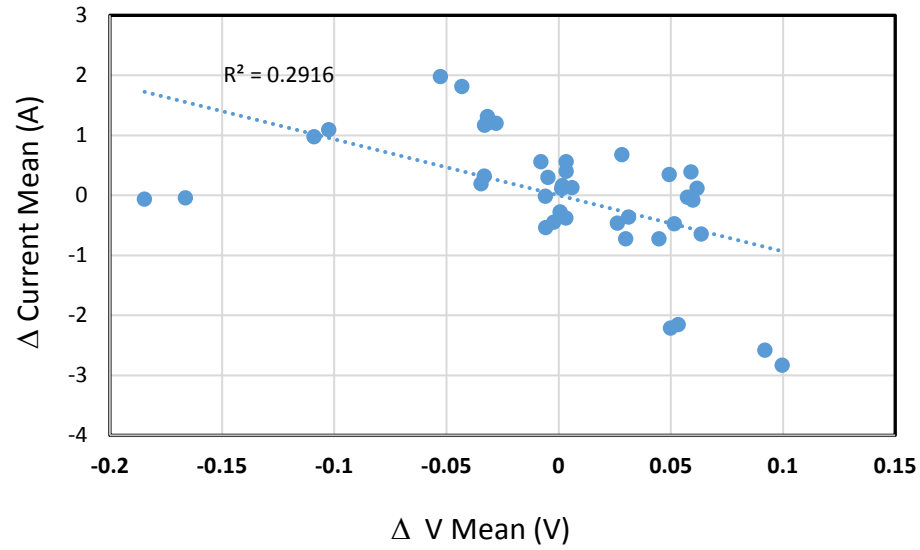
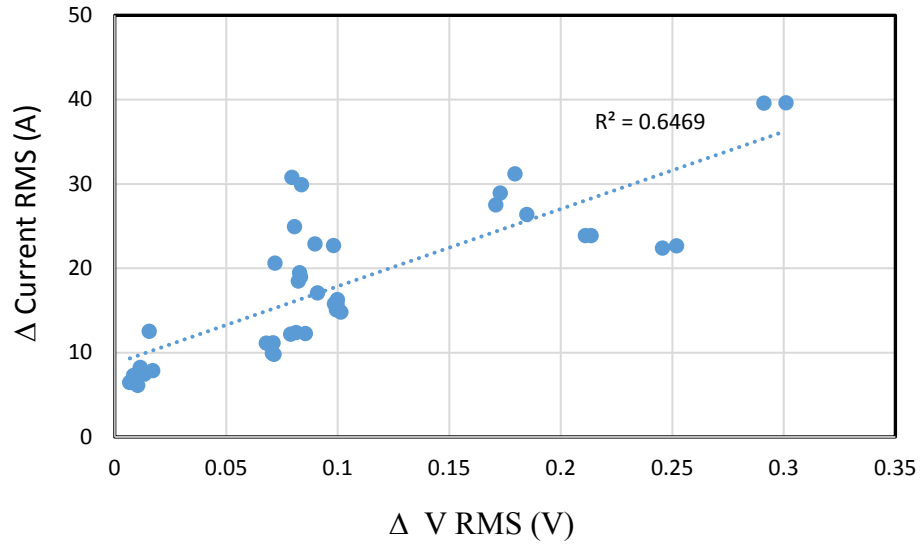


Figure 3.22. Correlation of Deviations of Current as a Function of Voltage within a Block for All Five Blocks (a) RMS, (b) Mean

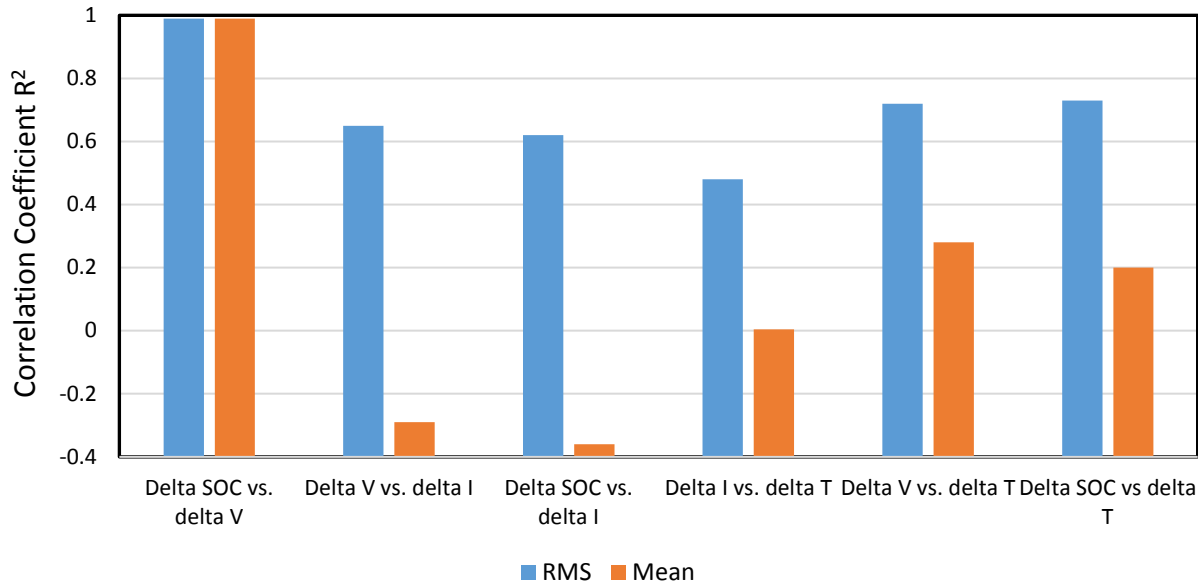


Figure 3.23. Correlation Coefficient R^2 for Various Parameter Pairs for Vaults within a Block for All Five Blocks (a) RMS, (b) Mean

3.4.4 Variation of Parameters across Blocks

Figure 3.24 shows results for deviations in vault parameters across all the blocks in the BESS. Note that the trends for deviations of vault parameters from all vaults within the BESS remained the same as the vault parameter deviations from all vaults within blocks. For example, the highest deviations are for 1-2, 3-5, and 3-6, the same as the results for deviation within a block. This indicates that all five blocks performed similarly, and hence the trends within blocks propagated when compared across all blocks. This underscores the need for maintaining uniform conditions within blocks to ensure optimum performance. Deviations for brief periods are not a cause for concern. However, if the uniformity of operating conditions is not maintained, the weak vaults (and cells within those vaults) can get weaker.

The strongest measured statistical relationship was between the deviation for SOC versus deviation in voltage, with a correlation of 0.99 for both RMS and mean. All other pairs investigated have an R^2 of 0.6 to 0.7 using RMS, while the mean R^2 was lower.

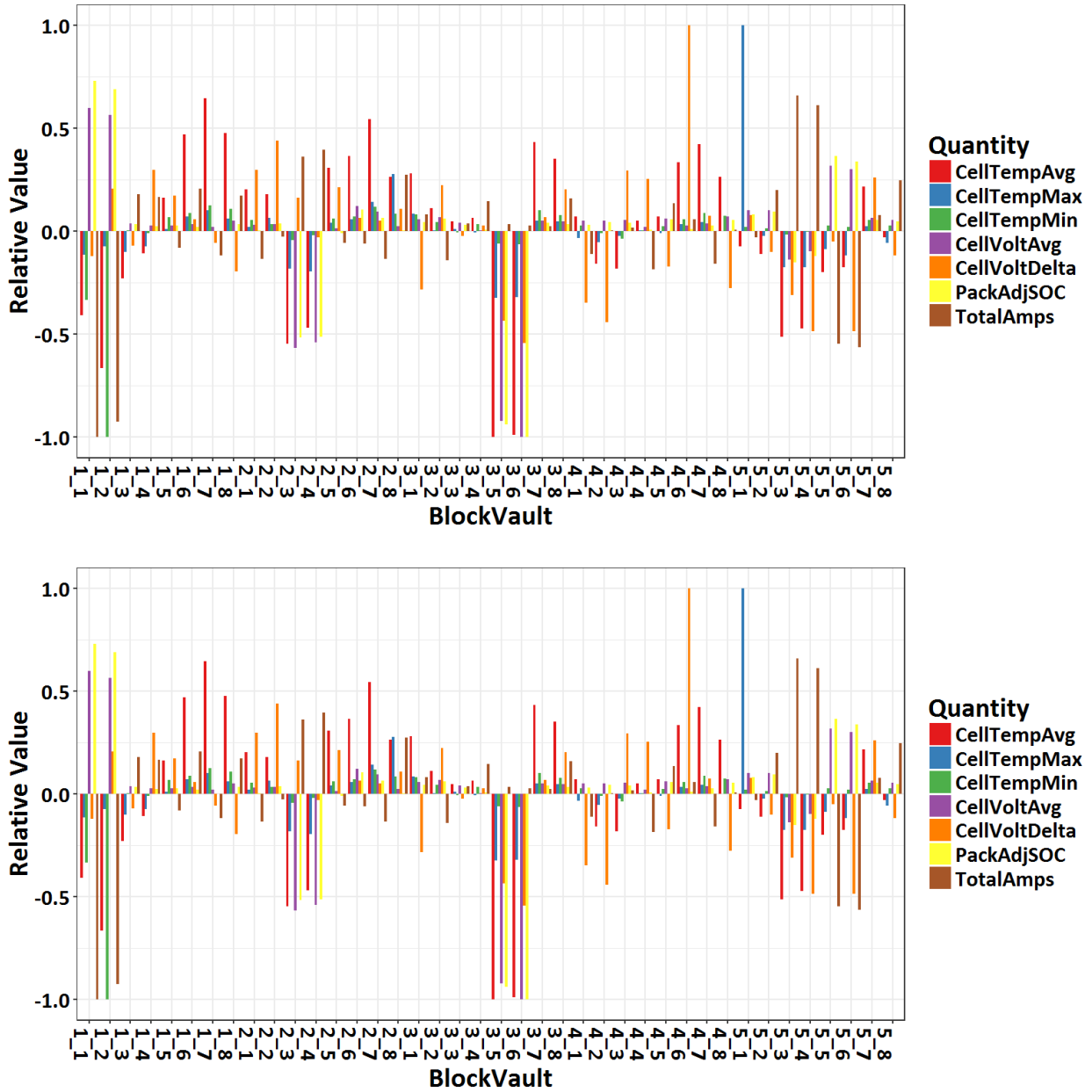


Figure 3.24. Deviation of Parameters for Vaults across all Blocks within the BESS (a) RMS, (b) Mean

Figure 3.25 shows the R^2 for ΔSOC versus ΔV and ΔV versus ΔT for deviations across all blocks. Note that the ΔSOC RMS is similar in magnitude to that for deviations of vault SOC's within a block, but is one order of magnitude higher than the corresponding value for deviations between vault pairs (Figure 3.25a).

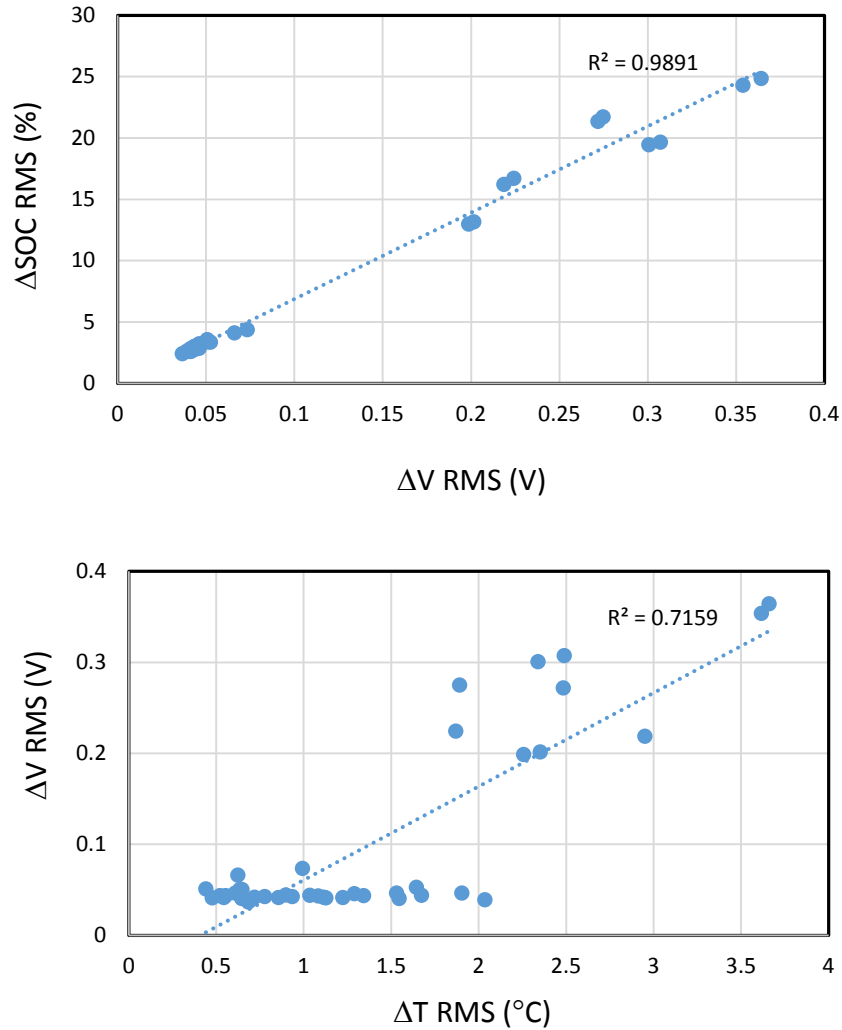


Figure 3.25. Correlation of Δ SOC versus Δ Voltage in Vaults across all Blocks (a) RMS, (b) Mean

Figure 3.26 demonstrates that the deviation over time exhibited good correlation for Δ SOC versus ΔV (both RMS and mean). The high correlation between RMS for Δ SOC (or V) and T decreases by 3X when the mean is considered. SOC (or V) has a high R^2 versus I and T when RMS is the measure. However, the correlation versus I decreases significantly when mean is the measure. This shows that as expected, higher differences in current should lead to higher differences in SOC, whereas the temperature differences do not lead to as high an SOC difference. This is also supported by the extremely low R^2 for ΔI versus ΔT . The negative correlation for SOC as a function of V versus I within blocks was also found when deviations across all blocks was considered. Note that except for SOC versus V, the R^2 for the mean of the deviation was lower than R^2 for RMS of deviations.

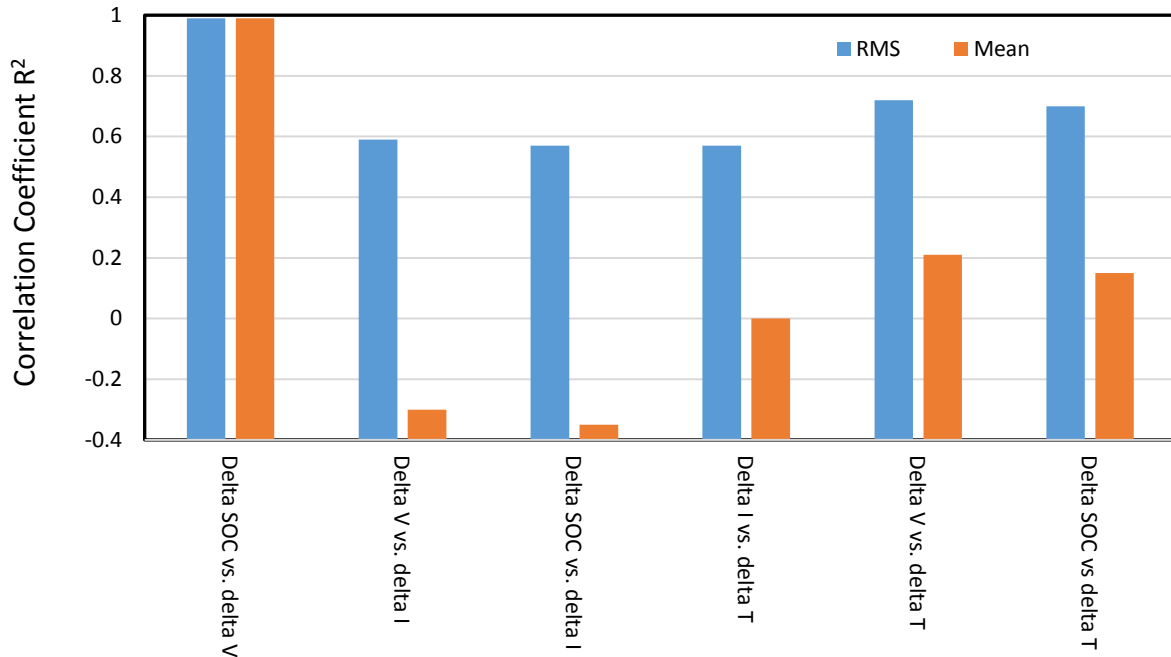


Figure 3.26. Correlation Coefficient for Deviation of Various Parameter Pairs across all Blocks

Table 3.5 shows the R^2 of the standard deviation for the various variables pairs within a rack, block, and across blocks, for both the mean and RMS values. Figure 3.27 graphically presents the same data. For the rack case, the values are simply R^2 for the RMS of the difference between vault pairs in the rack.

When considering RMS, the correlation coefficient R^2 between Δ SOC and Δ V is the highest. R^2 for Δ V versus Δ I, Δ SOC versus Δ I, and Δ I versus Δ T are also high. For the rack, Δ V versus Δ T and Δ SOC versus Δ T do not have a high correlation. In contrast, for the blocks and across blocks, Δ V versus Δ T and Δ SOC versus Δ T correlation is higher than the Δ V versus Δ I and Δ SOC versus Δ I correlation. As expected, Δ SOC and Δ V, due to their very high correlation, behave similarly with other variables.

When considering the mean, the R^2 for Δ SOC versus Δ V is still close to 1. The R^2 for other pairs decrease. The Δ V versus Δ I, Δ SOC versus Δ I R^2 is now greater than the Δ V versus Δ T, Δ SOC versus Δ T R^2 values. The correlation for Δ I versus Δ T totally breaks down for the mean case. The reason is the direction of change in current is the same, regardless of the sign of the temperature; hence, the correlation breaks down. However, temperature does effect the magnitude of the current through each vault, as seen from the high correlation for the RMS case.

Table 3.5. Correlation Coefficient R^2 for Deviations of Various Parameter Pairs for Vaults within Rack, Block, and across All Blocks

Parameter	R^2 Vaults Δ within Pair	R^2 Vaults Dev. within Block		R^2 Vaults Δ within Pair	
		RMS Dev. within Block	Mean. Dev. within Block	RMS across Block	Mean Across Blocks
Δ SOC vs. Δ V	0.89	0.99	0.99	0.99	0.99
Δ V vs. Δ I	0.65	0.65	-0.29	0.59	-0.3
Δ SOC vs. Δ I	0.59	0.62	-0.36	0.57	-0.35

Parameter	R ² Vaults Δ within Pair	R ² Vaults Dev. within Block		R ² Vaults Δ within Pair	
		RMS Dev. within Block	Mean. Dev. within Block	RMS across Block	Mean Across Blocks
ΔI vs. ΔT	0.53	0.48	0.004	0.57	0.0007
ΔV vs. T	0.19	0.72	0.28	0.72	0.21
ΔSOC vs. ΔT	0.12	0.73	0.20	0.7	0.15

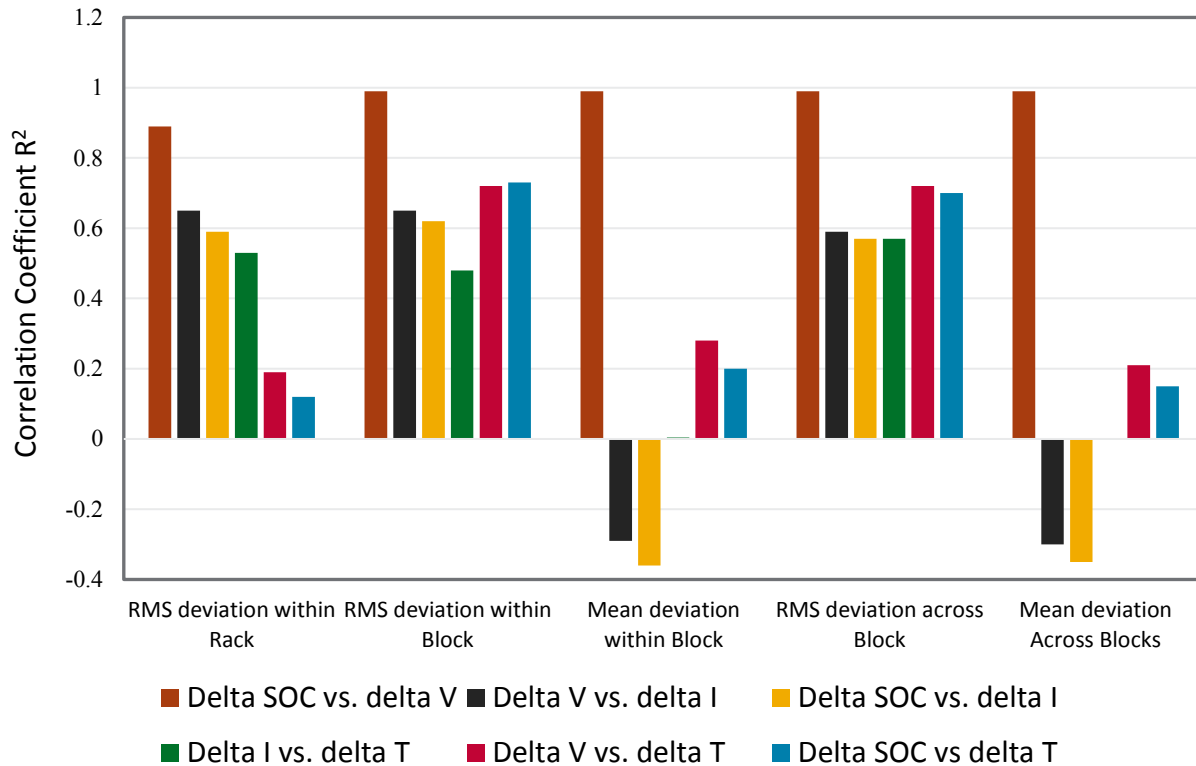


Figure 3.27. Correlation Coefficient R² for Deviations of Various Parameter Pairs for Vaults within Racks, Blocks, and across all Blocks

3.4.5 Charge at Various Rates

Figure 3.28 presents the difference between the power flow at the 15 kV line and the sum of the low voltage meters for Blocks 1–5. The difference is very small, and reflects the transformer losses, which amount to <0.2 percent of the power flowing through the BESS.

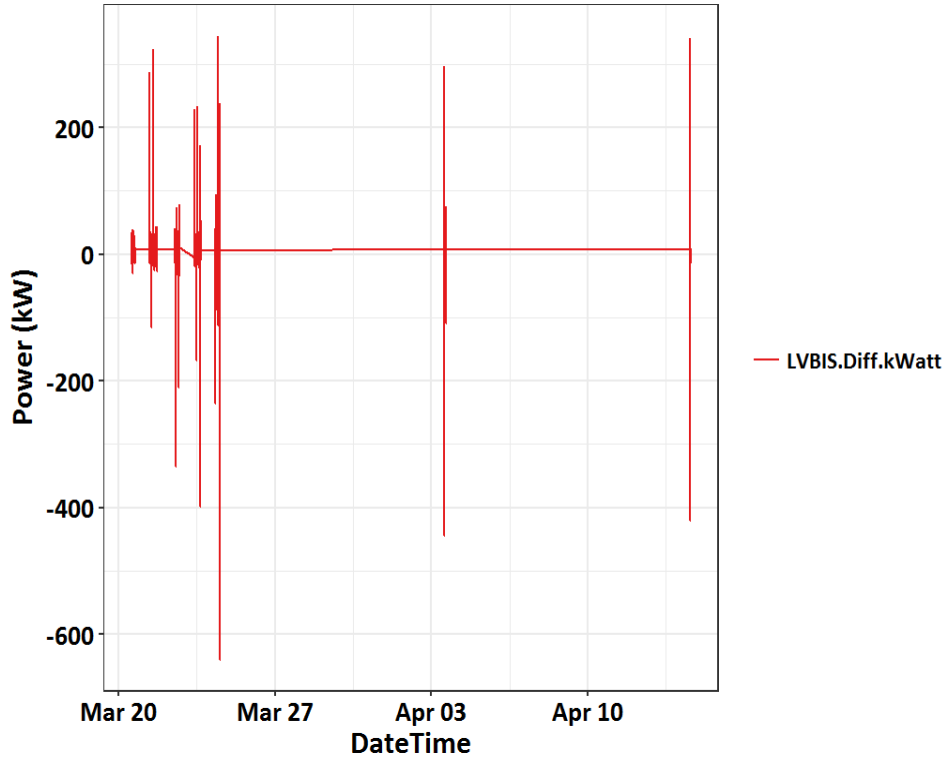


Figure 3.28. Difference between Power at the 12.47 kV and 430 V AC Level during Charge at Various Rates

Within each block, the maximum, minimum, and average cell temperatures were recorded, along with the difference between maximum and minimum cell temperature. The average cell voltage, difference between maximum and minimum cell voltage, current flow, and average SOC were all recorded. Under normal operation with all inverters working properly, the current through each vault is nearly equal. For each vault pair, the median current difference is <0.04 amperes, except during the start of charge or discharge when the difference shoots up to nearly 10 amperes. The average SOC for all vaults fall within a tight range. The difference between maximum and minimum cell voltage in each vault is in the 0.01V to 0.06V range, except at the start of charge or discharge when it spikes at 0.08 V to 0.15 V. Table 3.6 summarizes these observations for Block 1. Similar observations were made for the other blocks. Table 3.7 shows the results for the capacity test using variable-rate charging.

Table 3.6. Parameter Values for Vaults in Block 1 during Variable-Rate Charge Testing

Components	Parameter	Range at Max T		Range at Mid T		Range at Min T	
		Low T, °C	High T, °C	Low T, °C	High T, °C	Low T, °C	High T, °C
All 8 vaults in Block 1	Cell T Max	33	38	27	33	26	30
All 8 vaults in Block 1	Cell T Min	23	32	18	27	17	25
All 8 vaults in Block 1	Cell T Avg.	32	36	26	29	23.5	28
All 8 vaults in Block 1	Cell T Diff.	Vaults 1 and 2 had highest ΔT – 8-12°C range. The others were in the 2°-9° C range.					
All 8 vaults in Block 1	Cell V Δ	Delta V is 0.01 to 0.06V - except at start of charge or discharge when it shoots up to 0.08 to 0.15V.					
All 8 vaults in Block 1	Adj. SOC	Pretty tight range within 1 percent.					
All 8 vaults in Block 1	Current Diff. for Vault Pairs	0.08 A median. Very tight distribution, except during start of charge or discharge when the difference is as high as 10 to 30 A.					

Table 3.7. Parameter Values Results for 1 MW Discharge and Variable-Rate Charge

Cycle #	Charge Power (kW)	Discharge Power (kW)	Charge Energy (kWh)	Discharge Energy (kWh)	RTE	Cum RTE	Notes
1	593	1,010	882				All inverters working
2	597	1,006	897				All inverters working
3	591	1,010	899				All inverters working
1	1,088	1,022	947	738	0.78		Three inverters not working during discharge – 1A, 2D, 3D
2	1,085	1,011	892	754	0.85		
3	1,089	1,011	991	789	0.80	0.81	3 rd cycle started the next morning. Thus, it as a cold start. 3D and 1A inverters were down during discharge; high temperature possibly resulted in better performance
1	3,034	1,010	944	767	0.81		3D and 1A not working
2	3,094	1,016	936	726	0.78		3D and 5B not working
3	3,085	1,016	986	770	0.78	0.79	3 rd cycle started after next morning. Thus, it was a cold start. All inverters working
1	5,023	1,016	999	785	0.79		5C and 5A not working during discharge
2	4767	1,014	953	766	0.80	0.80	5B not working

The charge and discharge energy as a function of power are shown in Figure 3.29. The discharge energy for Cycle 2 is less than for Cycle 1 when charging at 3,000 kW and 5,000 kW. For 3000 kW discharge, Vaults 5-1 and 5-2 went into power-limiting mode during discharge. Inverters for Racks 5b and 5c were down at the beginning of Cycle 1. It is not clear if this situation persisted throughout the 5,090 kW charge testing.

For Cycle 3, the discharge energy is lowest at a 500 kW charge. The charge energy trend is clearer. As charge power increases, Cycle 2 charge energy decreases compared to Cycle 1 for charge powers in the 1,000–5,000 kW range. For Cycle 3, the charge energy is highest for the 1,000 and 3,000 kW charges. Due to these counteracting forces, the RTE is highest for the 500 kW charge at 86 percent, while the RTE for the 1,000, 3,000, and 5,000 kW charges is 79–81 percent. This shows that for various charge levels, the highest RTE is obtained at 500 kW, or C/2.5 rate charge. This is in line with what is known for lithium-ion batteries—the charge efficiency is most efficient around the C/2 rate. Higher charge rates lead to lower efficiencies.

For clarity, the average discharge and charge energy for each charge rate is plotted in Figure 3.30. The charge energy increases with charge power as expected due to the higher operating voltage. At high charge powers, the charge may be terminated before the actual Ah-related target SOC is reached, if the BMS measures SOC using cell operating voltage, where Ah stands for ampere-hours. This leads to a lower energy content in the BESS at the end of charge. Hence, the discharge energy decreases when preceded by charging at increasing power levels. However, the discharge energy following a 5,000 kW charge was higher than the energy following all other charge power levels. This could be because the BESS temperature was high after a 4C rate charge. Even after a one hour rest, the BESS temperature remained high, and resulted in a high discharge energy. Lithium-ion batteries are endothermic during charge and exothermic during discharge. At a 2.4C rate charge (3,000 kW), the reversible heat (endotherm) has a greater impact, thus resulting in less of a temperature rise. At a 4C rate charge, the temperature rise likely dominates the subsequent discharge rate performance.

Figure 3.31 shows the average temperature during charge and discharge for each charge power level. Due to the temperature effect and other reasons previously described, RTE is at its minimum at 3,000 kW and increases slightly at a 5,000 kW charge.

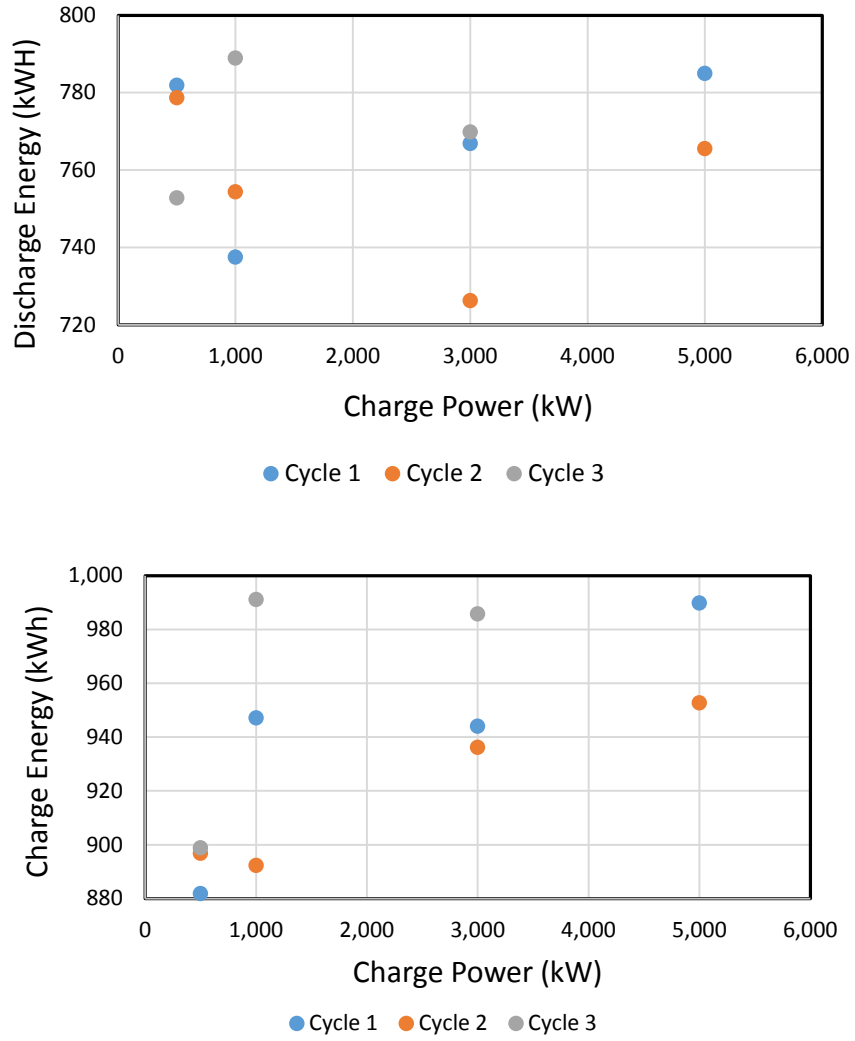


Figure 3.29. Discharge (a) and Charge (b) Energy for Various Charge Powers and 1,000 kW Discharge

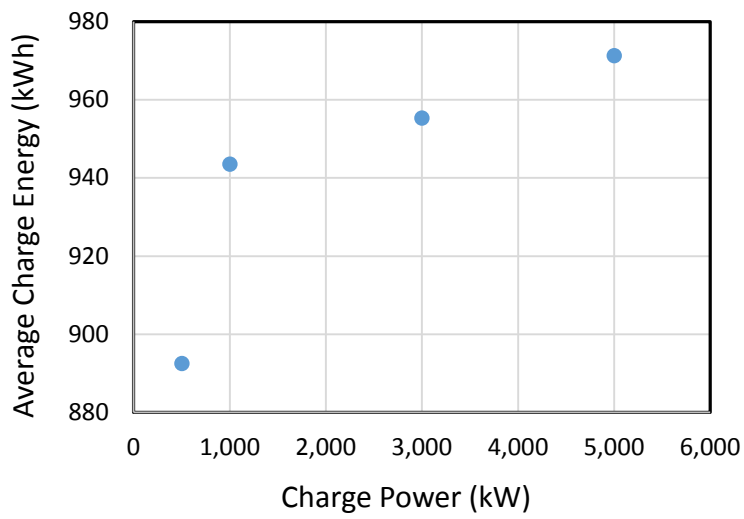
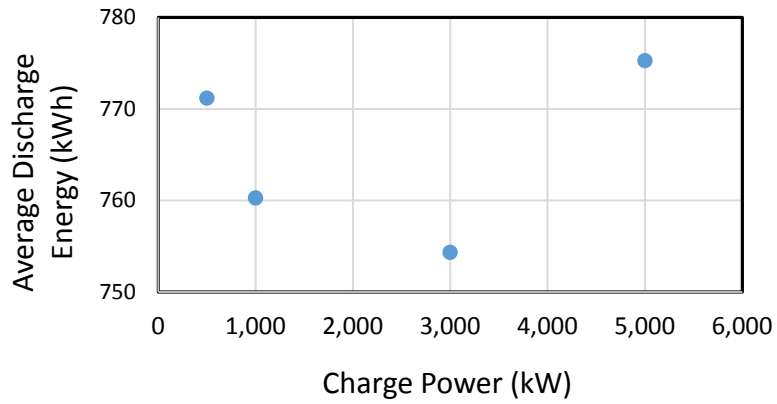


Figure 3.30. Average Discharge (a) and Charge Energy (b) as a Function of Charge Power

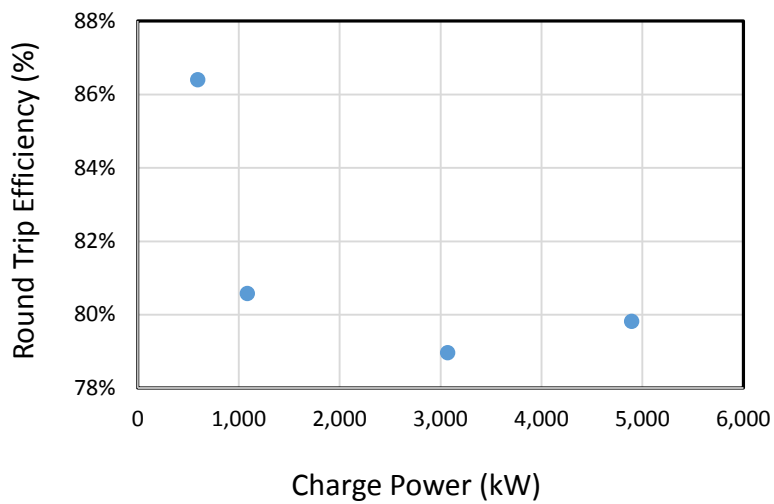


Figure 3.31. Cumulative RTE for Various Charge Powers and Discharge at 1,000 kW

The available energy for various charge powers and a 1,000 kW discharge level as a function of order in which the experiments were performed are shown in Table 3.8 and Table 3.9. At 3,000 kW and 5,000 kW charge rates, the discharge and charge energy decrease from Cycle 1 to Cycle 2. Both discharge (Figure 3.32) and charge energy (Figure 3.33) increase for Cycle 3 at a 3,000 kW charge rate. The charge energy increases very slightly with cycle number at 500 kW, while discharge energy decreases with cycle number, leading to a decrease in RTE with cycle number. At a 1,000 kW charge and discharge, the discharge energy increases with cycle number while the charge energy troughs at Cycle 2. No specific trend exists in terms of performance with respect to the order of experiments.

Table 3.8. Discharge Energy Obtained at Various Charge Power Levels with Order of Experiment Shown

Order	500 kW	1,000 kW	3,000 kW	5,000 kW
1	737	738	757	724
2	731	754	796	772
3	717	789	784	

Table 3.9. Charge Energy Obtained at Various Charge Power Levels with Order of Experiment Shown

Order	500 kW	1,000 kW	3,000 kW	5,000 kW
1	882	947	944	990
2	897	892	936	953
3	899	991	986	

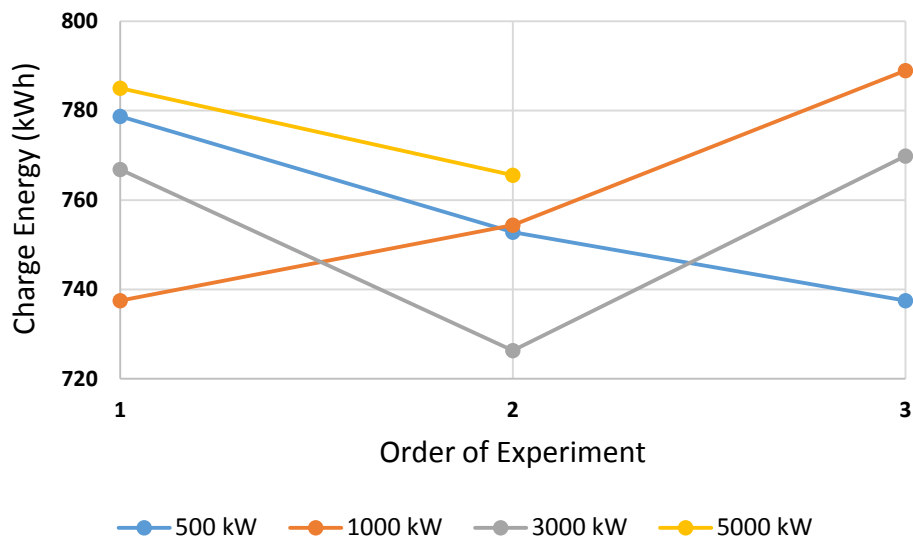


Figure 3.32. Effect of Order of Experiment on BESS Discharge Energy for Discharge at 1,000 kW and Various Rates of Charge

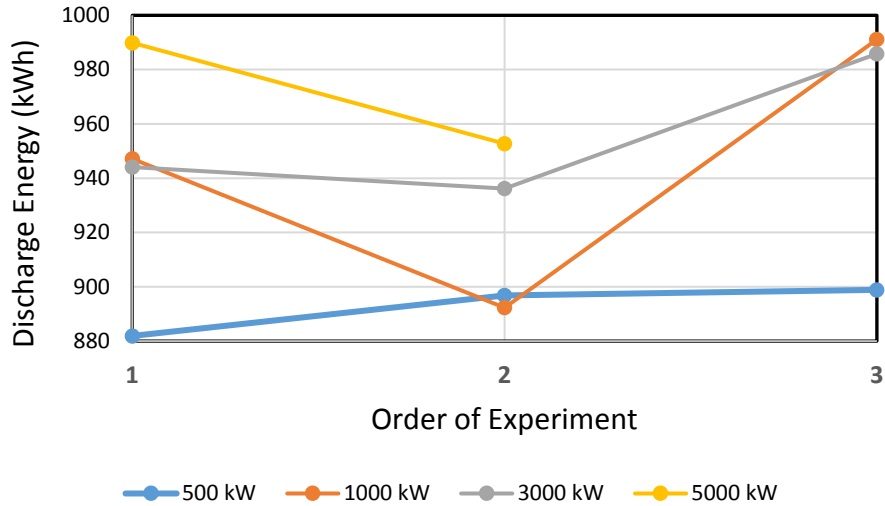


Figure 3.33. Effect of Order of Experiment in BESS Performance for 1,000 kW Charge and Various Rate Charge

The standard deviation for testing at various charge levels across a range of times for SOC, temperature, and voltage for vaults with respect to all the vaults in the BESS and to vaults within the block are shown in Figure 3.34. The temperature of the vaults were within two degrees of each other 68 percent of the time. The SOC standard deviation is 9 percent, while the voltage standard deviation is 0.12 V. For vaults within Block 5, the SOC standard deviation is quite high, at 20 percent, while the voltage deviation is around 0.275 V. This block also exhibits a higher standard deviation for temperature compared to other blocks, and dominates the overall standard deviation values. It should be noted that at the start of the test, inverters 5b and 5c were down during the initial discharge to 20 percent prior to starting cycling. Also, during the 1 MW discharge after the second charge at 3 MW, Banks 5-1 and 5-2 went into power-limiting mode.

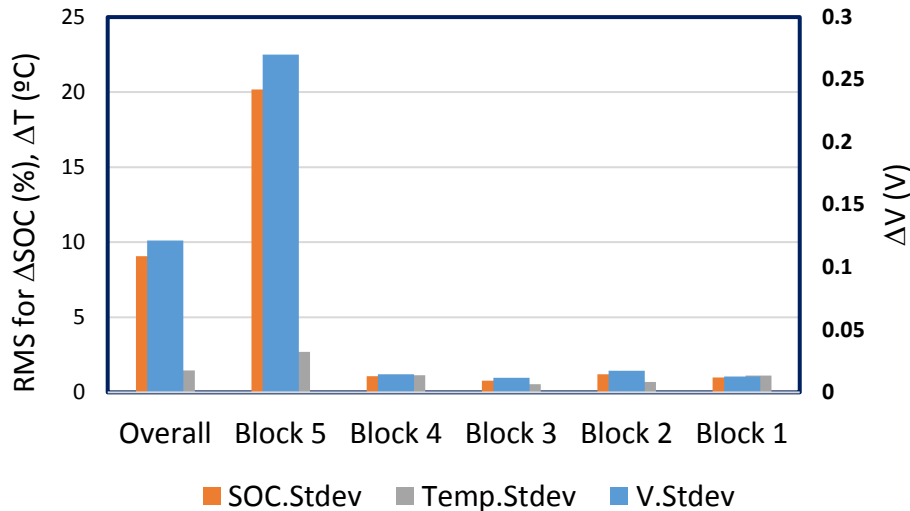


Figure 3.34. Standard Deviation for SOC, Temperature, and Voltage for Vaults within the BESS for Testing at Various Charge Powers

The 9 percent Δ SOC corresponds to 18 percent of the average BESS SOC, while the 0.12 V deviation corresponds to 3.5 percent of the average voltage per cell of 3.5V, and the Δ T of 1.5°C to 3.6 percent of the average temperature of 40°C. Plotting the Δ SOC versus Δ V gives a very linear line with an R^2 of 1.0, thus showing the vaults in the BESS perform in a uniform manner.

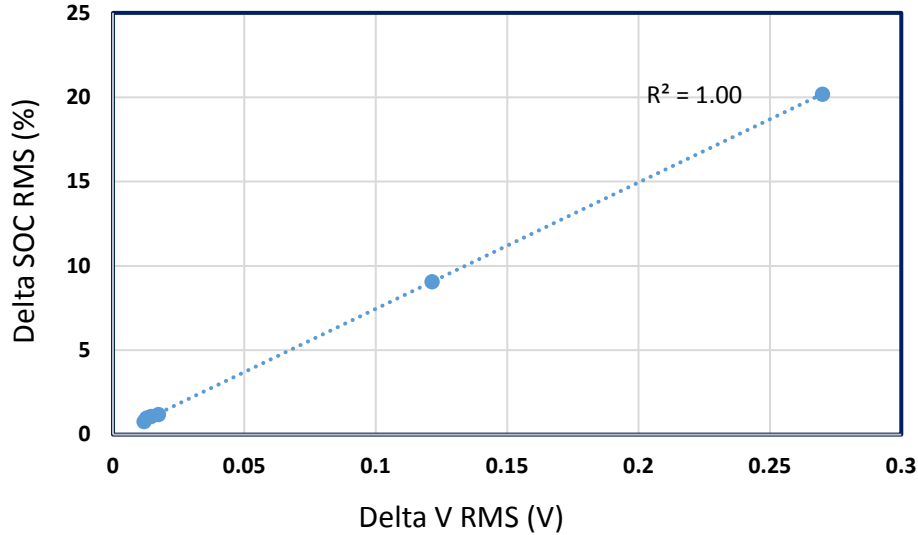


Figure 3.35. Standard Deviation of SOC versus Voltage for all BESS Vaults

3.4.6 Variation of Parameters within a Rack

The next level of analysis involves comparing vault pairs in each rack. The difference in the vault pair values of various parameters measured were computed as a function of time. The RMS value of this difference across the time range was plotted for each parameter, normalized with respect to the higher RMS value, for all vaults in the BESS (Figure 3.36).

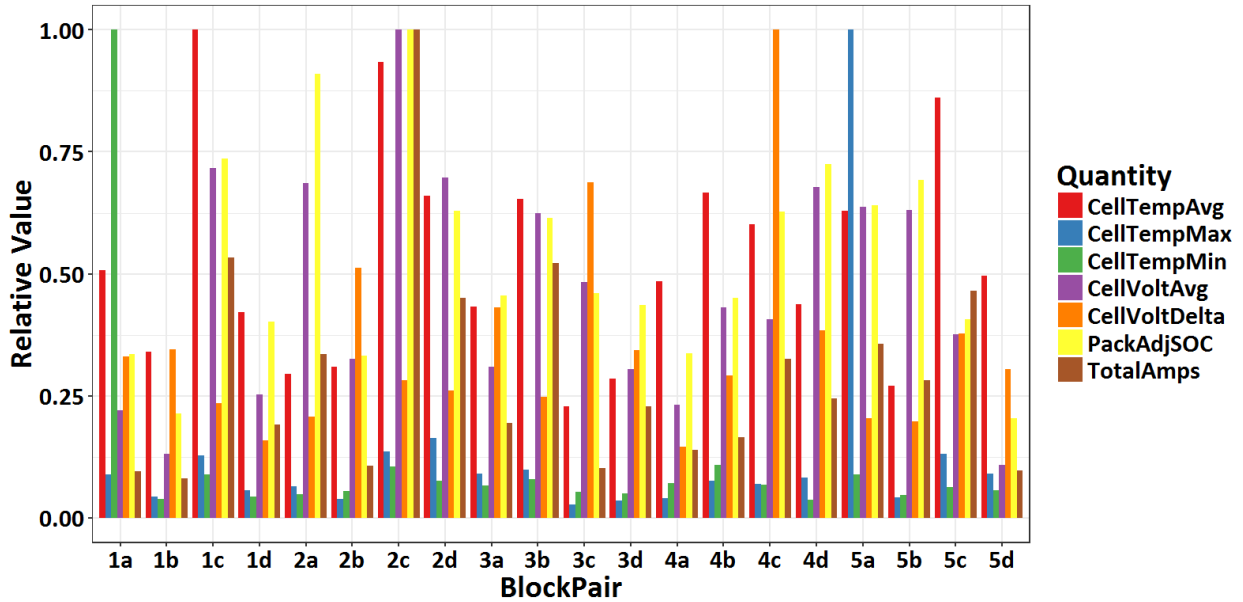


Figure 3.36. RMS of Difference between Vault Pair Values across the Time Range Normalized with Respect to Largest RMS Value for Various Charge Power Levels

The largest SOC difference occurs for Rack 5c, which also has the largest differences for average temperature, average voltage, and average current. Plotting the Δ SOC as the deviations in temperature, voltage, and current shows a linear relationship for deviation in voltage with an R^2 of 0.84, while the corresponding fits for amperes and temperature have R^2 of 0.20 and 0.46, respectively (Figure 3.37). This indicated that the operating voltage played a bigger role in driving SOC differences than current and temperature. A possible reason is that over a period of time the differences in current may cancel each other out, as low current in one vault may be followed by high current in the same vault as compared to its partner in the pair. It may be more instructive to plot the magnitude of the differences in current to verify this is indeed happening. When one vault has higher current, its temperature also rises. But the voltage may rise faster due to increase in SOC and higher polarization. As voltage and SOC increases, this could reduce current flow through this vault, thus directing more current through the other vault. The SOC, on the other hand, moves in line with the vault voltage.

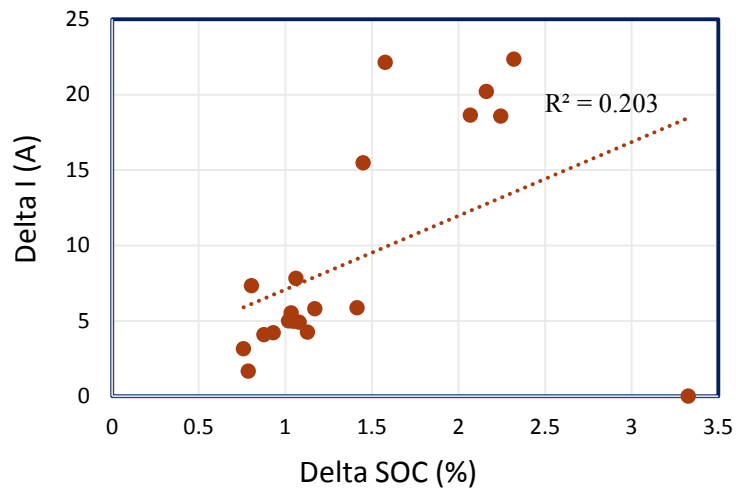
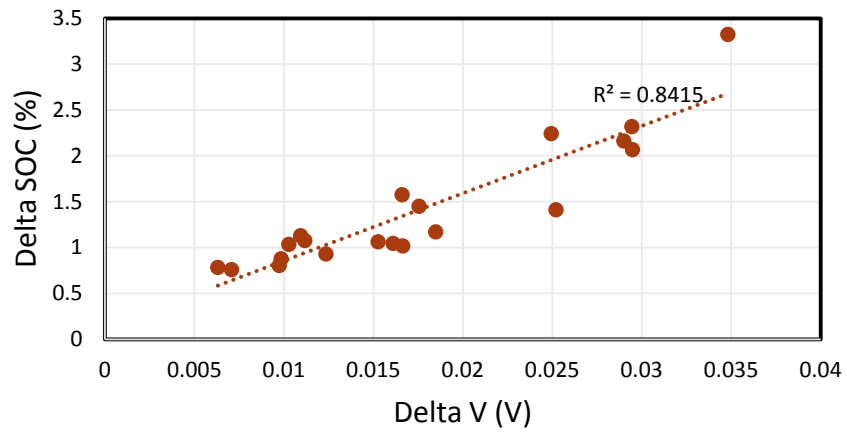
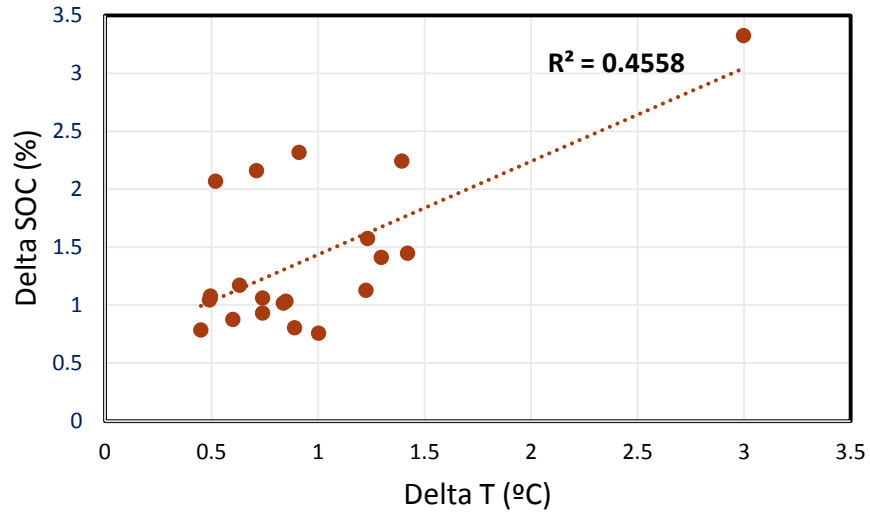


Figure 3.37. Linear Fit for SOC Deviation versus Voltage Deviation for Vault Pairs Compared to Other Pairs in the BESS

The median of the difference in current and the RMS of the difference in current between vault pairs are plotted in Figure 3.38. The high RMS correlates with a high bias (median value is high) as seen for vaults in Rack 2c, which is the same as during discharge. The positive value of the median means that during discharge, the current is higher in one vault, while during charge, the current is higher in the other vault in the rack pair. This is because the sign for charge current is different than the sign for discharge current. Also, the RMS is one order of magnitude higher than the median values. This is due to the high effect of the data points during the transition from zero current to charge or discharge, where there are spikes observed.

By taking the absolute value of the current, the confusion related to the sign of current affecting the interpretation of results can be removed. As seen from Figure 3.38, which presents the RMS of difference of various parameters within vaults in a rack, the RMS for Rack 2c is high for voltage, SOC, and current. Unlike during discharge, the RMS for Rack 2c for temperature is not high, possibly due to endothermicity of the charging reaction. Hence, the high median current difference for 2c is tied to the high RMS of the difference of cell temperature, voltage, SOC, and current between vaults in a rack. While RMS values for 1b, 2a, 4c, 4d, and 5a are high for current, this is not reflected in a high median value. An examination of Figure 3.38 for RMS values of various parameters for vaults within racks show high RMS values for 1b, 2a, 4c, and 5c for temperature, voltage, and SOC. These results demonstrate the effect of high current deviation on these parameters.

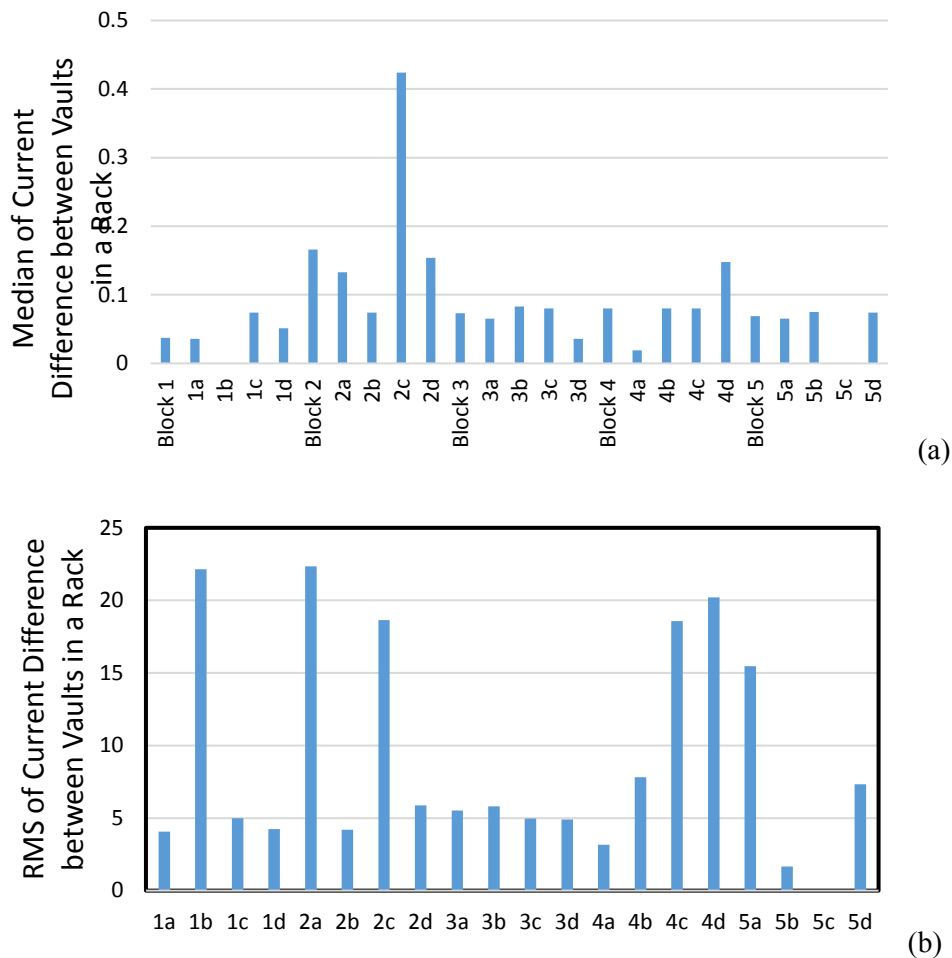


Figure 3.38. Correlation between the Median (a) and RMS (b) of Current Difference between Vaults in a Rack

3.4.7 Variation within a Block

Parameters for each vault were also compared with the remaining vaults in the same block (Figure 3.39). Figure 3.39a shows the RMS value of the difference, while Figure 3.39b shows the mean of the difference across the time investigated. One point that stands out is the voltage and SOC deviation are highly correlated, as was found for vault pairs within racks. For Vaults 5-5 and 5-6, all parameters deviate significantly. This could give insight into whether this particular inverter (5C) was not working for some of the time during testing. Note that inverters 5B and 5C were down at the start of the 500 kW charge testing. Vaults 5-1 and 5-2 also had high RMS values. During the second discharge, Vaults 5-1 and 5-2 went into power-limiting mode. The SOC and voltage for these vaults has a positive deviation, while the temperature and current have a negative deviation. This indicates that both SOC and voltage are negatively correlated with temperature and current, while for the multiple rate discharge runs the SOC and voltage were positively correlated with temperature.

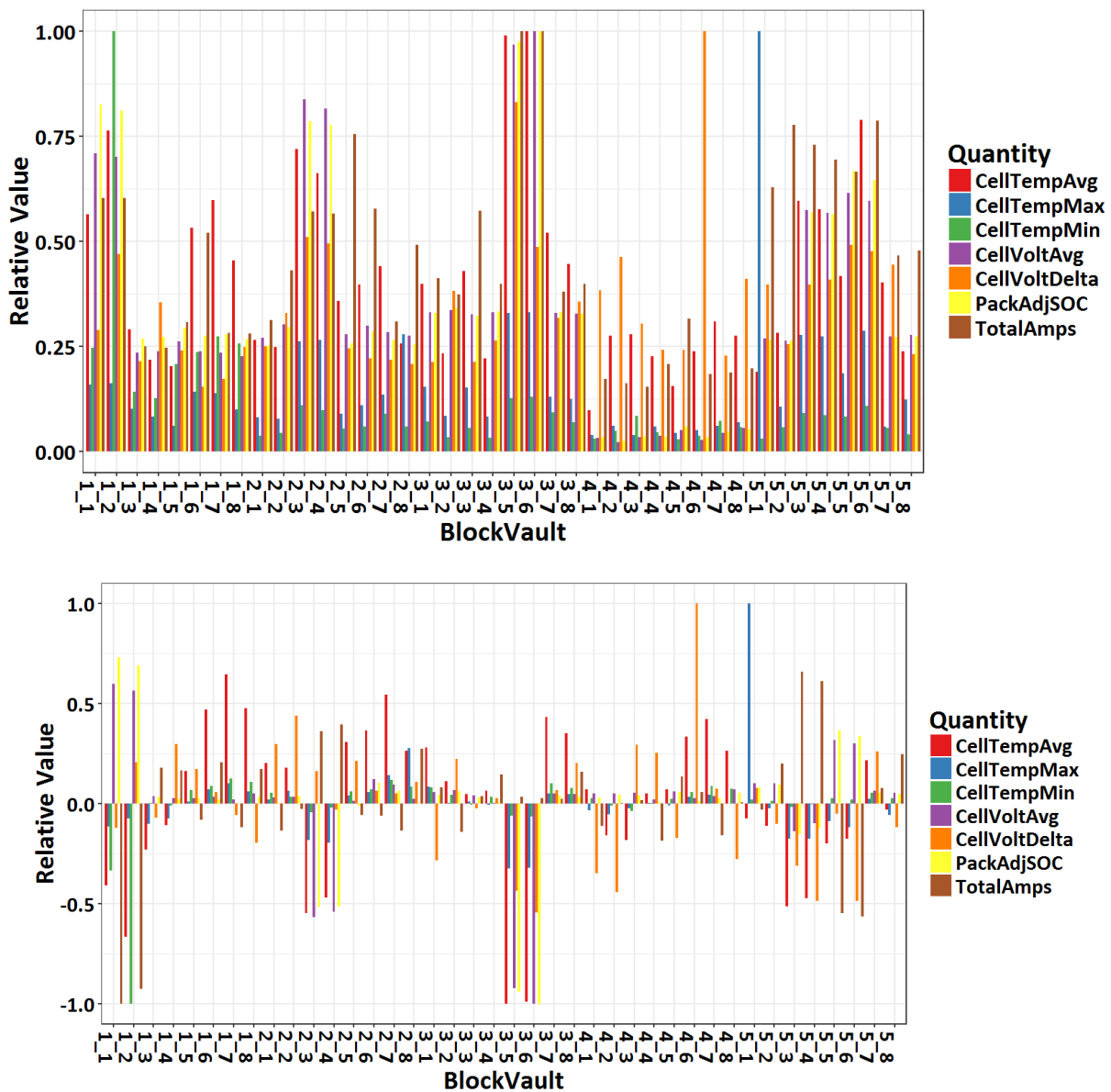


Figure 3.39. Deviation of Parameters for Vaults within Each Block

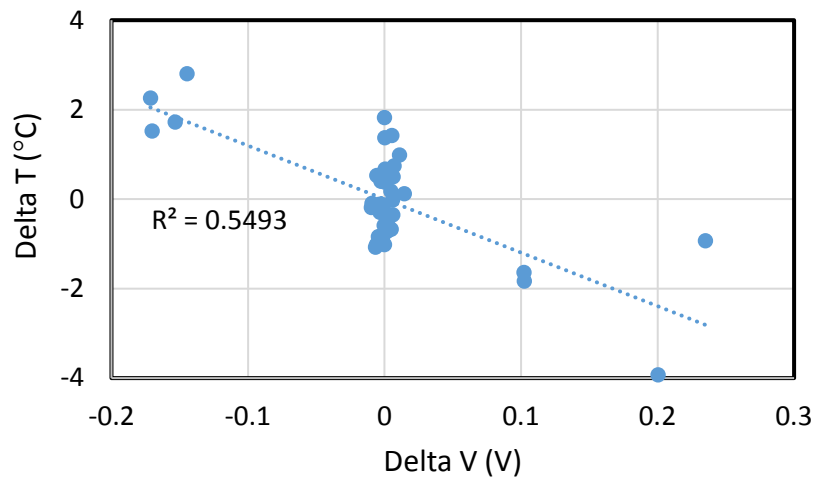
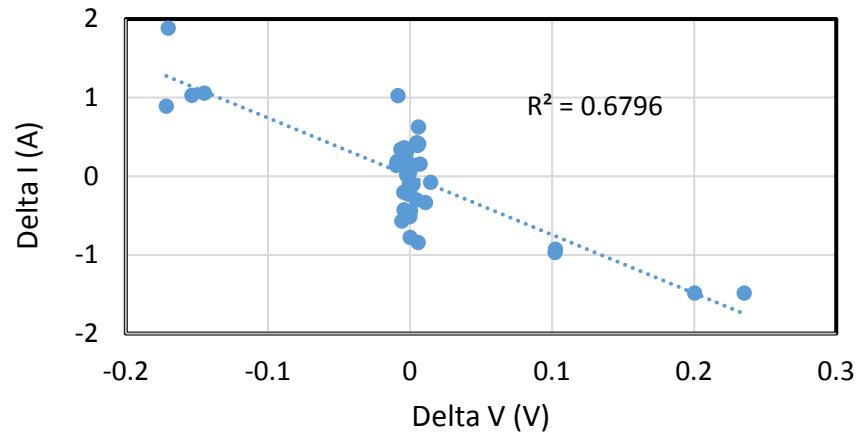
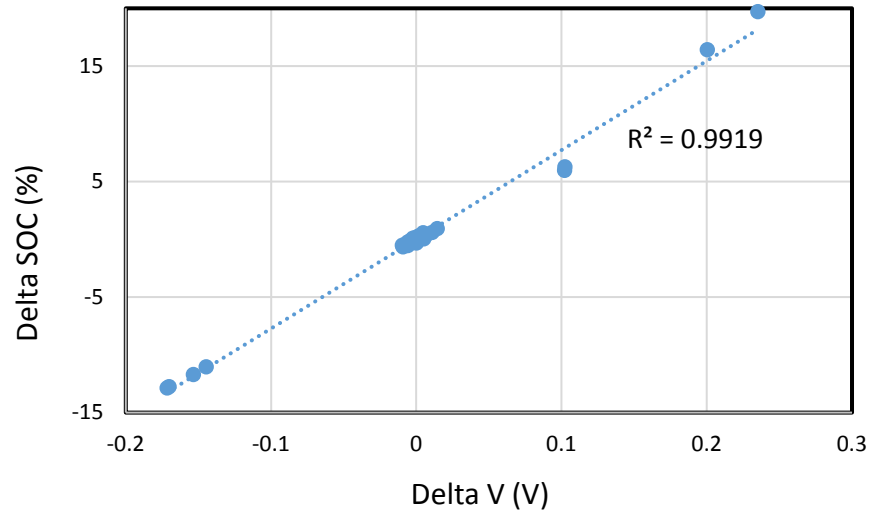


Figure 3.40. Correlation for Various Deviation Pairs within Each Block

3.4.8 Deviation Across all Blocks in the BESS

The trends for deviation of vault parameters within blocks remained the same when the vault parameter deviation from all vaults within the BESS was determined. This indicates that all five blocks performed similarly, and hence the trends within blocks propagated when compared across all blocks (Figure 3.41).

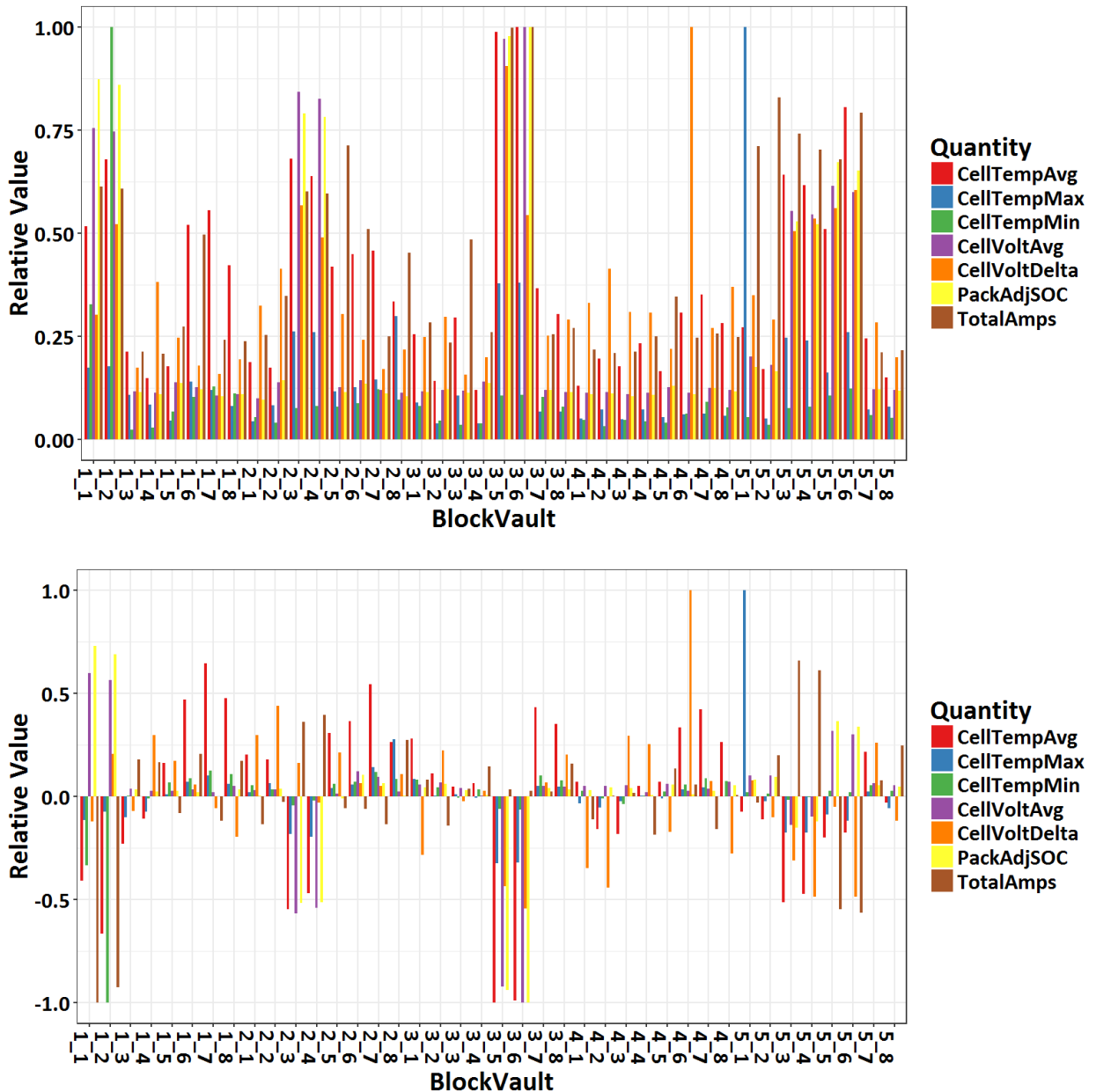


Figure 3.41. Deviation of Parameters for Vaults across All Blocks

The deviation of SOC follows a similar relationship with voltage as observed earlier, but the R^2 was 0.99, which is extremely high. The SOC versus I relationship was the same as observed earlier, with a negative correlation with respect to deviation in I mean. A similar relationship was found for voltage versus I mean. Similar to the last test, SOC and voltage have a negative correlation with respect to I mean. The

SOC and voltage had a negative correlation with respect to T mean, unlike the previous weak correlation with T mean. Figure 3.42 presents these results.

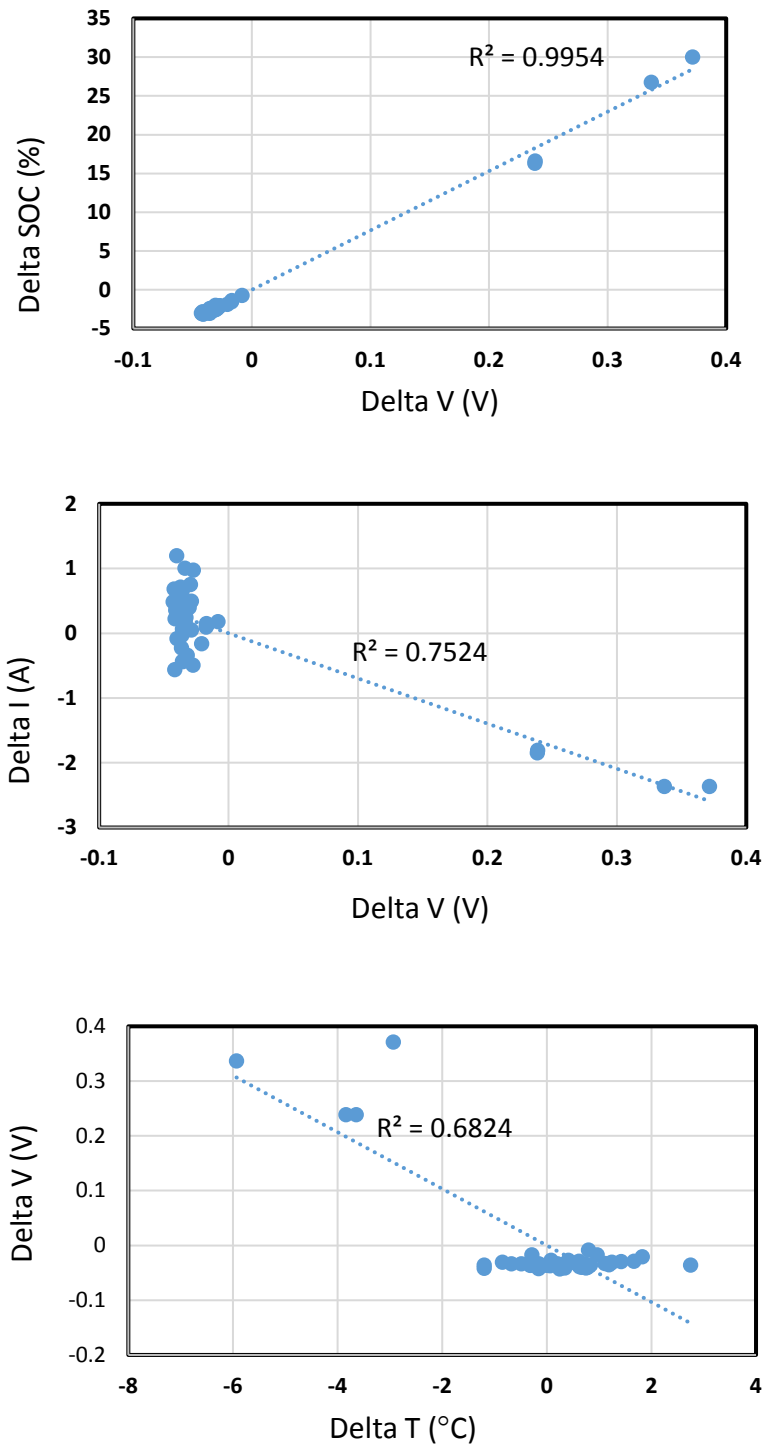


Figure 3.42. Correlation for Deviation Pairs across All Blocks

Figure 3.43 presents the correlation coefficient for the various pairs within a rack, block, and across all blocks. The trend for SOC versus V, V and SOC versus I was the same as for various rate discharge. However, for various rate charge, the SOC and V versus T curves have a negative correlation. Thus, as temperature of the vault increases with respect to the other vaults, its SOC decreases with respect to the other vaults. This could be related to the fact that the charging reaction is endothermic, while the discharge reaction is exothermic.

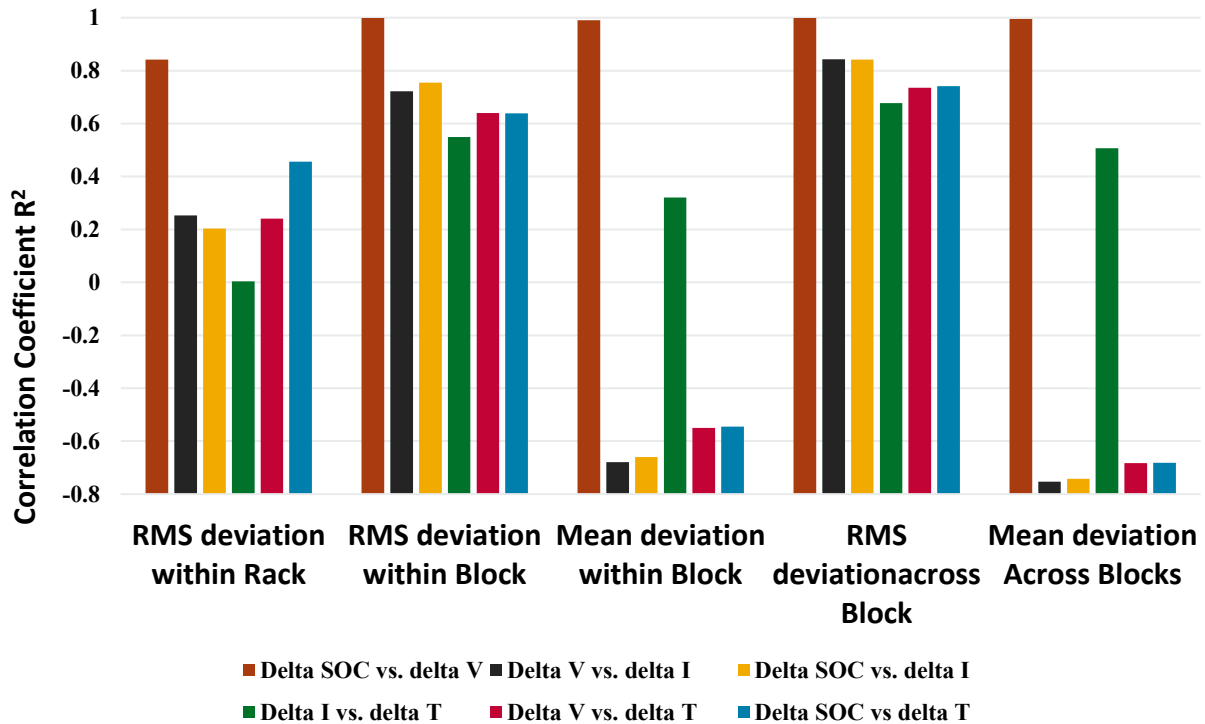


Figure 3.43. Correlation Coefficient for Deviation of Various Pairs within a Rack, a Block, and Across Blocks for Various Charge Rates

3.5 Response Time/Ramp Rate Test

The purpose of the response time / ramp rate test is to determine the time it takes for the BESS to ramp up to its full rated power from a state of rest. The BESS is taken to a starting SOC of 80 percent. It is subjected to a 5 MW discharge for 5 seconds. The response time is determined. In addition, the DC internal resistance is measured at the vault level by measuring the voltage drop at $t = 1$ through 5 seconds. Note that at $t = 1$ second, the SOC is 0.11 percent. Typically, we do not want to have a $\Delta SOC > 0.11\%$, since that changes the state of the DC battery. However, for a 5 MW rate discharge (or charge), this change in SOC occurs in 1 sec. Since the data is obtained once every second, it is not clear if the 1-sec value corresponds to the actual change in voltage. Hence, ΔV for 1-5 seconds was determined, and the internal resistance determined. The ohmic resistance was determined by curve fitting the data from $t=1$ to $t=5$, and extrapolating to $t=0$. A 15-min rest period allows determination of the total resistance from the voltage at $t=5$, 10, and, 15 minutes. Curve fitting using voltage values at $t = 1$ to 60 seconds allows estimation of the ohmic resistance of the DC vaults.

This is followed by bringing the BESS SOC down by 10% at 1,000 MW rate, followed by a 1-hour rest. At each SOC, a 5 MW charge pulse was applied, followed by a 15-minute rest, a discharge pulse, a 15-

minute rest. This is repeated until the SOC reaches 20 percent, at which time a 5 MW charge pulse was applied. The internal resistance at each SOC is determined by the same method. Table 3.10 shows the test procedure.

Table 3.10. Response Time and Ramp Rate Test Procedure

Minutes Required for 10% SOC Change	Charge / Discharge Power	SOC	Comments	Timing Notes
Bring to 80% SOC				
0.00	5	80%	Discharge at rated power (5MW) for 5 seconds	Began at 8:59:13am 5/25/2017
0.08	0		Rest for 15 minutes	
15.00	1		Discharge at 1MW until 70% SOC is reached	Began at 9:14:15am 5/25/2017
7.50	0	70%	Rest for 1 hour	Began at 9:17:15am
60.00	-5		Charge at 5MW for 5 seconds	Began at 10:19:01
0.08	0		Rest 15 minutes	
15.00	5		Discharge at 5MW for 5 seconds	Began at 10:34:03am
0.08	0		Rest for 15 minutes	
15.00	1		Discharge at 1MW till 60% SOC	Began at 10:49:01am
7.50	0	60%	Rest for 1 hour	
60.00	-5		Charge at 5MW for 5 seconds	Began at 11:49:10
0.08	0		Rest 15 minutes	
15.00	5		Discharge at 5MW for 5 seconds	Began at 12:04:02pm
0.08	0		Rest for 15 minutes	
15.00	1		Discharge at 1MW till 50% SOC	Began at 12:19:08
7.50	0	50%	Rest for 1 hour	Began at 12:25:13
60.00	-5		Charge at 5MW for 5 seconds	Began at 1:25:07pm
0.08	0		Rest 15 minutes	
15.00	5		Discharge at 5MW for 5 seconds	Began at 1:40:23pm
0.08	0		Rest for 15 minutes	
15.00	1		Discharge at 1MW till 40% SOC	Began at 1:55:03pm
7.50	0	40%	Rest for 1 hour	Began at 2:00:55pm
60.00	-5		Charge at 5 MW for 5 seconds	Began at 2:59:55pm
0.08	0		Rest 15 minutes	
15.00	5		Discharge at 5 MW for 5 seconds	Began at 3:15:04pm
0.08	0		Rest for 15 minutes	
15.00	1		Discharge at 1MW till 30% SOC	Began at 3:30:06
7.50	0	30%	Rest for 1 hour	Began at 3:35:48
60.00	-5		Charge at 5 MW for 5 seconds	Began at 4:35:43pm
0.08	0		Rest 15 minutes	
15.00	5		Discharge at 5 MW for 5 seconds	Began at 4:51:41pm
0.08	0		Rest for 15 minutes	
15.00	1		Discharge at 1 MW till 20% SOC	Began at 5:06:04pm

Minutes Required for 10% SOC Change	Charge / Discharge Power	SOC	Comments	Timing Notes
7.50	0	20%	Rest for 1 hour	Began at 5:10:15pm
60.00	-5		Charge at 5MW for 5 seconds	Began at 6:10:15
0.08	0		Rest 15 minutes	Began at 6:10:59

The ramp rate test was performed by entering the target power and then keeping it at the target power for 5 seconds, followed by a target power of 0. It took around 13 seconds to reach the target power. At each SOC, a charge pulse is applied until 5 MW is reached, following which the BESS is kept at 5 MW for 5 seconds, followed by ramp down to 0 power. After a 15 minute rest, this step is repeated for a discharge pulse. The BESS SOC is then brought down by 10 percentage points.

It took 12-13 seconds for the BESS power to reach 5 MW, with the power ramping up to rated power in 15 seconds. Hence, the applied current changed during this pulse test. This makes it potentially unreliable to determine the internal resistance by conventional means described earlier (i.e., measure the ΔV at the time corresponding to ΔSOC of 0.2 percent and divide by the current at this time).

The BESS power, average cell voltage, and average current as a function of time is shown in Figure 3.44, while V versus I plot is shown in Figure 3.45 for the discharge at 80 percent SOC. The current keeps increasing for about 13 seconds (Figure 3.44c), after which the BESS power reaches close to 5000 kW (Figure 3.44a), during which the average cell voltage decreases linearly (Figure 3.44b). Once the maximum power is reached, the current remains nearly constant, while the rate of voltage decrease slows down. The ΔSOC corresponding to 13 seconds is around 0.6 percent, while the ΔSOC at 6.5 seconds is ~ 0.16 percent. The reason this is not a linear rate of increase of ΔSOC is that the current increases with time.

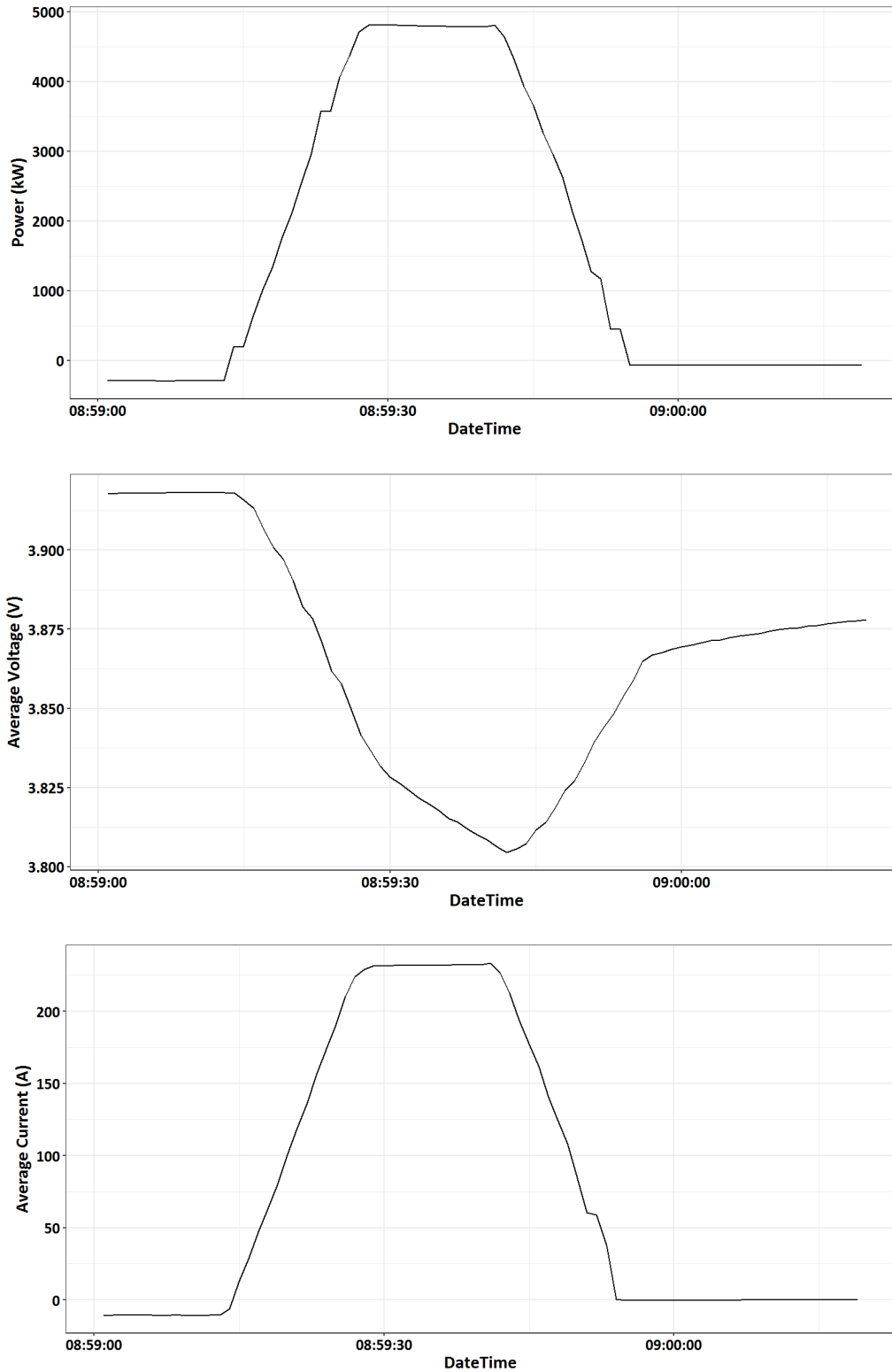


Figure 3.44. BESS Power, Average Cell Voltage, and Current through Each Rack during Ramp Up and Down to 5,000 kW Discharge

The lower rate of decrease of voltage is shown as a steep voltage drop in the V over I plot (Figure 3.45). This voltage drop is associated with a combination of factors – drop in SOC, increase in concentration polarization, increase in charge transfer over potential. Since power at an average of 2C rate has been flowing for 13 seconds prior to the constant power region, it can be assumed that most of the charge transfer related over potential has been captured within 13 seconds. The 5-seconds at ~ 5,000 kW corresponds to a Δ SOC of 0.5 percent, not sufficient to explain the voltage drop of 0.035 V per cell. It can also be assumed that concentration polarization plays a negligible role prior to the maximum power being reached.

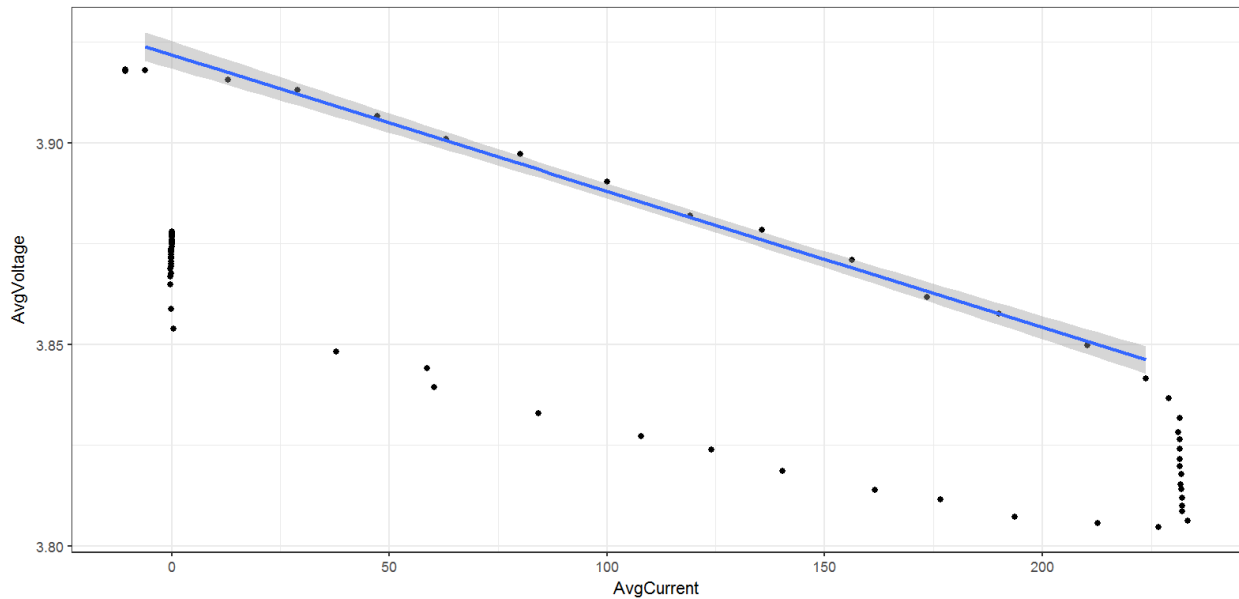


Figure 3.45. Plot of Average Cell Voltage versus Current through Vaults

Table 3.11 presents the results for the response time/ramp rate test during charging, while Table 3.12 presents results for 5 MW of discharge. The V versus I plot was used to determine internal resistance. Additionally, the potential drop at 0.15 percent Δ SOC was used to determine the internal resistance. The charge ramp rate is not a function of the BESS SOC, and is 6.5 percent of rated power for various rates of discharge (Table 3.11). For discharge, the ramp rate is highest at 80 percent SOC at 7.4 percent rated power, while it is in the 6.6-6.9 percent rated power for the other SOC's tested. The results for charge and discharge ramps are consolidated in Figure 3.46.

Table 3.11. Results for Response Time/Ramp Rate Test during 5 MW Charge

SOC	Actual SOC	Time to Rated Power (s)	Initial Power (kW)	Final Power (kW)	Ramp Rate (MW/s)	% Rated Power/s
80						
70	71	13.36	-56.7	-4460.0	-329.5	-6.6
60	62	13.68	-46.1	-4479.8	-324.2	-6.5
50	54	13.89	-34.3	-4464.0	-318.9	-6.4
40	45	13.33	2.6	-4456.1	-334.5	-6.7
-30	36	13.56	5.3	-4452	-328.7	-6.6
20	29	13.21	34.3	-4393	-335.1	-6.7

Table 3.12. Results for Response Time/Ramp Rate Test during 5 MW Discharge

SOC	Actual SOC	Time to Rated Power (s)	Initial Power (kW)	Final Power (kW)	Ramp rate (MW/s)	% Rated Power/s
80	80	13.87	-292.7	4812.0	367.9	7.4
70	72	13.29	-92.3	4301.9	330.7	6.6
60	64	12.62	-46.1	4293.9	343.9	6.9
50	55	12.92	-38.2	4392.5	338.0	6.8
40	46	12.61	-23.7	4309.7	343.6	6.9
30	37	12.82	-1.3	4311.0	336.4	6.7
20		1				

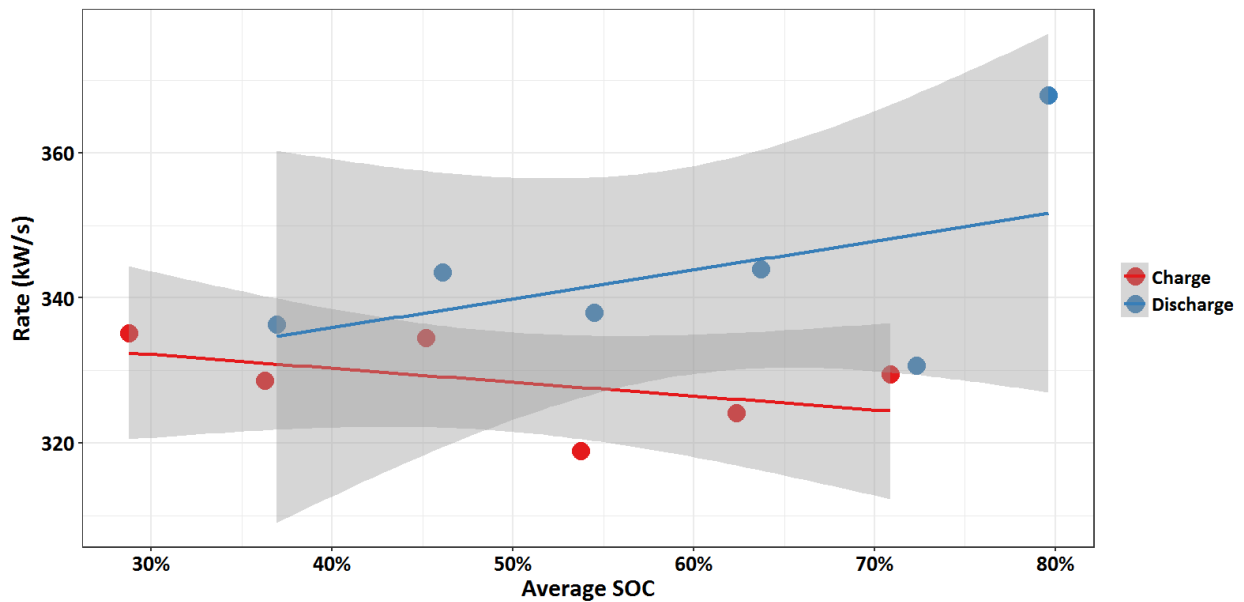


Figure 3.46. Ramp Rate of BESS for Charge and Discharge

The ramp rate for each block is shown in Figure 3.47 for charge and discharge. Blocks 1, 3, and 4 have a similar ramp rate, while Block 5 has 50 percent of the ramp rate of Blocks 1, 3, and 5. Block 2 has a 68 percent ramp rate compared to these blocks. During discharge, the ramp rate for Blocks 2 and 5 decrease with decreasing SOC, while the stronger blocks have a stable ramp rate across the SOC range investigated. The charge ramp rate is stable for all blocks.

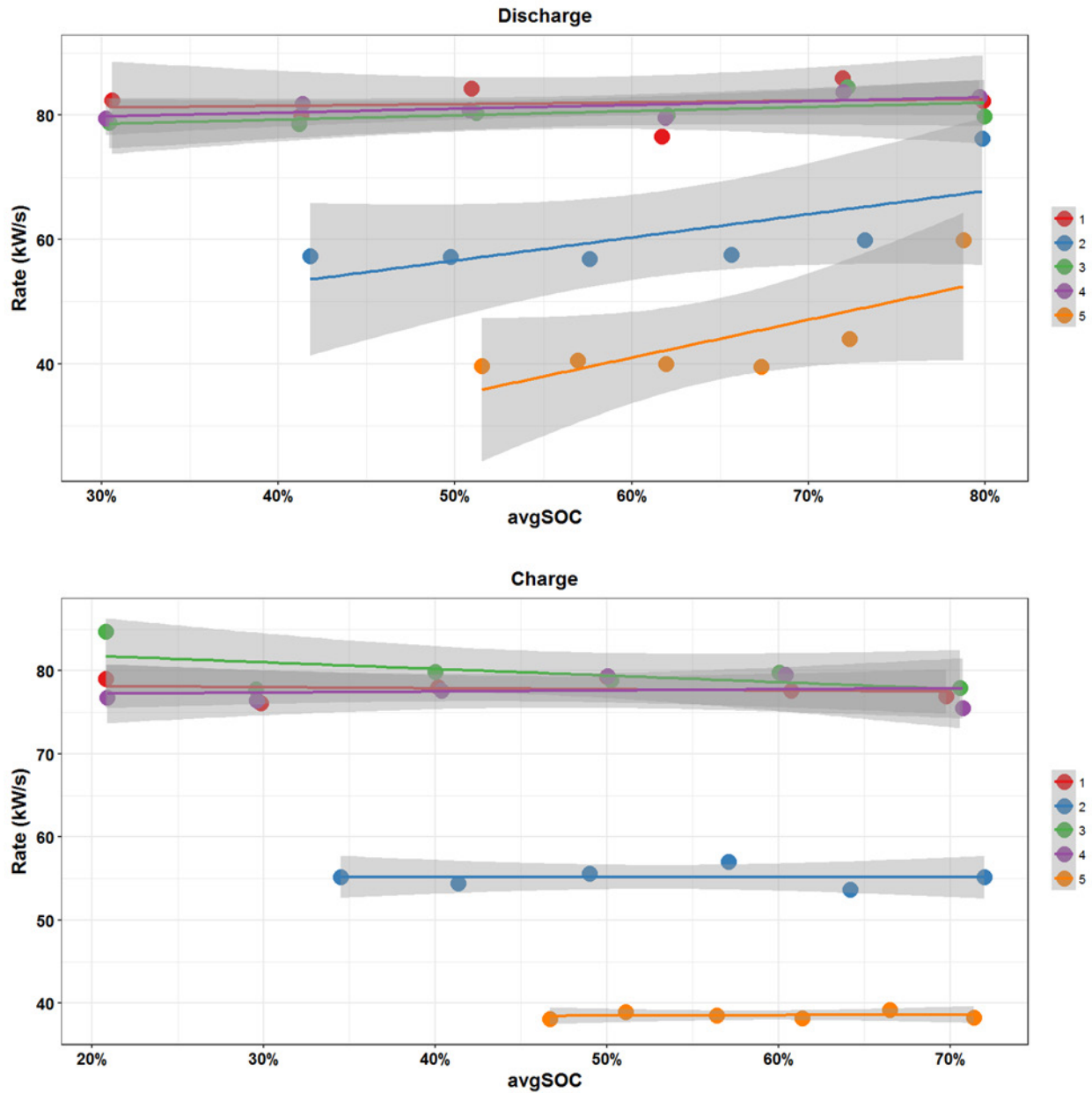


Figure 3.47. Ramp Rate for Blocks during Charge and Discharge

3.6 Internal Resistance Test Results

Table 3.13 and Table 3.14 show the per cell resistance. Data for average cell voltage and current through each vault is available. From this, the average cell resistance in each vault is computed, taking into account there are six parallel strings in a vault and 144 cells in series in each string. Hence, the per cell resistance in a vault is calculated using Equation (3.1):

$$R_{cell_{vault}} = \frac{\Delta V_{vault} \times 6}{I \times 144} \quad (3.1)$$

Where $R_{cell_{vault}}$ is the average resistance of each cell in the vault in ohms, ΔV_{vault} is the change in voltage in volts for $\Delta SOC = 0.2\%$, and I is the current in amperes through the vault.

The average cell resistance in each rack ($R_{cell_{rack}}$) is computed using the average of the ΔV for the two vaults in the rack, and the average of the current I through each vault in the rack in Equation (3.1).

The average cell resistance in a block ($R_{cell_{block}}$) is computed using the average of the ΔV for the eight vaults in the block and the average of the current I through each vault in the block in Equation (3.1).

The average cell resistance in the BESS ($R_{cell_{BESS}}$) is computed using the average of the ΔV for the 40 vaults in the block, and the average of the current I through each of the 40 Vaults in Equation (3.1).

From the per cell resistance, the vault, rack, block, and BESS resistance are calculated using Equations (3.2)–(3.5):

$$\frac{RV_{vault} = R_{cell_{vault}} \times 144}{6} \quad (3.2)$$

$$\frac{RR_{rack} = R_{cell_{rack}} \times 144}{6 \times 2} \quad (3.3)$$

$$\frac{R_{Block} = R_{cell_{Block}} \times 144}{6 \times 2 \times 4} \quad (3.4)$$

$$\frac{R_{BESS} = R_{cell_{BESS}} \times 144}{6 \times 2 \times 4 \times 5} \quad (3.5)$$

It was reported in Schweiger et al. 2010 that the SOC change needs to be less than 0.1 to 0.2 percent during pulse testing to determine internal resistance or else the change in OCV with SOC can affect the internal resistance values. In this test, it took 13 seconds for the BESS power to reach 5,000 kW. The internal resistance was measured using the slope of the V versus I curve during this period, and the numbers were checked using the change in voltage and current at ΔSOC of 0.2 percent. As shown in Figure 3.48, the median resistance measured by both methods across all vaults is nearly the same (this data was for 80 percent SOC discharge).

Table 3.13 and Table 3.14 and Figure 3.48 show the BESS-based cell resistance for charge and discharge. For charge, the resistance increases steeply at 20 percent SOC, while remaining flat for other SOCs. The resistance is nearly flat for discharge, with a slight increase at 37 percent SOC.

Table 3.13. Results for Response Time/Ramp Rate Test - Charge

Target SOC	Actual SOC	Per Cell Internal Resistance at the BESS Level (Milliohms)
80		
70	71	2.08
60	62	2.06
50	54	2.14
40	45	2.13
-30	36	2.11
20	29	2.30

Table 3.14. Results for Response Time/Ramp Rate Test - Discharge

Target SOC	Actual SOC	Per Cell Internal Resistance at the BESS Level (Ohms)
80	80	2.03
70	72	2.04
60	64	1.98
50	55	2.01
40	46	1.93
30	37	2.06
20		

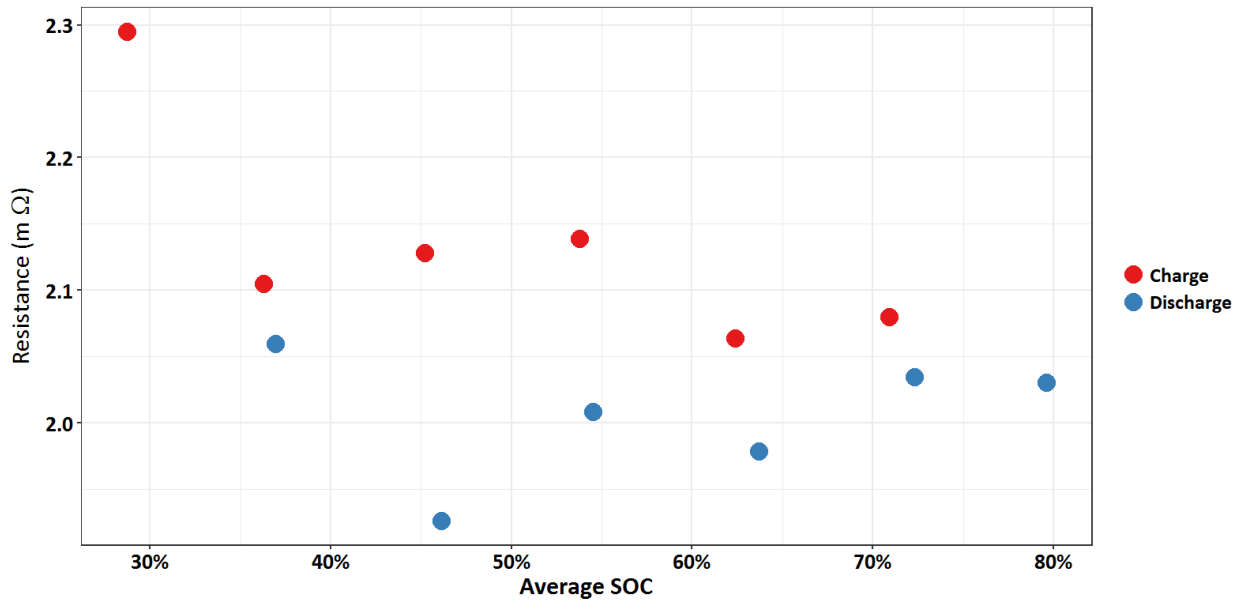


Figure 3.48. Per Cell Resistance on the BESS Level for Charge and Discharge at Various SOCs

The per cell resistance was calculated on the following basis as described earlier:

- Vault
- Rack
- Block
- BESS

Figure 3.49 shows the median of the per cell resistance on a vault basis. Vault 2-5 has the highest resistance – about 3.1 milliohms or 50 percent higher than the 2 milliohms for the rest of the vaults. Both methods used here yield results within 5 percent of each other as seen from Figure 3.49a and Figure 3.49b.

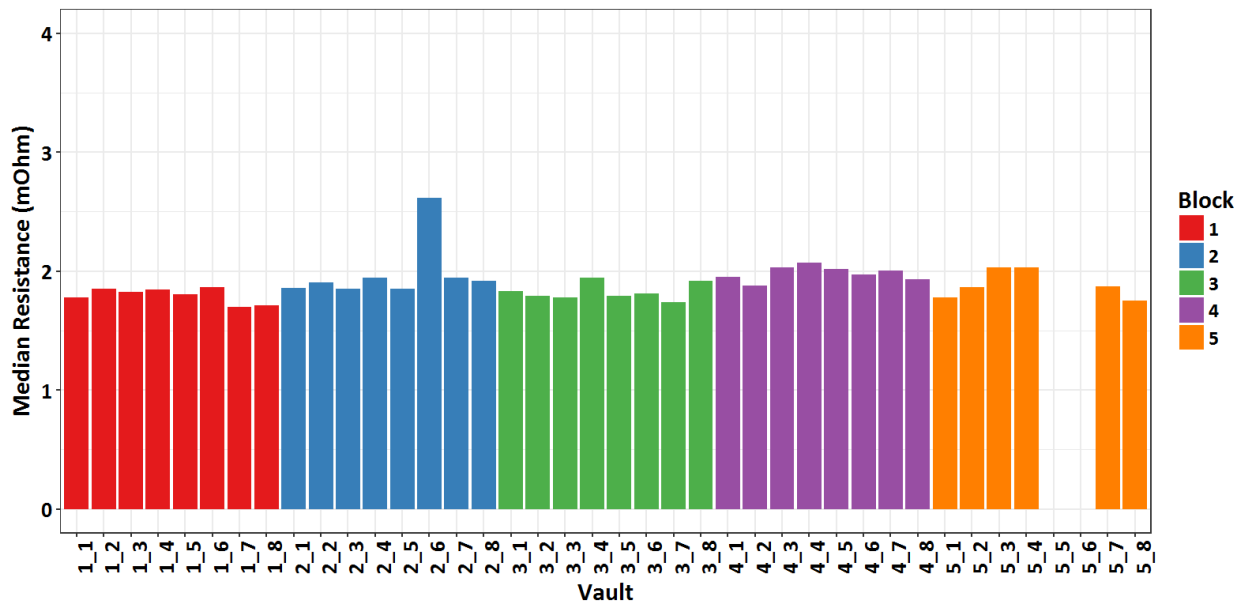
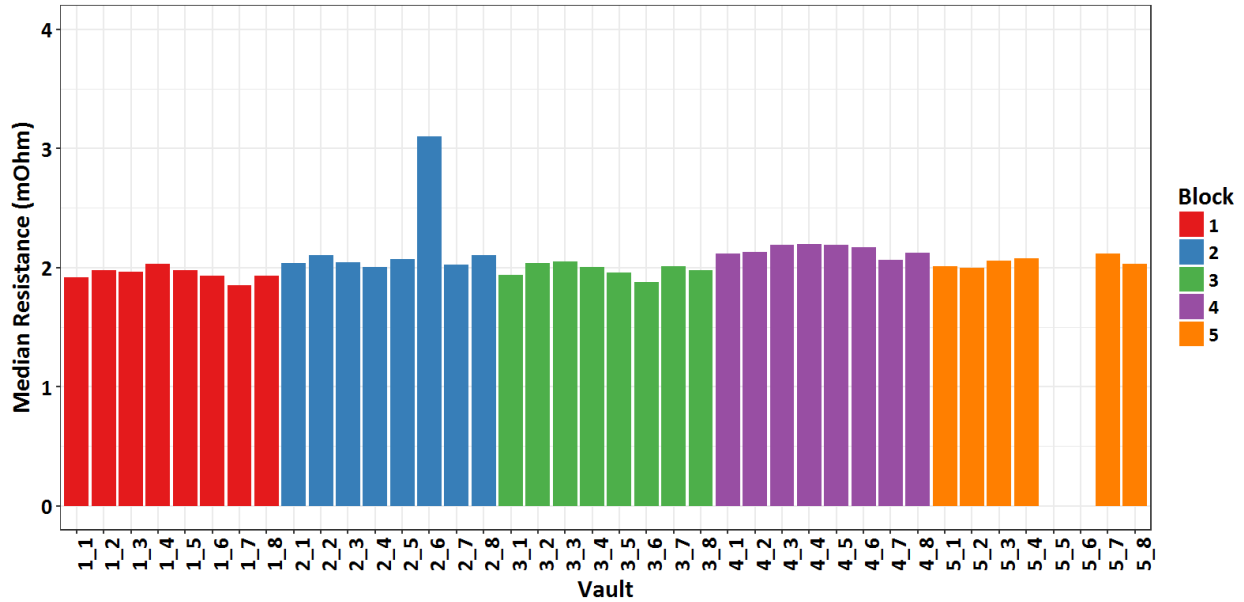


Figure 3.49. Per Cell Resistance on Vault Basis for All SOC (a) Based on Slope of V versus I Plot, and (b) Based on Voltage and Current at Δ SOC of 0.2%

To investigate the resistances for each vault at each SOC during the charge and discharge pulse, the vault resistances were plotted for all the conditions tested (Figure 3.50). The trend remained unchanged across all SOC for both charge and discharge pulses. Vault 2-5 resistance is higher than the resistance of all other vaults across all SOC investigated for both discharge and charge pulses.

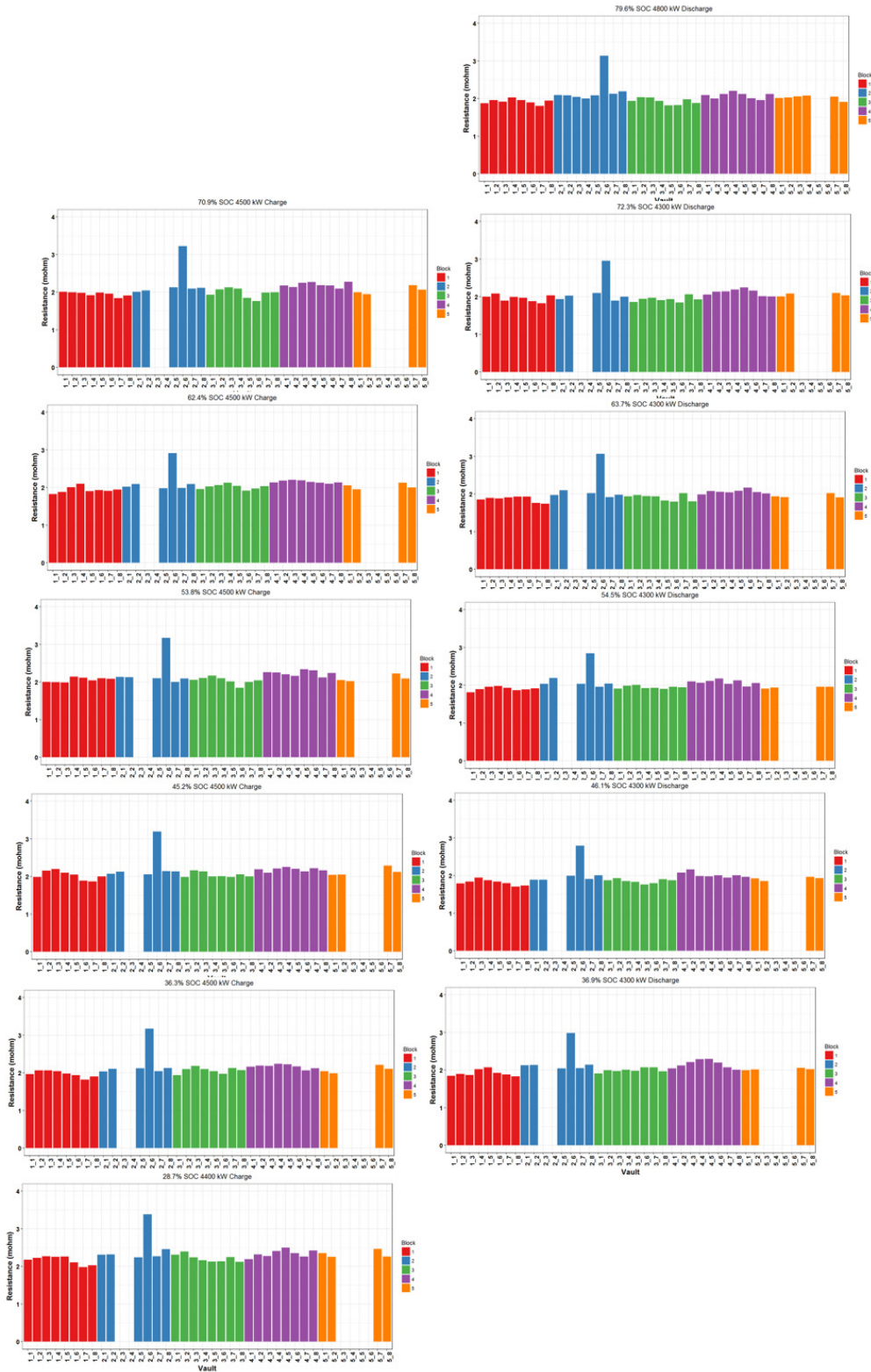


Figure 3.50. Per Cell Resistance on Vault Basis for Charge and Discharge Pulses Across all Tested SOC

Figure 3.51a shows the per cell resistance on a rack basis, while Figure 3.51b shows the per cell resistance on a block basis. Again, these values are the median resistance across all SOC.

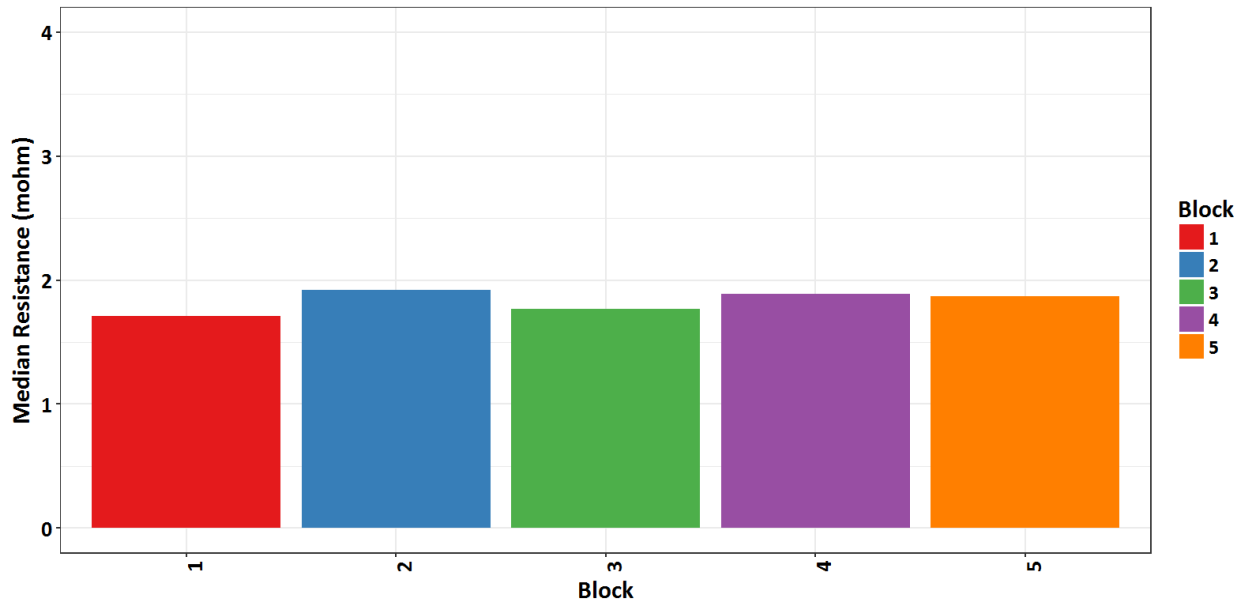
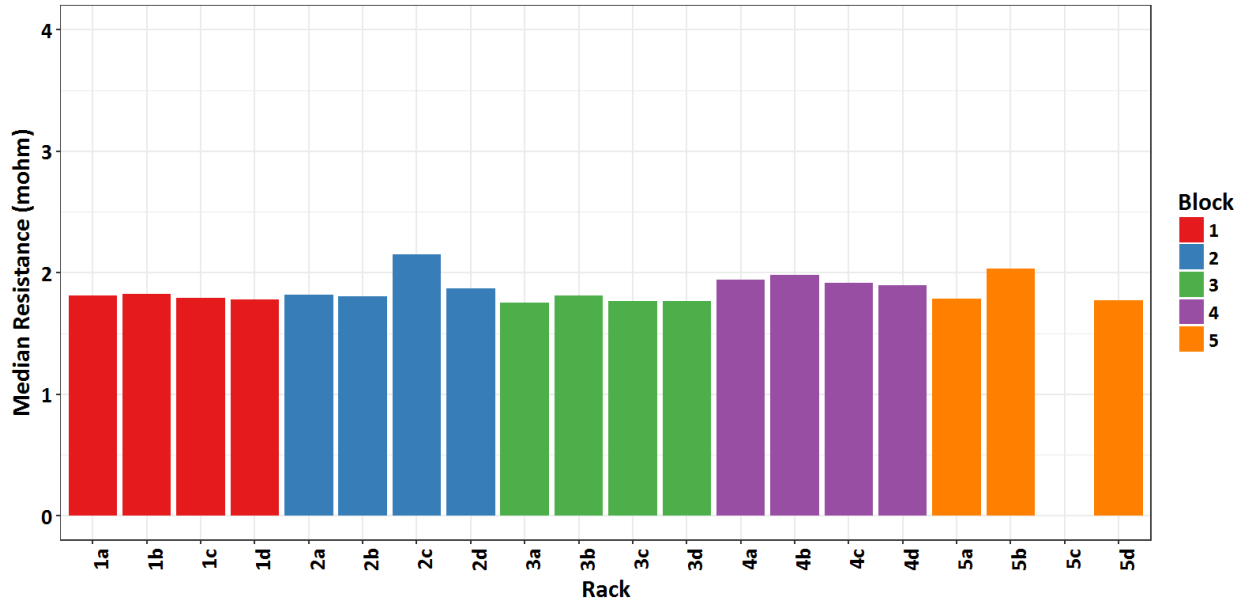


Figure 3.51. Median per Cell Resistance on a Rack and Block Basis for Charge and Discharge across All SOC on a (a) Rack Basis, and (b) Block Basis

To investigate the resistances for each rack at each SOC during the charge and discharge pulse, the per cell resistance for each rack was plotted for all the conditions tested (Figure 3.52). The trend remained unchanged across all SOC for both charge and discharge. Figure 3.53 shows similar results for per cell resistance on a block basis.

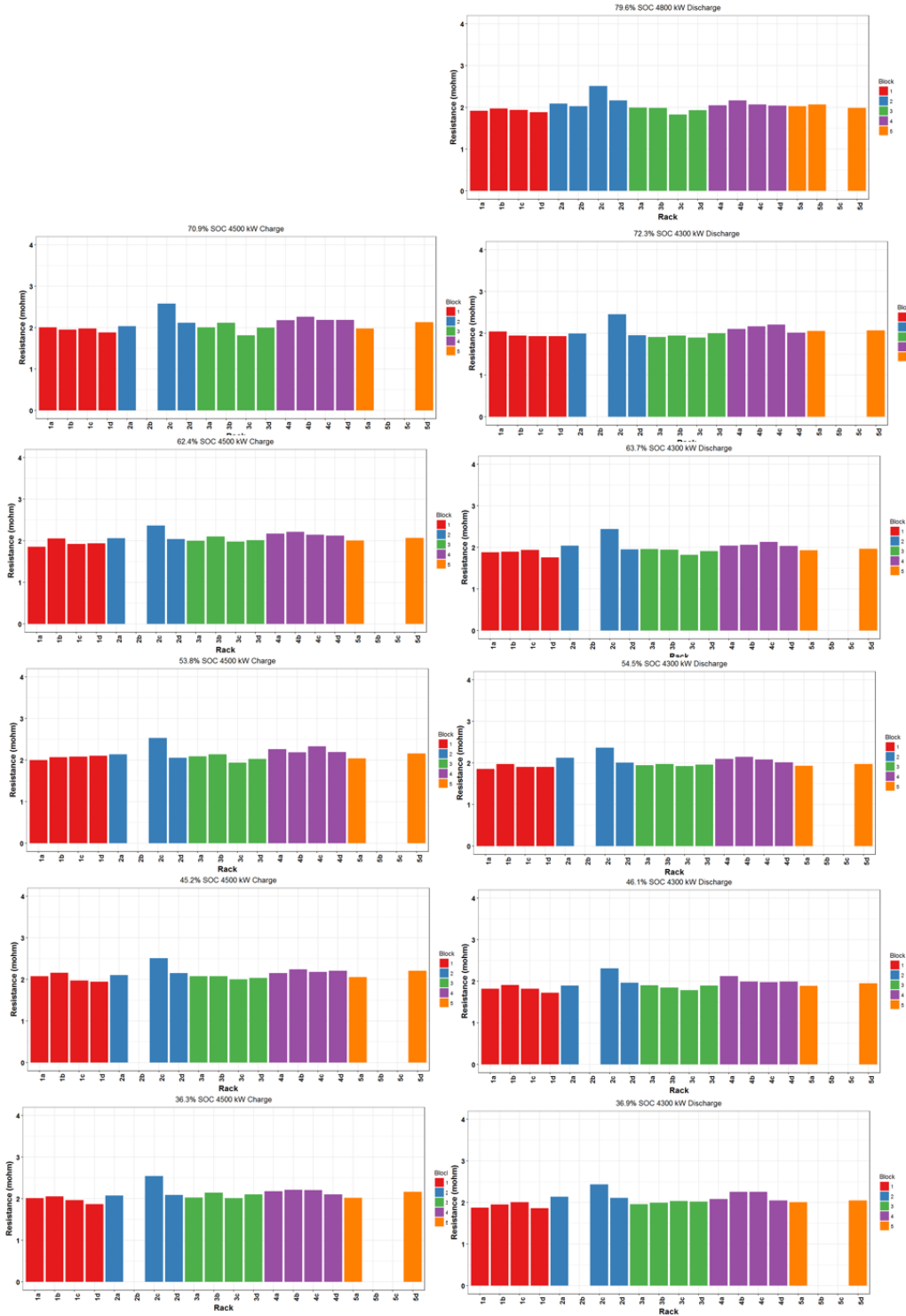


Figure 3.52. Per Cell Resistance on a Rack Basis for Charge and Discharge across All SOCs Tested

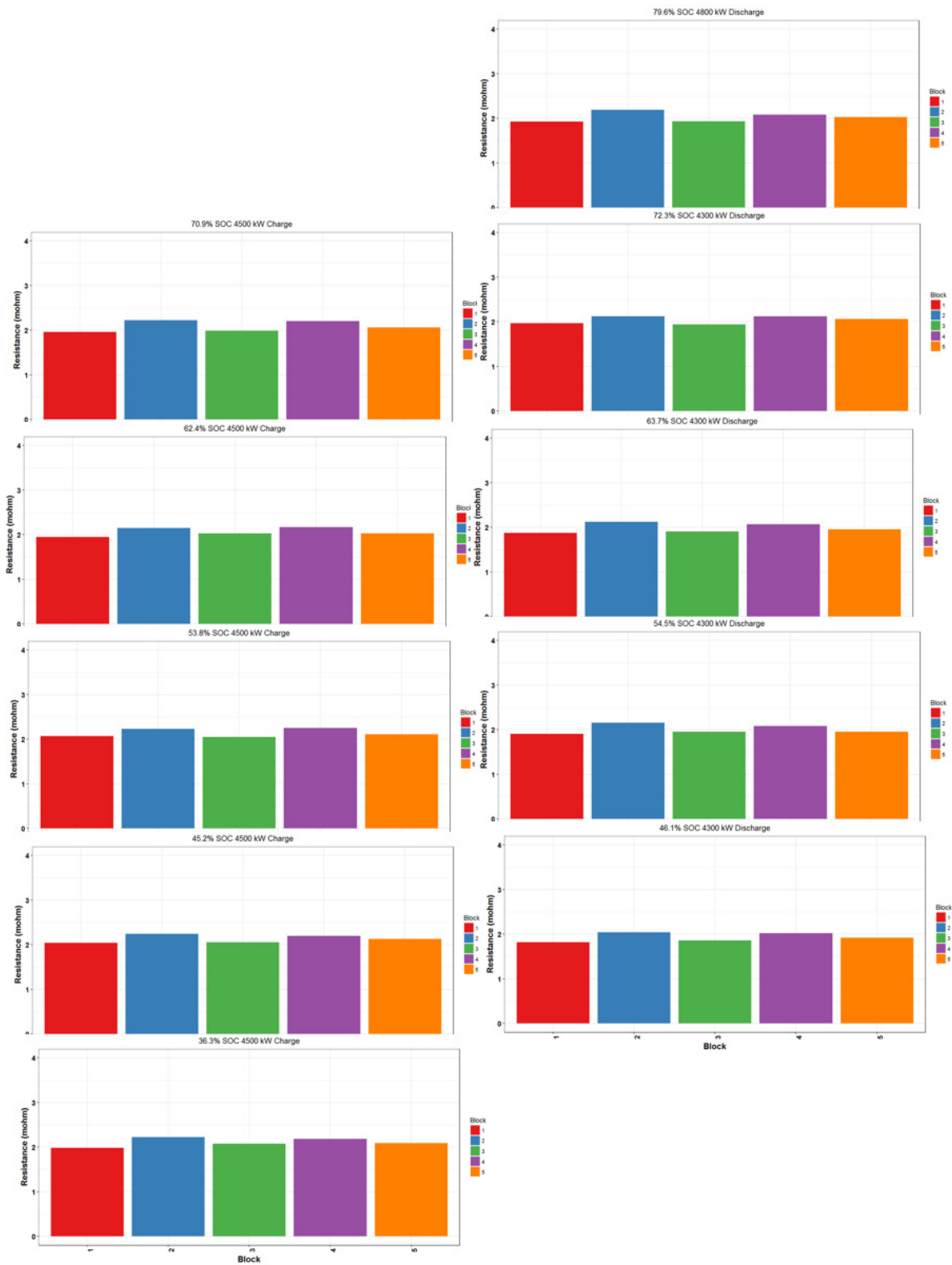


Figure 3.53. Per Cell Resistance on a Block Basis for Charge and Discharge across SOCs

For one run following the above tests, the BESS was set in the ramp mode, which resulted in the BESS reaching the target 5 MW power in 1.05 sec seconds corresponding to a ramp rate of over 4765 kW/s,

which is an order of magnitude higher than found earlier. This shows that the BESS responds quite rapidly, provided the correct mode is used to ramp it up or down. The ramp rate results are shown in Table 3.15. The BESS does not reach 5000 kW, topping out at 4702 kW in one second, corresponding to a ramp rate of 4766 kW/s, or 95.3% of rated power/s. The Blocks took 0.5 to 2.5 seconds to reach maximum power, which ranged from 770 to 1070 kW, or 77 to 107% of each Block's rated power. For Block 3, the power remained at 157 kW for 2 seconds before reaching the maximum power of 1045 kW in 2.5 seconds, while for Block 1, the power remained at 899 kW for 2 seconds before maximizing at 1042 kW in 2.5 seconds. It is not clear why the Block power remained at an intermediate power level for 2 seconds before increasing to the maximum value in 2.5 seconds. It is possible All Blocks with maximum power > 1000 kW took 1.5 to 2.5 seconds to reach maximum power, resulting in low ramp rate of 420 to 720 kW/s (42 to 72% of rated power/s). Block 2 with a maximum power of 772 kW had a high ramp rate of 781 kW/s, while Block 5 with a maximum of 796 kW had the highest ramp rate of 1611 kW/s. The sum of the maximum power of all five Blocks at 4722 kW is close to the BESS maximum power of 4702 kW. This appears to indicate that the 2-s duration for which Block 1 and Block 5 remain at 899 kW and 157 kW respectively is probably not accurate, since that would add to a lower total power in one second. Similarly, the 1-second duration at 586 kW also appears to be too high for the same reason. Hence the ramp rates calculated for Blocks 1, 3 and 4 underestimate their real ramp rate, as reflected in the fact that the sum of the ramp rates of the five Blocks are lower than the BESS ramp rate by 809 kW/s. By assuming that Blocks 1, 3 and 4 reach their maximum power in 1 second, the sum of their ramp rates at 4779 kW is close to the BESS ramp rate at 4765 kW/s. The values of the initial high power for each Block appears to be correct, since their sum adds to the initial ramp rate for the BESS at 0.5 s. This indicates that for some Blocks, data is not collected every 0.5 seconds, resulting in repeat values of the power.

Table 3.15. Fast Ramp Rate Results

	Maximum Power	Minimum Power	Time to Max power	Ramp Rate	Corrected Ramp Rate (kW/s)	Time to initial high power	Initial high power (kW)	Ramp rate
BESS	4702	-63	1	4765	4766	0.5	2623	5370
Block 1	1042	-12.4	2.5	421	1053	0.5	899*	1822
Block 2	772	-8.6	1	781	781	0.5	454	925
Block 3	1045	-13	2.5	424	1058	0.5	157*	340
Block 4	1067	-13	1.5	720	1080	0.5	586	1067
Block 5	796	-9.6	0.5	1611	806	0.5	796	1611
Sum								
Block 1-5	4722			3957	4779		2892	5765

* Constant for 2 seconds

For this run, the internal resistance was again determined by both methods described. For every 0.1 percent change in SOC, the estimated time at 5,000 kW is 0.9 seconds. It took 1-1.5 seconds to reach 5,000 kW. Assuming an average power of 2,500 kW during the ramp up from 0 to 5,000 kW, the expected Δ SOC after one second is ~ 0.05 percent. Hence at 1.5 seconds, the anticipated Δ SOC is ~ 0.14 percent, and at two seconds, the anticipated Δ SOC is 0.19 percent.

Due to lack of sufficient number of points within two seconds, the slope of V versus I was used to determine the internal resistance for up to the point where I stops changing. The criterion of 0.15 percent

Δ SOC was used to determine the internal resistance of the cells. The per cell resistance was about 1.5 milliohms, less than the two milliohms found earlier.

3.7 Frequency Regulation

The DOE-OE Protocol uses a modified 24-hour PJM duty signal that combines signals of average and high standard deviations. Figure 3.54 shows the signal and the response of the BESS. Due to the inability of the SSPC to process 4-second commands, the signal times were simplified to align with the battery response times. This modification was necessary to address timing issues with respect to data being entered into the system and to address communication lags. The test was also compressed to under one hour. Results indicate that the BESS follows the signal quite well. Note that due to the operator having to enter each signal value manually, testing was restricted to the first 20 minutes of Figure 3.54.

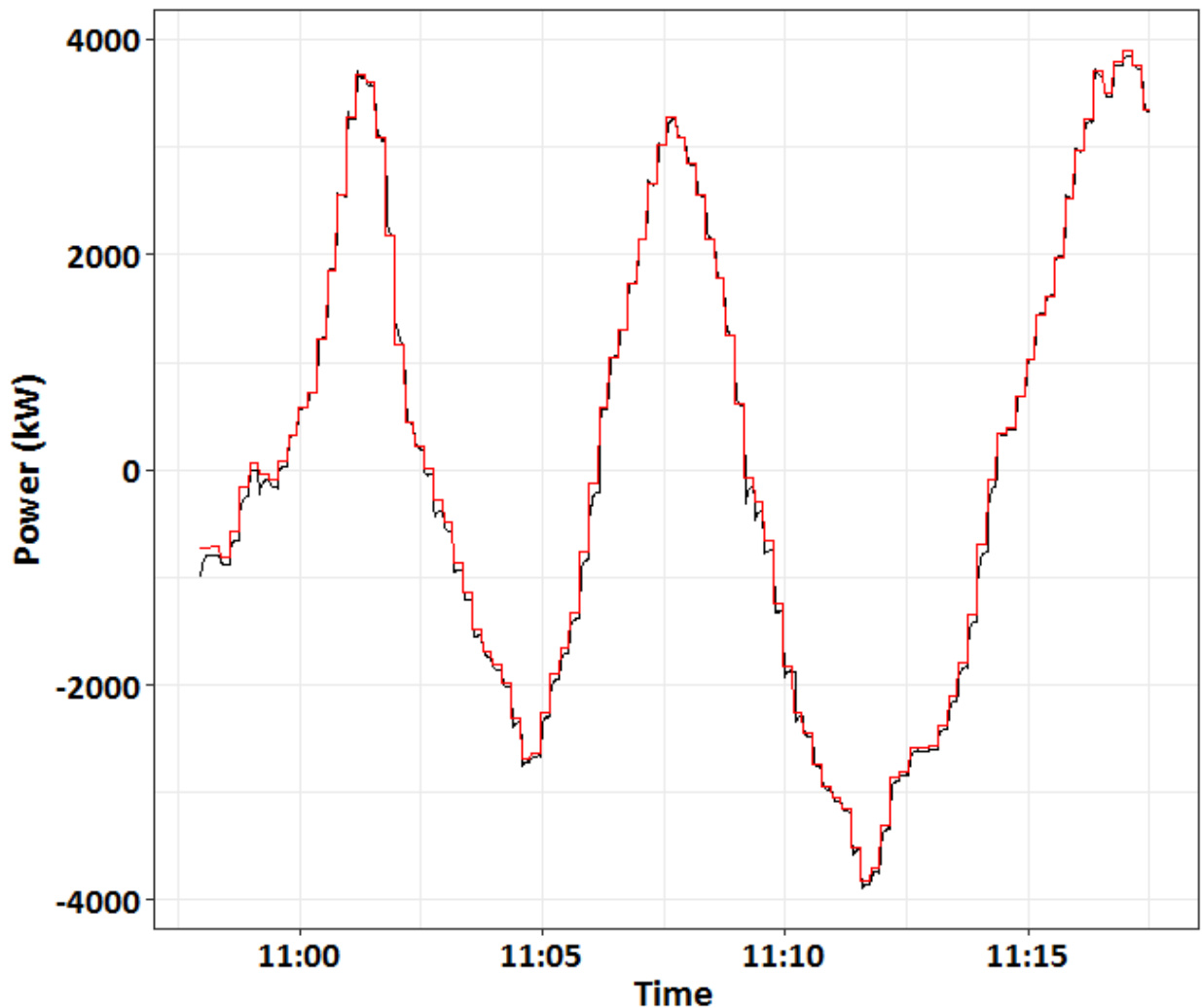


Figure 3.54. Frequency Regulation Tracking – Signal (Red) and Response (Black)

The histogram of the error (response – signal) is shown in Figure 3.55. The Cauchy distribution curve fit the histogram well since its kurtosis is high. Note that the data is skewed slightly to the right of the Cauchy distribution. Hence this metric, Cauchy Scale Error, was added to the list of metrics.

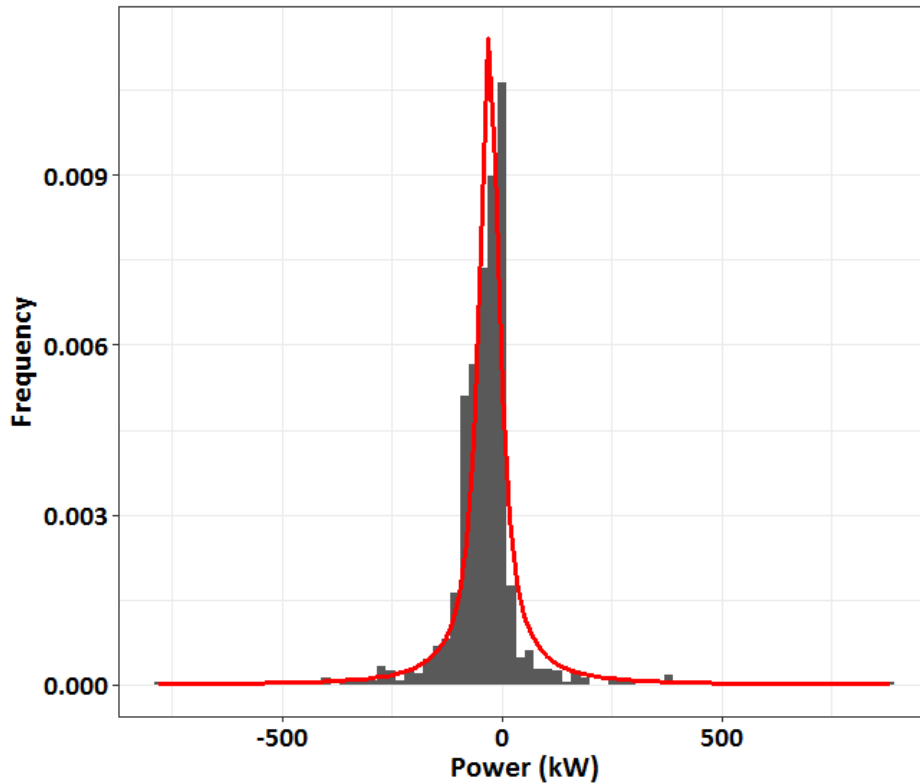


Figure 3.55. Histogram of the Frequency Regulation Error

Figure 3.56 shows the response error as a function of power. As shown, in the 500 to 3,000 kW range, the line that fits the data is on the x-axis; that is, the error is zero. For discharge powers lower than 500 kW, the error becomes more negative (i.e., the response power is less than the signal). During charge, the error is always less than 0 (i.e., magnitude of charge power greater than signal) and peaks when the signal is 400 kW. This plot demonstrates three points:

1. The BESS tracks the signal better during discharge as seen by the blue fitted line located on the X-axis for > 500 kW
2. The BESS response during discharge is lower than the signal at signal power < 500 kW
3. The BESS response during charge is greater in magnitude than the signal.

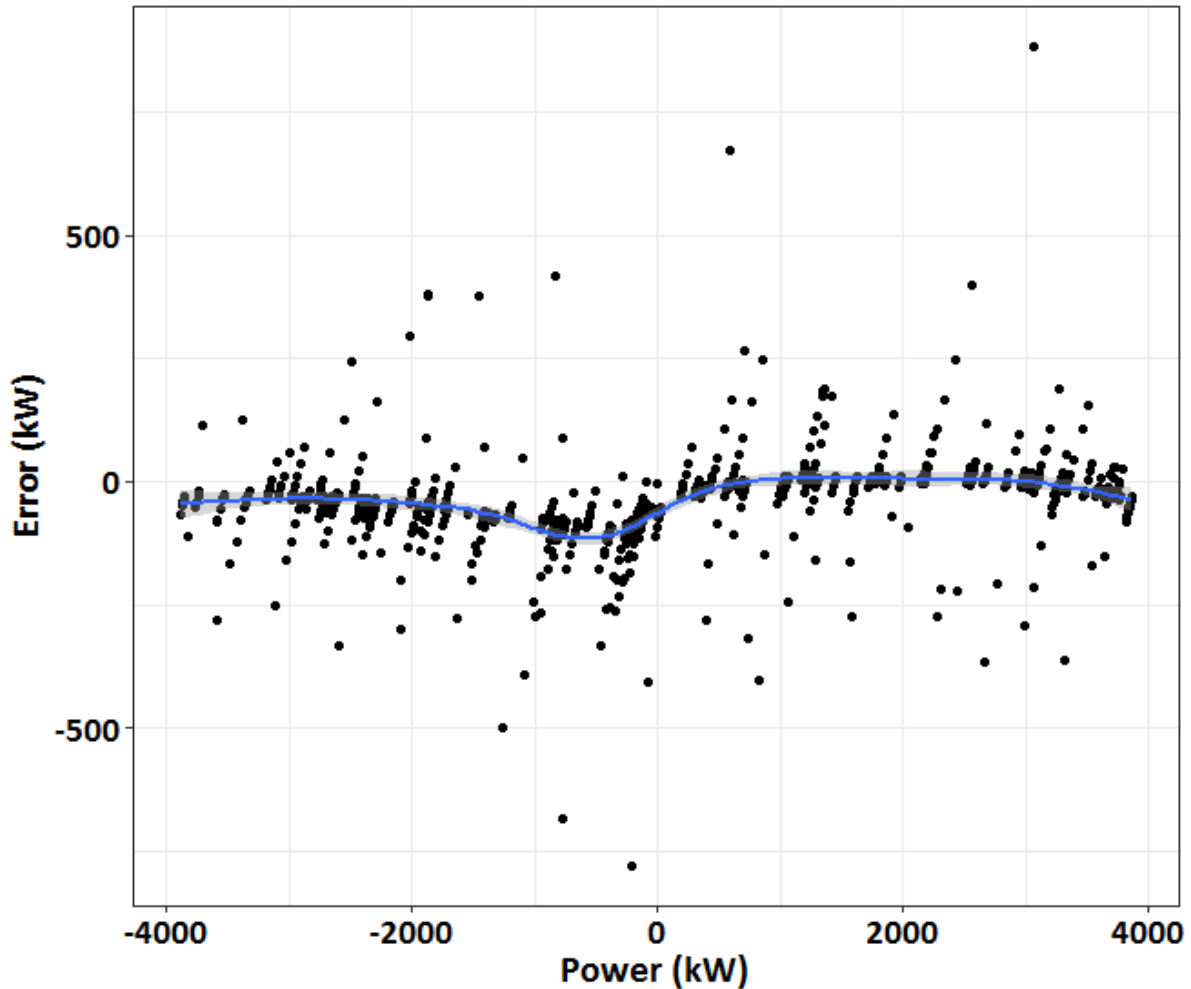


Figure 3.56. Tracking Error as a Function of Power

FR test results are provided in Table 3.16. For FR, the percentage signal tracked is calculated based on two criteria:

- Response is within x percent of signal, where x is shown in Table 3.16 to be 1 percent, 3 percent, and 5 percent
- Response is within 1 to 2 percent of rated power

For low signal values, this is a tough criterion to meet, as evidenced by a low tracking of 35 percent for the requirement of the response being within 1 percent of signal. The corresponding tracking using 1 percent of rated power as a criterion provides a tracking of 60 percent.

Table 3.16. Frequency Regulation Metrics

Date	Value	Normalized on Average Power	Normalized Rated Power
Duration (min)	19.6		
Average Temperature, °C	26.9		
SOC Max	0.787		
SOC Min	0.6		
Initial SOC			
Final SOC			
Average of Absolute Power (kW)	1850		
Maximum Charge Power (kW)	3884		
Maximum Discharge Power (kW)	3860		
RTE	NA		
RTE, No Aux	0.72		
RMSE (kW)	NA		
RMSE, No Aux (kW)	95.1	0.05	0.02
Cauchy Scale Error (kW)	NA		
Cauchy Scale Error, No Aux (kW)	27.6	0.015	0.0055
Mean Absolute Error, kW	NA		
Mean Absolute Error no Aux, (kW)	57.4	0.03	0.01
% Time Signal Followed	NA		
% Time Signal Followed, No Aux (1% of signal)	35%		
% Time Signal Followed, No Aux (3% of signal)	60%		
% Time Signal Followed, No Aux (5% of signal)	69%		
% Time Signal Followed, No Aux (1% of rated power)	60%		

As noted earlier, if the response is within a certain percent of the signal or of rated power, the BESS is considered to have tracked the signal. Clearly, as the percentage is increased, the BESS signal tracking target is easier to meet. Figure 3.57 shows the BESS signal tracking as a function of various percentages of either the signal or rated power.

When the BESS response error is within 2 percent and 4 percent of rated power, BESS signal tracking is 87 percent and 96 percent, respectively. Hence, if percent of rated power is the criterion for signal tracking, the BESS tracks the signal extremely well for the requirement of BESS tracking error < 4 percent of rated power. However, when the requirement of BESS tracking error is for BESS signal to be within 4 percent of the signal, the BESS signal tracking is only 65 percent. The BESS signal tracking plateaus at 74 percent when the criterion is tracking error < 8 percent of the signal. In other words, using a fixed percent of the signal as a criterion for BESS signal tracking is more severe than using a fixed percent of rated power.

To further illustrate this point, the RMSE, mean error, and Cauchy scale error are very small percentages of the mean power of 1,850 kW, (1.5-5 percent), and an even smaller percentage of the BESS rated power (0.6-2 percent). It is not clear which criterion is more applicable to real-world requirements. Entities such as CAISO may prefer the criterion as a fixed percentage of the signal, while from the perspective of the BESS operator, it makes sense to represent it as a fixed percent of its rated power.

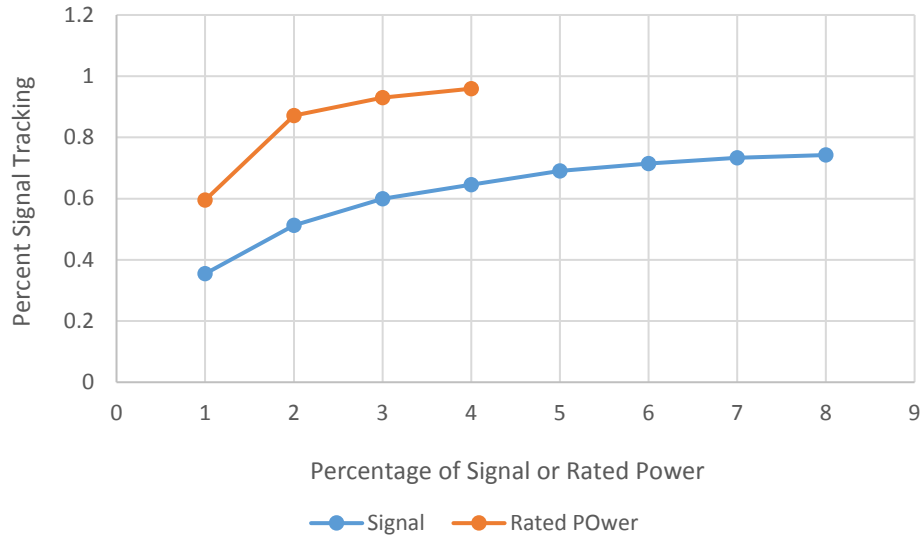


Figure 3.57. Percent Signal Tracking for Frequency Regulation at Various Percentages of Signal and Rated Power

4.0 Energy Storage Valuation Methodology and Cost Estimates

4.1 Use Cases

PNNL began its assessment of energy storage benefits by reviewing a briefing report prepared by PGE outlining the benefits of the SSPC (PGE 2016). The use cases originally identified by PGE included those outlined below:

1. Respond to transactive node/transactive signal
2. 400 kW of demand response benefit
3. 1.3 MWh of energy shift from on-peak costs to off-peak costs
4. 2 to 4 MW of real-time voltage & frequency for system operations
5. Kilovolt-ampere reactive (kVAR) support and control on the distribution feeder
6. \approx 1.2 MWh of off-peak ability to absorb excess wind power
7. 5 MW load response to under-voltage load shedding events
8. Real-time solar integration algorithms utilizing Kettle Brands' solar output signal
9. Frequency response test and deployment
10. Distribution automation using advanced, intelligent relays
11. CVR
12. Use as a dispatchable standby generation (DSG) resource
13. Emergency power for the Oregon National Guard Command Center at the Salem Airport
14. Intra-hour load balancing
15. Black start capability for up to 1 MW load on the rural feeder.

After reviewing that document and meeting with PGE on several occasions, those use cases were transformed into the following (use cases provided by PGE are indicated in brackets as appropriate):

1. Arbitrage (PGE UC3)
2. Participation in the Western Energy Imbalance Market (EIM)
3. Demand response benefit (PGE UC2)
4. Regulation up and down services (PGE UC14)
5. Primary frequency response (PGE UC9)
6. Spin reserve
7. Non-spin reserve (PGE UC12)
8. Volt-VAR control (PGE UC4 and UC5)
9. CVR (PGE UC11).

PNNL has identified two new use cases: PNNL UC2 (EIM) and PNNL UC6 (spin reserve). Use cases defined by PGE that will not be evaluated include UC1, UC6, UC7, UC8, UC10, UC13, and UC15. These use cases were deemed to either not be feasible, not be of measurable value, or are addressed through other use cases.

4.1.1 Energy Arbitrage

Arbitrage is the practice of taking advantage of differences between two market prices. In the context of electric energy markets, energy storage can be used to charge during low-price periods (i.e., buying electricity) in order to discharge the stored energy during periods of high prices (i.e., selling during high-priced periods). The economic reward is the price differential between buying and selling electrical energy, minus the cost of RTE losses during the full charging/discharging cycle. The battery system could provide up to approximately 1.25 MWh of energy to bid into the wholesale energy market.

Energy price data was obtained from Powerdex for the 2011–2016 time period. The hourly price data provided by Powerdex formed a portion of the basis of the calculations. Figure 4.1 presents hourly 2015 price data for illustrative purposes. Prices range from a high of over \$220/MWh to a low of \$-3.14/MWh.

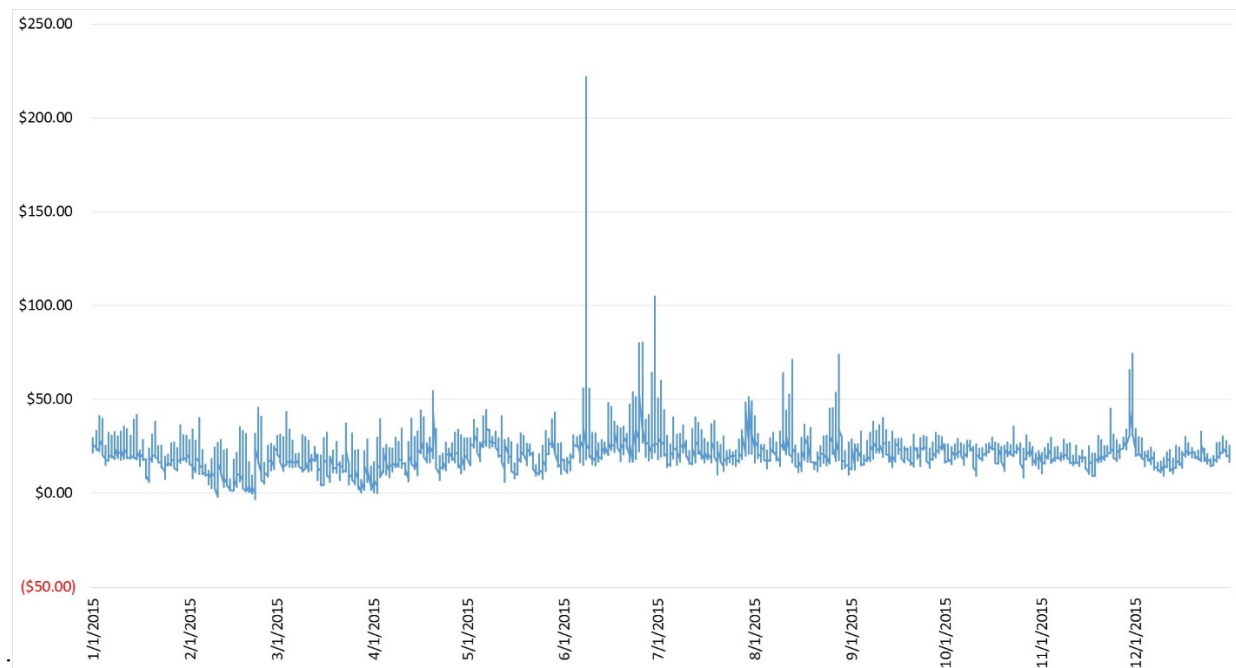


Figure 4.1. Hourly Mid-Columbia Price Index Values for 2015

4.1.2 Western Energy Imbalance Market

PGE will be joining the Western EIM operated by the California Independent System Operator (CAISO) in 2017. Under the EIM, CAISO performs 5- and 15-minute dispatch of least-cost electricity to balance generation and load in its wholesale energy market. Figure 4.2 presents a map of current and planned Western EIM participants (CAISO 2017).

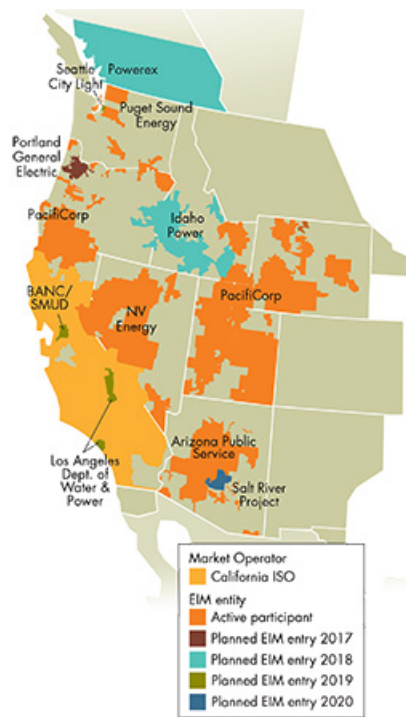


Figure 4.2. Western Energy Imbalance Market

PGE could use the SSPC as an asset while participating in the EIM. This use case functions very similarly to UC1 (arbitrage) inasmuch as it offers PGE an opportunity to participate in the wholesale pricing of energy. To evaluate the benefit of using the SSPC in the EIM, PNNL acquired 5- and 15-minute data for the PacifiCorp West load aggregation point nearest the PGE service territory (ELAP_PACW_APND). Data were obtained from the CAISO OASIS system for 2015 and 2016.

Under one scenario, EIM and Mid-C prices were developed on an hourly basis with the lowest hourly value among the two serving to charge the SSPC and the highest used when discharging the SSPC. The assumption under this scenario is that PGE would bid the SSPC into either market on an hourly basis. With an offer to sell previously stored energy at a bid price lower than the market price, the resource would be dispatched to discharge until the stored energy was depleted. In this scenario, we assume that its capacity would be fully dispatched in the 15-minute intervals and nothing would be left for 5-minute dispatch. An alternative scenario was also run in which PGE would bid the SSPC into the EIM on an hourly basis but it would be dispatched by CAISO subject to 5-minute real-time market (RTM) prices.

4.1.3 Demand Response Benefit

Demand response programs allow utilities to purchase reductions in load capacity when demand exceeds generation capacity. Commercial and industrial businesses can sell their capacity during peak demand periods to reduce load to meet generating capacity. As noted in the Section 4.1.5 pertaining to primary frequency response, approximately 300 kWh of energy must be reserved to obtain that high-value benefit. Based on historical data, the battery could be called to provide up to three hours of demand response. With a total energy capacity of 1.25 MWh and 300 kWh reserved for primary frequency reserve, only 950 kWh is available for demand response. With a three-hour target window, the total demand response capacity is limited to 317 kW.

There are four relevant demand response programs offered by PGE:

- The curtailable tariff program, which is a firm contracted capacity product for large industrial customers
- The bring-your-own-thermostat program, which offers incentives to test smart thermostats that PGE can control
- The behavioral demand response program, which features day-ahead notification to residential customers
- The automated demand response (ADR) program, which is the highest value program and the one most appropriate for the SSPC, involves participation in which PGE has paid up to approximately \$100/kW-year. The ADR program calls total up to 40 event hours per year, some with as little as a 10 minute notification.

Based on historic event data, the ADR program requires participation from 2–6pm in the June–August and December–February timeframes. Between 2013 and 2016, there were 27 ADR events. ADR events for 2016 are presented in Table 4.1. These were used as the basis of the estimation calculations presented in section 5.0. As shown, there were eight ADR events in 2016 ranging from one to three hours in duration. The total event statistics were scaled down to a 317 kW demand response contract. In this case, the SSPC is used to avoid paying out under the ADR program.

Table 4.1. 2016 ADR Events

Date	Beginning Time	Duration (Hours)	MW Contracted	MW Achieved	MWh Achieved	Battery MW Achieved	Battery MWh Achieved
1/6/2016	5:00 PM	2	13.1	5.3	10.6	0.3	0.6
2/17/2016	5:00 PM	1	11.2	8.0	8.0	0.3	0.3
2/24/2016	4:00 PM	1	11.2	7.3	7.3	0.3	0.3
7/28/2016	4:00 PM	3	11.1	8.9	26.6	0.3	0.9
8/12/2016	4:00 PM	3	10.3	8.1	24.3	0.3	0.9
8/18/2016	4:00 PM	3	10.3	7.8	23.3	0.3	0.9
12/8/2016	5:00 PM	3	8.6	3.5	10.6	0.3	0.9
12/14/2016	5:00 PM	3	8.6	6.0	17.9	0.3	0.9

In modeling participation in the demand response program, two cases were established. In the base case, it is assumed that PGE can predict demand response events at least one hour in advance and in so doing can reserve energy for other use cases. In the alternative case, it is assumed that the battery must be held at full state-of-charge to ensure availability of 950 kWh of energy, which is the rated energy minus the frequency response set aside of 300 kWh, awaiting a call in the afternoon hours (2–6pm) during the aforementioned months when demand response events may occur. The alternative case demonstrates the financial cost associated with an inability to predict events.

4.1.4 Regulation Up/Down

The electric power system must maintain a near real-time balance between generation and load. Balancing generation and load instantaneously and continuously is difficult because loads and generators are constantly fluctuating. Minute-to-minute load variability results from the random turning on and off of millions of individual loads. The services needed to meet such a balancing requirement are referred to as

“ancillary services”, which are necessary to generate, control, and transmit electricity in support of the basic services of generating capacity, energy supply, and power delivery.

Regulation up/down services are required to continuously balance generation and load under normal conditions. Regulation is the use of online generation, storage, or load that is equipped with automatic generation control (AGC) and that can change output quickly to track the moment-to-moment fluctuations in customer loads and to correct for the unintended fluctuations in generation. Regulation helps to maintain system frequency, manage differences between actual and scheduled power flows between control areas, and match generation to load within the control area. Regulation service has been identified as one of the best “values” from energy storage for increasing grid stability because of the high cost of regulation services.

In this project, regulation prices were obtained from the Northwest Power Pool (NWPP) production cost analysis performed in a previous project (Samaan 2013). The amount of regulation services in each hour is limited by both the power and energy capacities of the SSPC. Such constraints have been modeled in the optimal scheduling process. When regulation services are being called, battery storage needs to charge/discharge in order to follow AGC signals. Charging and discharging operations affects the battery SOC. Nevertheless, because regulation signals are small-duration and energy neutral over time, the cost associated with energy changes in the BESS is very small compared to the total revenue from regulation services.

4.1.5 Primary Frequency Response

Under this use case, a Western Electricity Coordinating Council (WECC)-wide frequency response event triggers a required response from PGE. In compliance with North American Reliability Corporation (NERC) Standard BAL-003-1—Frequency Response and Frequency Bias Setting, PGE must provide up to 36 MW of generation capacity when required. NERC performed a 1-year test during which time the SSPC demonstrated a capacity to quickly respond to events. The SSPC is now part of the PGE operational plan for providing frequency response under NERC Standard BAL-003-1.

Frequency response events as of yet do not result in notifications by WECC or NERC. Rather, the SSPC is set to automatically respond to unexpected frequency excursions. Based on the set points (high and low) established by a frequency regulation screen, the SSPC responded 181 times over 13 months for an average of 13.9 times month. Over roughly 10 months in 2016, PGE registered 18 frequency response events requiring SSPC responses, for an overage of 1.8 events per month. Of these events, the SSPC responded 15 times. Thus, the screen governing the SSPC response successfully responded to a frequency response event 83.3 percent of the time but triggered nearly eight times as many responses as were required by NERC.

Figure 4.3 illustrates a typical frequency response event at the SSPC. The green line represents the power output level by the SSPC during the event. The power output level was around 4 MW over the first four minutes of the event before tapering down to zero. The orange line represents the SOC of the battery over the course of the event, which fell from 80 percent to approximately 54 percent. The red line represents the system frequency, which triggered the response. Notice the droop in system frequency that triggered the event. The entire event required energy over roughly six to seven minutes. PNNL measured the energy output of this event at approximately 300 kWh and PGE validated that the SSPC control algorithm is designed to generate a 300 kWh response.



Figure 4.3. Frequency Response Event

In addition to the SSPC, frequency response is being provided by the Pelton Round Butte Hydroelectric Plant. PGE has not estimated the impact of providing frequency response on the economic life of the Pelton Round Butte Hydroelectric Plant or the marginal costs of meeting this requirement. CAISO, however, has contracted with two entities for primary frequency response: Seattle City Light (SCL) and BPA. The SCL contract transfers 15 MW/0.1 Hz of frequency regulation to SCL at a contract price of \$1.22 million or \$81/kW-year (CAISO 2016a). The BPA contract transfers 50 MW/0.1 Hz of frequency regulation to BPA at a contract price of \$2.22 million or \$44.40 per kW-year (CAISO 2016b). The weighted average of these two values (\$52.8/kW-year) was used in the base case while the SCL value was used as an alternative measure.

Given the short-duration nature of these events, PNNL evaluated the benefit based on a 5 MW capacity despite the limited energy content of the SSPC. Under the base case, it is assumed that the events cannot be predicted until shortly before they occur, and as a result, 300 kWh of energy must be held in reserve at all times. An alternative case assumes the events can be predicted, thus the need to hold energy in reserve was eliminated for this case.

4.1.6 Spin and Non-Spin Reserves

Spin and non-spin reserves are called to restore the generation and load balance in the event of a contingency such as the sudden, unexpected loss of a generator. Any resource that can respond quickly and long enough can supply contingency reserves. Faster response has greater value to the power system.

Spin reserve is provided by power sources already online and synchronized to the grid that can increase output immediately in response to a major generator or transmission outage, and can reach full output within 10 minutes. For generators, the spinning reserve is the extra generating capacity that is available by increasing the power output of generators that are already connected to the power system. Unlike regulation up service that is exercised from hour to hour, spinning reserve is not called upon unless the

contingency occurs. The frequency that a contingency will occur is very low and can be safely ignored in economic assessment.

Non-spinning reserve or supplemental reserve is the extra generating capacity that is not currently connected to the system but can be brought online after a short delay. For battery storage, it can be modeled the same way as spin reserve.

In this project, both spin and non-spin prices have been obtained from NWPP production cost analysis performed in a previous project (Samaan 2013). Both spin and non-spin reserves are limited by battery power capability. In addition, because it is required that spin and non-spin reserve must sustain the provision of energy for at least an hour, energy capacity puts another constraint on spin and non-spin reserve services.

4.1.7 Volt/VAR and Conservation Voltage Reduction

BESS with reactive power capability may be able to provide Volt/VAR related benefits to power the transmission and distribution system. Volt/VAR optimization and CVR, which is essentially a form of Volt/VAR optimization, is typically implemented as an area wide project consisting of multiple feeders. A BESS connected to a substation or at another location within the area of the Volt/VAR project may be directed for sourcing or sinking VAR by the distribution automation system or a Volt/VAR controller at the substation. VAR sourcing ability of a BESS could be used to serve local VAR demand and VAR sinking ability could be used to reduce voltage to provide CVR benefits.

CVR has been exercised by a number of utilities in the past—for example, Anderson (2016), Dominion (2012), Wilson (2012), Pinney et al. (2014), Sergici et al. (2016), Solar City (2016)—as a network-wide scheme consisting of multiple substations and feeders, voltage regulators, and capacitor banks. A summary of CVR benefits achieved in a few field studies conducted in the past are provided in Table 4.2.

Table 4.2. Previous Field Studies on CVR

Year	Study Location/ Details/ Methodology	Benefit Metrics
1987	Snohomish Public Utility District, Washington.	2.1% voltage reduction resulted approximately same reduction in energy consumption. Customer bill reduction \$6.28/customer-yr.
2007	Northwest Energy Efficiency Alliance. 3% voltage reduction at Boise substation. End of line voltage feedback. 24 hours on/24 hours off.	1.5% - 2.5% energy reduction (kWh); 1.8% - 2.6% demand reduction (kW).
2008	Plum Creek Timber. 40 MW load. Project sponsored by BPA and Flathead Electric cooperative.	Overall demand reduction – 3.72%.
2009	Midlothian Virginia. 2x34.5 kV urban circuits. Voltage regulation in the lower 5% band (114 to 120 V).	2.8% reduction in energy consumption.
2010	Ripley Power and Light. Demand reduction VVO. 3 substations and 9 feeders.	Energy reduction range of 1.3% to 5.4% across all feeders; demand reduction up to 3.4% or 1.64 MW.

Year	Study Location/ Details/ Methodology	Benefit Metrics
2010	AEP Ohio GridSmart project in Gahanna. 13.2 kV feeder regulators and capacitor banks.	Average energy reduction over 3%; station peak demand reduction over 3% (higher than energy reduction %); approximately 1/3 reduction in tap operations.
2011	Murray State University. Program sponsored by TVA. Two OLTC, 4 feeders.	4.38% peak reduction; 4.82% energy conservation; 27.5% mean reactive reduction.
2012	4 substations in Iowa Lakes Electric Cooperative set up for 2.5% (3 V) reduction.	CVRf: 1.04-1.05. Verification of CVR benefit is challenging because load changes due to CVR only is difficult to isolate.
2012	Dominion Virginia Power. Compared pre-CVR period with CVR period using day-pairing approach.	CVRf: 0.92
2013	Indianapolis Power and Light Company. CVR turned on for a few short periods in 2012 and 2013.	CVRf: 0.7-0.8
2014	West Penn Power Company	1.5% reduction in voltage resulted a range of CVRf with an average value of 0.86
2015	SCE territory. Application of smart inverters at LV feeders to enhance CVR benefit in the overall feeder. Voltage at certain customer services were shifted up using smart photovoltaic inverter so that CVR voltage for the overall system could be reduced further to increase savings.	0.38% additional reduction in energy consumption and 0.41% additional reduction in peak demand.

This section outlines an approach used to estimate/predict Volt/VAR application benefits of BESS to integrate with PNNL’s Battery Storage Evaluation Tool (BSET) for determining an overall optimized operation strategy for BESS bundling of multiple services. An approach was designed to estimate the potential benefit based on the actual service (e.g., CVR or local VAR support) a BESS would perform while engaged in a given Volt/VAR application at each time interval (e.g., an hour) over a given time period (e.g. 24 hours/ 1 week/ 1 year etc.). This approach required detailed network information (e.g., active and reactive load profiles, BESS power profile, voltage sensitivity with reactive power) and required tests to be conducted. A few important considerations for estimating the benefits are discussed below before moving into the actual methodology.

4.1.7.1 Considerations

1. Whether responding to a Distribution Automation System’s (DAS) command implementing a network-wide Volt/VAR or CVR scheme or responding to just a local controller, the ability of a BESS to provide benefits for these use cases is physically limited by the available capacity of the BESS inverter to sink/source VAR. Given that the main purpose of a BESS is to provide or demand active power, its VAR capability would be limited as compared to a pure VAR source and should be considered in estimating the benefits of Volt/VAR and CVR services.
2. For CVR applications, the amount of voltage change that could be achieved by sinking VAR by the BESS, or in other words the voltage sensitivity with respect to VAR, is a particularly important consideration. This information could be obtained by analyzing the results of load flow analysis

previously conducted by the utility’s planning department or from tests conducted by measuring voltage change in response to change in VAR at a location.

3. Finally, a mechanism is necessary to translate the change in VAR flow or change in voltage into tangible benefits (e.g., gain in capacity, reduction in power consumption). For a local VAR support application, this can be accomplished by finding the capacity gain as a result of reducing the burden of sourcing VAR from the upstream network. For a CVR application, this can be achieved by the CVR factor, which is defined as the percent reduction in power consumption due to a 1-percent reduction in voltage. CVR factors could be determined from tests, or empirical assumptions based on decades of field research (e.g., 0.8 percent reduction in mean energy consumption for 1 percent reduction in voltage (Pinney et al, 2014) could also be utilized).

4.1.7.2 Data Requirement from Utility and Benefit Screening

The following data was collected from PGE to assess the potential of volt/VAR benefits and actual benefit estimation:

1. Historical and forecast (if any) of active and reactive power flow from substation,
2. Historical and forecast (if any) of active and reactive power flow at the BESS location, if different from substation,
3. Historical power factor data at substation and at BESS location (if different from substation),
4. Information on any VAR sources (e.g., capacitor banks) used to support network during peak demand periods and their historical dispatch/switching profile,
5. Information on any future plan to install additional VAR sources for supporting system voltage and power factor, and
6. Voltage profile at substation and the remote end(s) of feeder(s).

4.1.7.3 Local VAR Support Benefit

Meeting local reactive demand using the VAR capability of power inverters in the BESS may be able to provide system benefits by relieving the burden of transmitting VAR from the upstream network. Often the peak demand or stressed condition of a network is associated with low voltage, particularly at the remote end of a feeder. Networks with high industrial loads also suffer from low power factor. Different VAR sources (e.g., capacitor banks, static VAR compensators) are used to compensate for these issues. An illustrative system is shown in Figure 4.4, where active and reactive power, P_{sub} and Q_{sub} , respectively, flows from the substation to serve the connected feeders. A BESS with VAR capability, sourcing Q_{ESS} amount of VAR, would be able to reduce the VAR that has to be brought from the upstream network or has to be supplied by other sources and therefore can support system voltage and power factor. At any given k -th instant, $Q_{ESS}(k)$ would be limited by the available VAR capacity of a BESS inverter, $Q_{ESS-cap}(k)$, expressed as shown below.

$$Q_{ESS-cap}(k) = \sqrt{S_{ESS}^2 - P_{ESS}^2(k)} \quad (4.1)$$

where, S_{ESS} is the BESS inverter apparent power capacity in kVA and $P_{ESS}(k)$ is the BESS active power in kW at k -th instant.

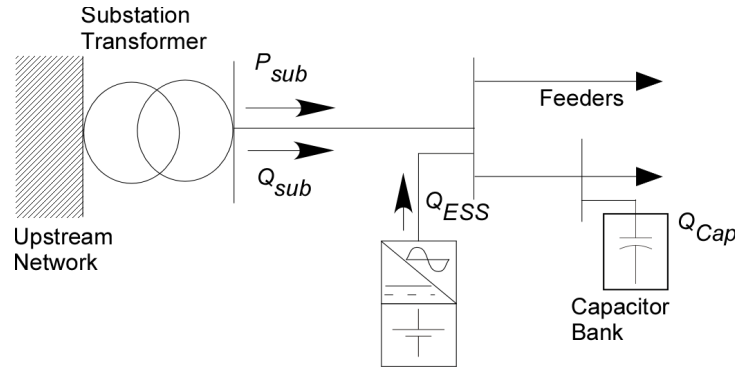


Figure 4.4. A Fictitious System Showing a BESS Meeting Local VAR Demand

4.1.7.4 Benefit Estimation

1. Hourly VAR capability of the BESS is determined/predicted using Equation (4.1), based on the predicted active power output of the BESS determined from the services provided by the BESS.
2. Using the VAR capability predicted in Step 1, the reduction in VAR to be imported from upstream network is determined.
3. Reduction in the burden to import VAR from the upstream network is translated in to equivalent capacity release using the approach described in Section 4.1.7.5. The benefit is estimated based on the released capacity of the upstream system and capacity price in an applicable market setting.
4. If it is assessed based on the data provided by the utility that BESS local VAR support will reduce or eliminate the need for additional VAR sources (e.g., capacitor banks), the equivalent cost could be included in estimating benefits.

4.1.7.5 Determining Upstream Network Capacity Release

Providing VAR from a local BESS would relieve the upstream network from the burden of supplying VAR and this could be used to supply additional loads. In an electricity market, capacity service is priced based on per kW cost estimate of installing peaking power generation resources (e.g., combustion turbine generator). An approach to estimate the amount of capacity released by supplying VAR locally could be to map the VAR supplied by the BESS on an AC system's capability curve and determine the release of equivalent active power capacity, as illustrated in Figure 4.5.

It can be assumed that an upstream AC source with a capacity of S_{SYS} MVA is supplying P_{SUP1} MW and Q_{SUP1} MVAR at a given hour to the feeder where a BESS is installed. If the local BESS inverter now supplies Q_{ESS} MVAR, the MVAR supplied by the upstream AC source will be reduced from Q_{SUP1} to Q_{SUP2} MVAR. Assuming a lossless ideal circuit, Q_{SUP2} could be roughly estimated by subtracting Q_{ESS} from Q_{SUP1} . The difference between the remaining active power capacity of the AC source (P_{RAC1}) when it was supplying Q_{SUP1} MVAR and the remaining active power capacity (P_{RAC2}) when it is supplying Q_{SUP2} is considered as capacity released (P_{REL}) by supplying VAR locally and used for capacity benefit calculation. The expression for determining P_{REL} is given in Equation (4.2).

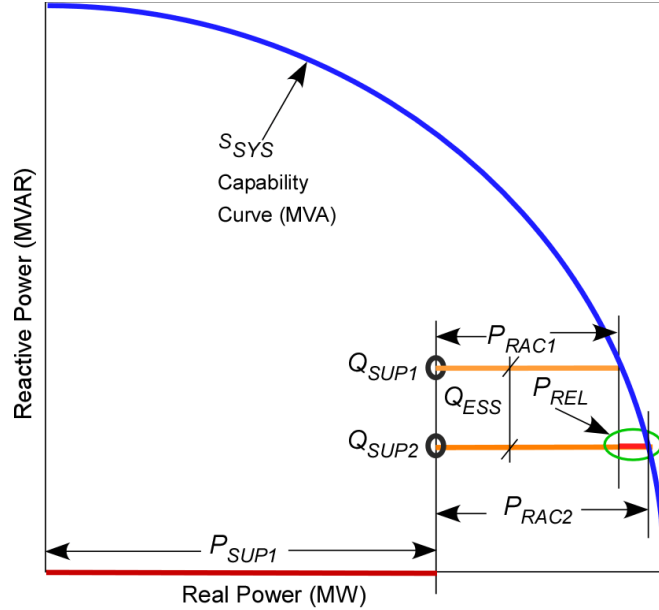


Figure 4.5. Release of Upstream Network Capacity in Terms of Synchronous Generator Capability

$$\begin{aligned}
 P_{REL} &= P_{RAC2} - P_{RAC1} \\
 P_{RAC1} &= \left(\sqrt{S_{SYS}^2 - Q_{SUP1}^2} \right) - P_{SUP1}, P_{RAC2} = \left(\sqrt{S_{SYS}^2 - Q_{SUP2}^2} \right) - P_{SUP1} \\
 Q_{SUP2} &= Q_{SUP1} - Q_{ESS}
 \end{aligned} \tag{4.2}$$

An assumption on the capacity of the upstream AC source (S_{SYS}) can be made based on the maximum demand of the feeder being supplied by the AC source over a given period. A safety factor (e.g., 10%) could be introduced to overrate the capacity. The release in upstream capacity was monetized using PGE's \$120/kW-year capacity price (Navigant 2017).

4.1.7.6 CVR Benefit

CVR is essentially maintaining voltage across the network preferably within the lower half (114–120 V on a 120 V scale) of the allowable range of 114–126 V. The task of BESS benefit estimation in a CVR application essentially requires determining the contribution of a given BESS in accomplishing the target reduction of voltage across the network by consuming VARs as directed by the CVR control system. Consider the illustration of a distribution system in Figure 4.6.

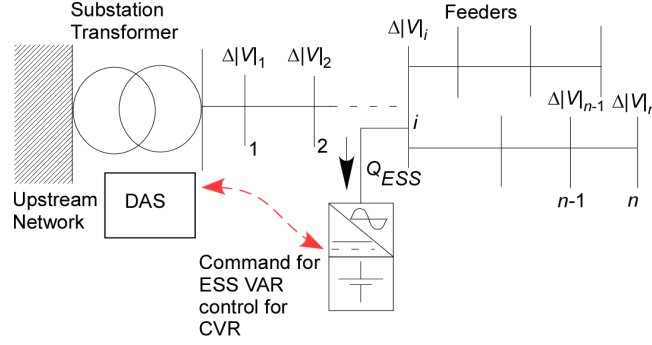


Figure 4.6. Illustration of a BESS Performing CVR in a Distribution Network

A control system implementing feeder wide CVR directs the BESS at the i -th node to sink a certain amount of VAR for achieving the target CVR voltage. Theoretically, CVR benefit contributed by the BESS at any given k -th instant of time would be the sum of reductions in active and reactive power consumptions at each of the nodes as given below.

$$\begin{aligned}
 P_{red}(k) &= \sum_{i=1}^n CVR_{fp} \times \Delta|V(k)|_i \times P_i(k) \\
 Q_{red}(k) &= \sum_{i=1}^n CVR_{fq} \times \Delta|V(k)|_i \times Q_i(k)
 \end{aligned} \tag{4.3}$$

where, P_{red} , Q_{red} are respectively the reductions in active and reactive power; CVR_{fp} , CVR_{fq} are the experimentally/empirically/otherwise determined CVR factors for active and reactive power, respectively; $\Delta|V|_i$ is the percent reduction in voltage at the i -th node of the feeder; and, P_i , Q_i are respectively the active and reactive power at the i -th node of the feeder.

Benefit estimation from power consumption at each of the load nodes in a feeder may be practically difficult to accomplish due to lack of data. Therefore, reduction in total load measured at the substation will be used in this approach. The maximum VAR that the BESS could consume at a given k -th instant will depend on its available capacity determined by Equation (4.1). The entire VAR capacity, however, may not necessarily be used for CVR. In a real-world scenario, the amount of VAR to be consumed by the BESS will most likely be determined by the DAS or a CVR control system. For the purposes of benefit estimation, a limit for VAR sinking needs to be determined based on site specific considerations and utility recommendations.

The CVR benefit was estimated by monetizing the reductions in hourly active power flow from the Oxford substation using 2016 Mid-Columbia electricity prices. Tests were conducted at the Oxford substation by regulator tapping and inverter control to determine the CVR factor (0.86) for benefit assessment.

4.1.7.7 Benefit Estimation

1. Using the projected $P_{ESS}(k)$ and BESS apparent power capacity S_{ESS} , the VAR capability of the BESS for each interval k , $Q_{ESS-cap}(k)$, was projected using Equation (4.1).
2. Using voltage sensitivity information, change in voltage at each time interval k , $\Delta V(k)$, by exercising VAR control with the capability of $Q_{ESS-cap}(k)$ was determined. Utility recommended maximum VAR

sinking limit was applied as necessary. PGE conducted voltage sensitivity tests at three locations on the feeder and constructed a voltage sensitivity model with respect to variations in reactive power.

3. Reduction in power consumption at each time interval was estimated using CVR factors determined from tests conducted at PGE as described in Section 4.1.7.8.

4.1.7.8 CVR Factor Determination Tests

PNNL and PGE personnel discussed possible approaches to determine a CVR factor; after discussion, the following tests were carried out.

1. Reduce voltage at the substation through tapping the substation on circuit tap changes by two steps and observe reduction in power consumption, as discussed in Uluski (2010).
2. Reduce voltage at the substation up to 3 percent by sinking VAR by the BESS inverter and observe the reduction in power consumption.

PNNL analyzed test results to identify voltage drop events and corresponding voltage and power profiles. The CVR factor was then determined by averaging the ratio of percentage change in power consumption to percentage change in voltage across all the data points in the identified voltage drop events. Signal processing techniques were applied to filter out high frequency components from the measured power data to aid the identification of power variations caused by voltage variations. As discussed in Uluski (2010), the CVR factor determined at the instant of voltage reduction is the initial CVR factor, which would slowly decrease and become stable at a value less than 50 percent of the initial value. This was considered in determining the CVR factor for the circuit under test.

4.2 Valuation Modeling Approach

BSET was used to run a one-year simulation of energy storage operations. The model was used to perform a look-ahead optimization hourly to determine the battery base operating point. The simulation was then used to determine the actual battery operation. The detailed modeling and formulation of this method can be found in Wu et al. (2015). This strategy is illustrated in Figure 4.7, which shows 1-minute output of a BESS. The top panel of the figure shows the prices of a balancing up service (blue line), a balancing down service (black dashed line), and the energy price (red line). Each price line is also identified in the figure. The balancing up price is zero, so the BESS does not provide any balancing up service throughout the day. The optimization tool performs tradeoffs between the balancing down and energy services. The energy service bid is shown as a black dashed line in the middle panel. The actual output of the BESS is presented as the red line, and deviates from the initially scheduled pattern in order to provide balancing down service and in mitigating an outage at around 7:00 p.m. The bottom panel shows the SOC of the BESS. As services are provided, the revenue or value derived from the service is logged as is the time the BESS is engaged in providing each service. Energy costs incurred during charging and RTE losses are included in the formulation.

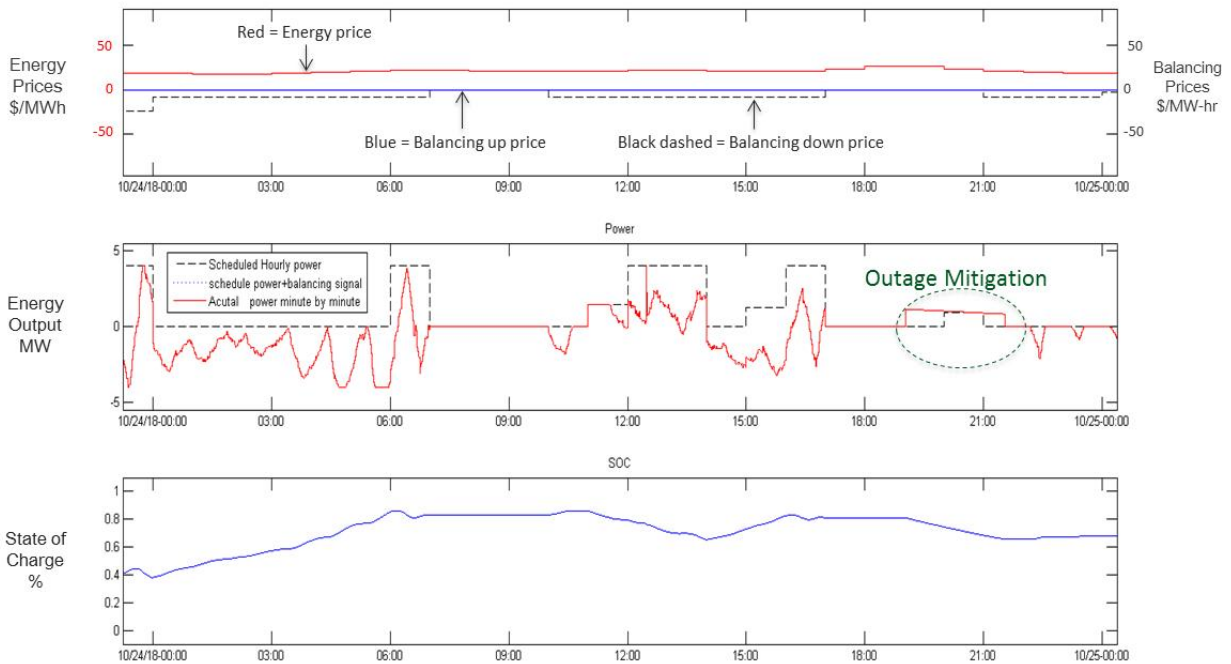


Figure 4.7. 24-hour Energy Storage Schedule

The economic benefit assessment has been performed for both individual services and bundle services in section 5.0. BSET was used to define the potential economic benefit of the SSPC on an annual basis and to determine the number of hours each BESS would be actively engaged in the provision of each service under optimal conditions.

4.3 Estimating Energy Storage Costs and Revenue Requirements

The SSPC was originally conceived as a groundbreaking research and development (R&D) project that would advance PGE’s understanding and technical capacity around integration of energy storage, smart grid technologies, and microgrid resources. Even real-time optimization and transactive energy systems were developed and tested as part of SSPC development. Due to the R&D nature of the project and the nascent stage of development for the grid-scale lithium-ion batteries deployed in the system, original system costs reached \$20.4 million. Due to learning and reductions in battery and component costs, PGE estimates that the SSPC today would cost roughly \$10.1 million. These costs, stratified by major components, are presented in Table 4.3. PGE estimated fixed annual O&M costs at \$75,000.

Table 4.3. PGE Estimated Costs for SSPC

Cost Component	SSPC Original Cost	SSPC Cost Today
SSPC Building	\$3,400,000	\$1,000,000
Software	75,000	250,000
Batteries	6,000,000	3,000,000
Inverters	6,000,000	3,000,000

Cost Component	SSPC Original Cost	SSPC Cost Today
Interconnection	750,000	750,000
Interim Battery Costs	4,061,016	2,030,508
Total PV Costs	\$20,361,016	\$10,105,508

In reviewing BESS deals being done across the United States, these costs appeared to be above current market prices. Therefore, PNNL has also considered alternative cost scenarios based on data presented in Lahiri 2017. These costs are based on deals being monitored by DNV GL, and are stratified somewhat differently than those presented by PGE. PNNL took the mid-point of these values, applied them to a 20-year battery installation, and estimated the present value costs of the existing SSPC if built today at \$5.4 million (Lahiri 2017). It is assumed battery replacement will take place after 10 years. Costs were also estimated for 5 MW of power capacity with 5, 10, 15, and 20 MWh of energy capacity at \$8.1, \$11.8, \$15.4, and \$18.9 million, respectively.

Table 4.4. Lahiri 2017 Estimated Costs

Cost Component	Low	High
DC Modules and BMS (\$/kWh)	\$325	\$700
Power Conversion System (\$/kW)	350	500
Power Control System (\$/kW)	80	120
Electrical BoP (\$/kW)	80	120
Construction and Commissioning (\$/kWh)	120	200
Fixed O&M Costs (\$/kW-year)	6	12
Major Maintenance (\$/kW)	150	400
Year Between Major Maint.	5	8
Battery Replacement (\$/kWh)	\$100	\$100

For energy storage to be cost competitive, the benefits must not only exceed the costs; they must exceed all associated revenue requirements, including all taxes, debt, and returns to investors. A detailed pro forma for the BESS was prepared to estimate revenue requirements. Major parameters used in the pro forma are presented in Table 4.5.

Table 4.5. Major Parameters Used in Estimating BESS Revenue Requirements

Parameter	Assumptions
Analysis Time Horizon	20 years
Battery Operating Lifetime	10 years
Federal Income Tax Rate	35%
State and Local Income Tax Rate	7.69%
After-Tax Weighted Cost of Capital	6.32%
Long-Term Rate of Inflation	2.25%
Property Tax Rate	1.4%
Discount Rate	6.32%

Based on the combination of costs and assumptions outlined previously in this section, revenue requirements were produced that accounted for full system costs, including all taxes, debt, and returns to investors. Revenue requirements for all five cost scenarios are presented in Table 4.6.

Table 4.6. BESS Revenue Requirements

Scenario	Revenue Requirements (Millions)
PGE Actual Expenditures	\$28.4
PGE Estimate if SSPC Built Today	\$14.6
Lahiri 2017 for 5MW/1.25MWh BESS	\$7.9
Lahiri 2017 for 5MW/5MWh BESS	\$11.5
Lahiri 2017 for 5 MW/10MWh BESS	\$16.4
Lahiri 2017 for 5 MW/15MWh BESS	\$21.2
Lahiri 2017 for 5 MW/20MWh BESS	\$26.1

5.0 Economic Results

One of the primary objectives of this research effort is to enhance the value that the SSPC can provide to PGE. In doing so, the analysis could be useful to other utilities facing similar investment decisions and those trying to extract maximum value from existing energy storage assets. At present, the SSPC is used exclusively to provide primary frequency response. While it can be confirmed that this is the highest value service for the SSPC, it is not the only one.

The SSPC is currently underutilized, operating an average of 14 hours per month, or 1.9% of available hours. While the findings of this section demonstrate that the SSPC will not yield benefits that exceed revenue requirements as initially designed and built, they do suggest there is a great deal of currently unrealized value. Further, they demonstrate that if the system was built today at the much lower prices evident in the marketplace, benefits would equal 74 percent of the revenue requirements. If the BESS was optimally scaled, benefits would exceed revenue requirements. The remainder of this section discusses the economic results of this assessment.

5.1 Evaluation of SSPC Benefits and Revenue Requirements

The first step in estimating the benefits associated with SSPC operation was to evaluate the benefits of each service individually. Table 5.1 and Figure 5.1 presents the results of these individual assessments. The results demonstrate that if the battery was used exclusively for each service, the total value could exceed \$7.5 million annually in aggregate. However, the capacity of the BESS to generate value is constrained by its operating characteristics and its ability to provide energy when needed for each application. That is, some services are in conflict and cannot be provided simultaneously.

There is competition for the energy in the SSPC both from an intertemporal and on an application basis. Knowledge of the battery's characteristics and the landscape of economic opportunities matters in terms of optimizing value. To resolve these conflicts, the research team employed BSET. When the model co-optimizes the benefits under the base case, limiting the value to what is technically achievable by the SSPC, economic value declines to \$5.9 million over a 20-year period in present value (PV) terms. Note that in the individual assessments, charging costs are embedded in each value. In the co-optimized case, they are reported separately.

The base case scenario, on which the values reported in Table 5.1 are based, employs the following assumptions:

- Arbitrage is run for 2016 using both Mid-C and EIM prices with 300 kWh of energy set aside for primary frequency response events
- 317 kW of demand response is provided and the events can be predicted
- 5 MW of primary frequency response with 300 kWh of energy set aside at all times for events
- All ancillary services co-optimized with 300 kWh of energy set aside for primary frequency response events
- After all other service-based commitments have been met, the remaining capacity of the SSPC is used to provide Volt-VAR and CVR support as needed.

The value of the base case is much lower when co-optimized because the energy to power ratio of the SSPC is low at 0.25, and roughly one-fourth of its energy must be held in reserve for primary frequency response at all times. The energy must be held in reserve because primary frequency response events

cannot be predicted. The lack of available energy limits the ability of the SSPC to generate value in more energy-intensive applications such as the ancillary services (e.g., regulation up/down, spin and non-spin reserves).

Table 5.1. Individual vs. Co-Optimized Benefits

Service	Individual	Co-Optimized
Charging Costs		\$(449,115)
Arbitrage (Mid-Columbia)	\$75,590	\$746,299
Energy Imbalance Market	\$373,778	
Demand Response	\$540,259	\$428,155
Regulation Up	\$727,250	\$374,609
Regulation Down	\$908,795	\$656,706
Primary Frequency Response	\$2,971,424	\$3,568,826
Spin Reserve	\$831,079	\$100,622
Non-Spin Reserve	\$720,221	\$46,124
Volt-VAR / CVR	\$393,619	\$393,619
Total	\$7,542,017	\$5,865,846

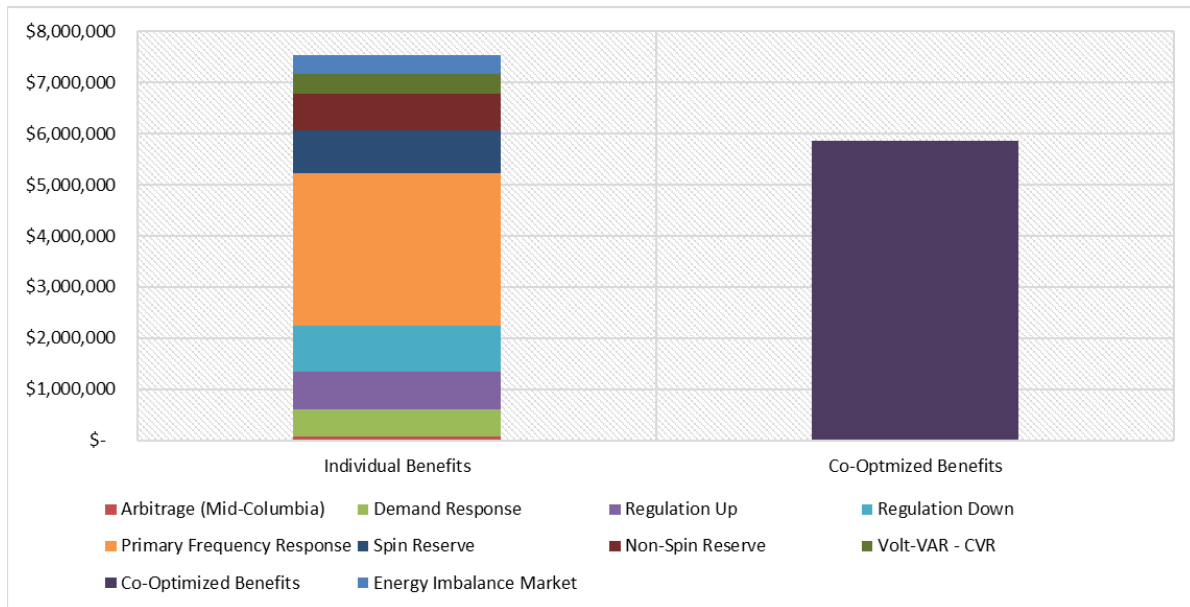


Figure 5.1. Individual Benefits Estimates by Use Case vs. Co-Optimized Benefits

SSPC benefits for the base case (\$5.8 million) fall far short of the revenue requirements for the SSPC as originally designed/built (\$28.4 million). It is important to understand, however, that the SSPC was developed as an R&D facility that advanced PGE and the region’s understanding of smart grid, energy storage, distributed energy, and microgrid systems (Figure 5.2).

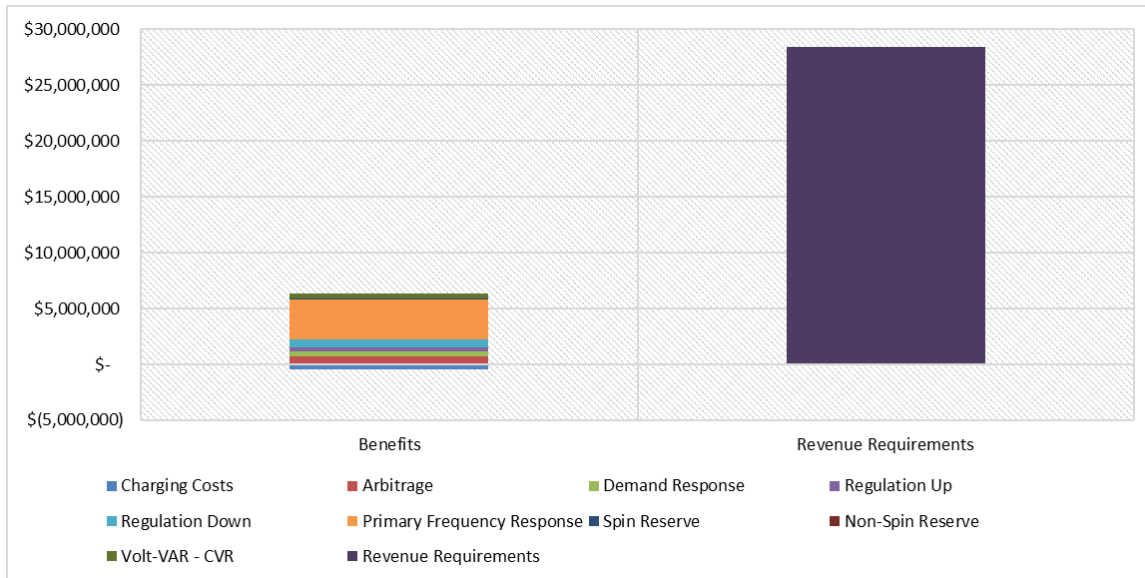


Figure 5.2. Base Case Benefits and Revenue Requirements for SSPC

Table 5.2 and Figure 5.3 present the results of a scenario that evaluates costs based on current prices as estimated in Lahiri (2017) and presented in section 4.3. Results indicate that co-optimized benefits equal 74 percent of system revenue requirements when current prices are used. The primary benefit is the one currently being realized by PGE, primary frequency response, which PNNL values at \$3.6 million over 20 years. However, all other use cases or services yielded an additional \$2.3 million in currently unrealized benefits over 20 years in PV terms. Of those services, arbitrage when also bidding into the Western EIM held the most revenue potential at \$0.7 million, followed by regulation down (\$0.7 million), demand response (\$0.4 million), and Volt-VAR/CVR (\$0.4 million).

Table 5.2. Co-Optimized 20-Year Benefits vs. Revenue Requirements (Base Case-Lahiri 2017 Costs)

Service	Individual	Revenue Requirements
Charging Costs	\$(449,115)	
Arbitrage (Mid-Columbia)	\$746,299	
Energy Imbalance Market		
Demand Response	\$428,155	
Regulation Up	\$374,609	
Regulation Down	\$656,706	
Primary Frequency Response	\$3,568,826	
Spin Reserve	\$100,622	
Non-Spin Reserve	\$46,124	
Volt-VAR / CVR	\$393,619	
Total	\$5,865,846	\$7,893,775

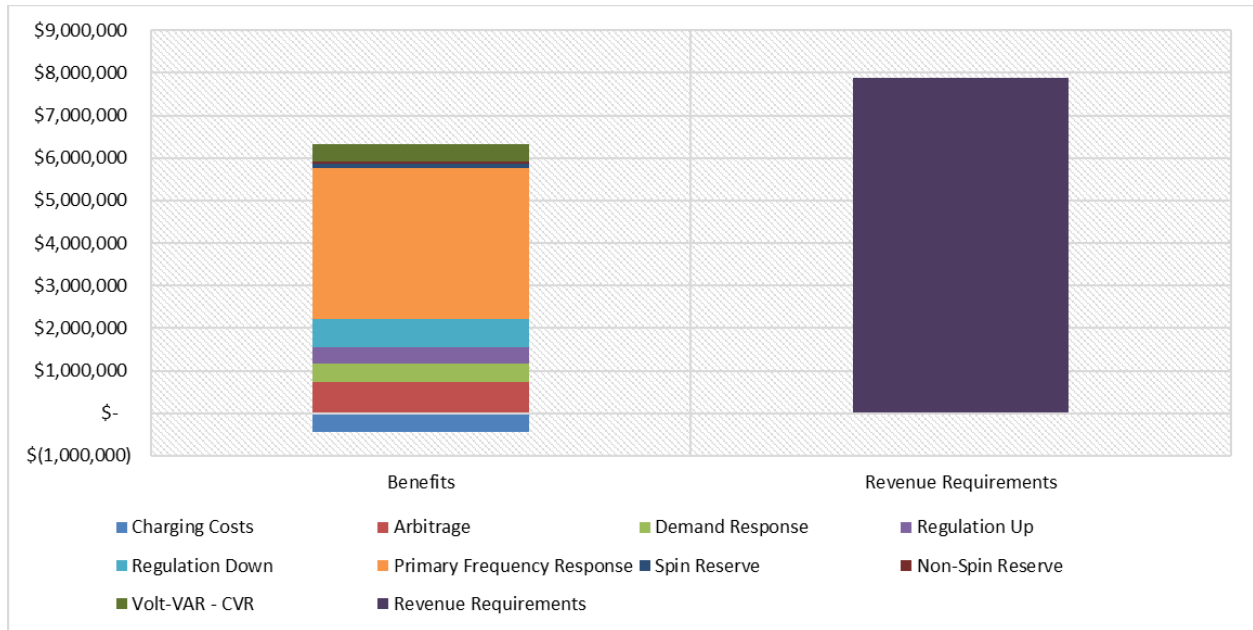


Figure 5.3. Benefits and Revenue Requirements, Using Current-Day Pricing, for a 5 MW/1.25MWh Energy Storage System

When the SSPC was originally designed, it was meant to be operated as a component of a larger microgrid system with attention placed on engineering rather than economic goals. Thus, the SSPC holds a small energy capacity (1.25 MWh) in relation to its power capacity (5 MW). With an energy to power ratio of only 0.25, it is not well suited to engage in most energy-intensive application such as arbitrage or ancillary services. Thus, PNNL studied scenarios with energy to power ratios closer to industry standards (1.0-4.0).

With an energy to power ratio less than approximately 0.5, the cost is higher than total benefits and the return on investment (ROI) is thus less than 1, as shown in Figure 5.4. As the ratio increases, benefits increase at a higher rate than the costs and therefore the ROI continues to increase until the energy to power ratio reaches a value of 2. Once the ratio surpasses 2, benefits increase at a lower rate than costs causing the ROI ratio to decrease. At an energy to power ratio of approximately 3.5, costs surpass benefits and the ROI ratio falls once again below 1.0.

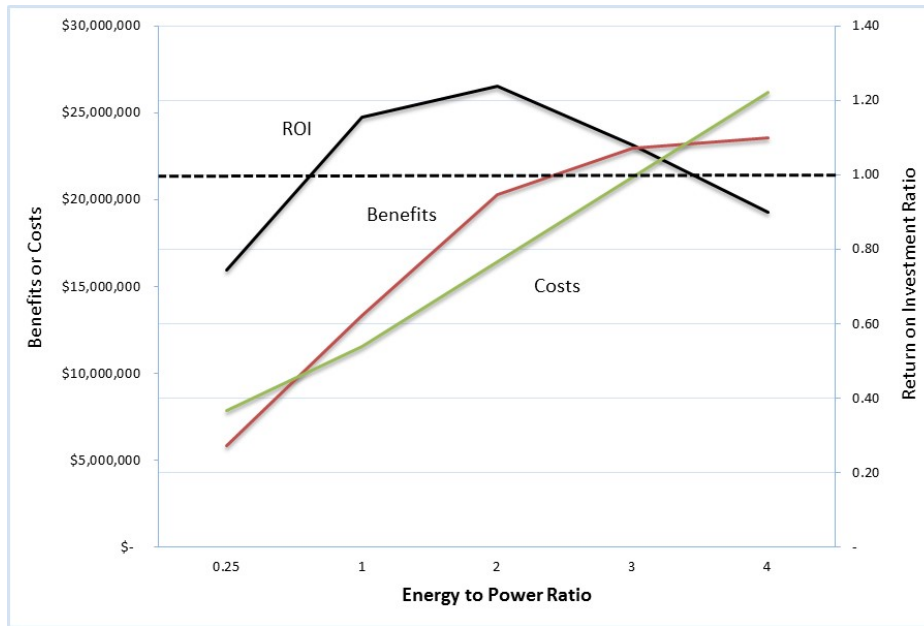


Figure 5.4. Impacts of Energy to Power Ratio on Costs, Benefits, and ROI

5.2 Application Hours and Values

Though nine value streams are available, the SSPC when operated in an optimal manner would remain idle roughly 22 percent of the time. The SSPC is idle when energy prices and RTE losses result in operating costs that would exceed the value of services provided. Energy arbitrage alone and ancillary services alone would be provided 32 percent and 26 percent of the time, respectively. Energy arbitrage and ancillary services would be provided during the same hour 20 percent of the time.

Figure 5.5 presents the annual hours engaged in the provision of each service. Note that in some cases, multiple services would be provided simultaneously. When the BESS is not sitting idle, it is most often engaged in providing arbitrage (1,265), followed by regulation up (1,025 hours), and spin reserve (655 hours).

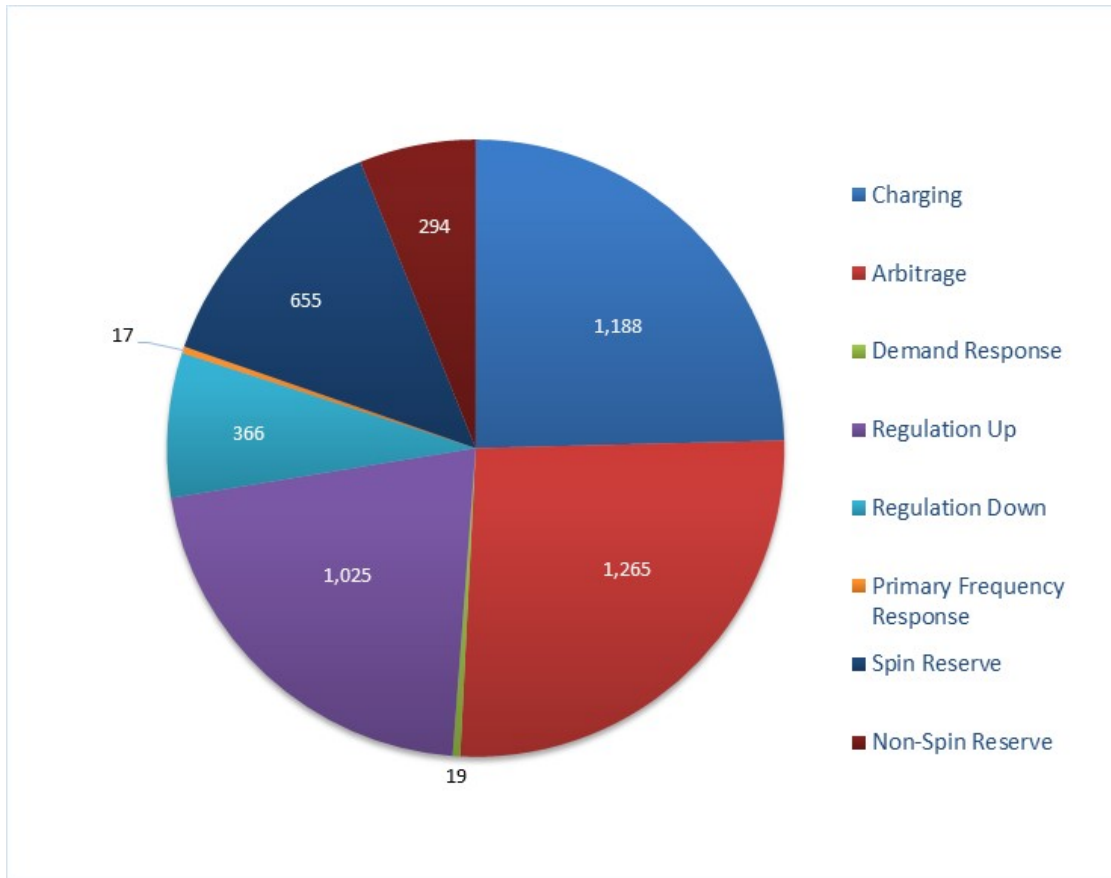


Figure 5.5. Annual Application Hours of the Energy Storage System under Base Case

Figure 5.6 presents the 20-year benefits for each service. As shown, primary frequency response and demand response provide tremendous value despite the fact that those services are concentrated in a very small number of hours each year—17 and 19, respectively. While the SSPC would be optimally engaged in arbitrage and ancillary services 78 percent of the time, those services only generate 27 percent of the total value. Note that Volt-VAR/CVR services are not charted in Figure 5.4 because they are provided at least partially in every hour of the year; varied as necessary based on the available capacity of SSPC batteries and inverters.

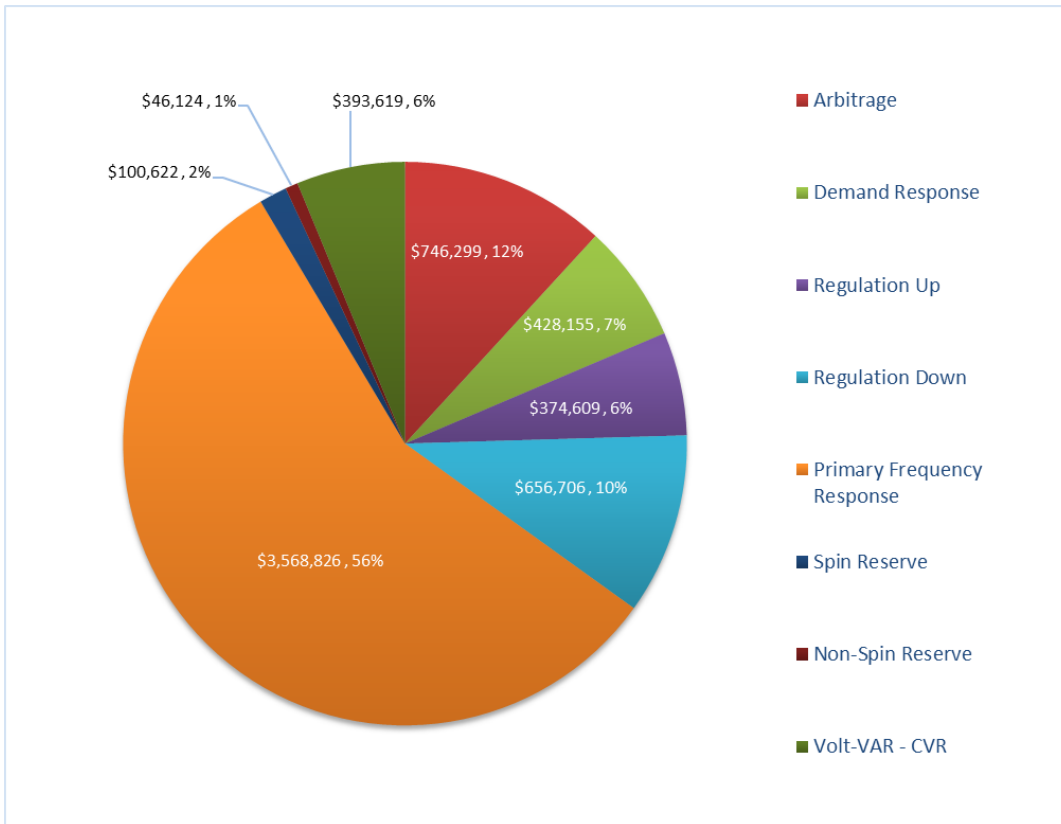


Figure 5.6. 20-year PV Benefits Derived from Each Service under Base Case

5.3 Participation in the Western EIM

Under the EIM, balancing authority scheduling coordinators must report load-balanced resource schedules to CAISO 75 minutes before dispatch time (Figure 5.7). Resources are then stacked in increasing order of cost per unit and CAISO dispatches resources from the common pool to serve regional load on a least-cost basis.

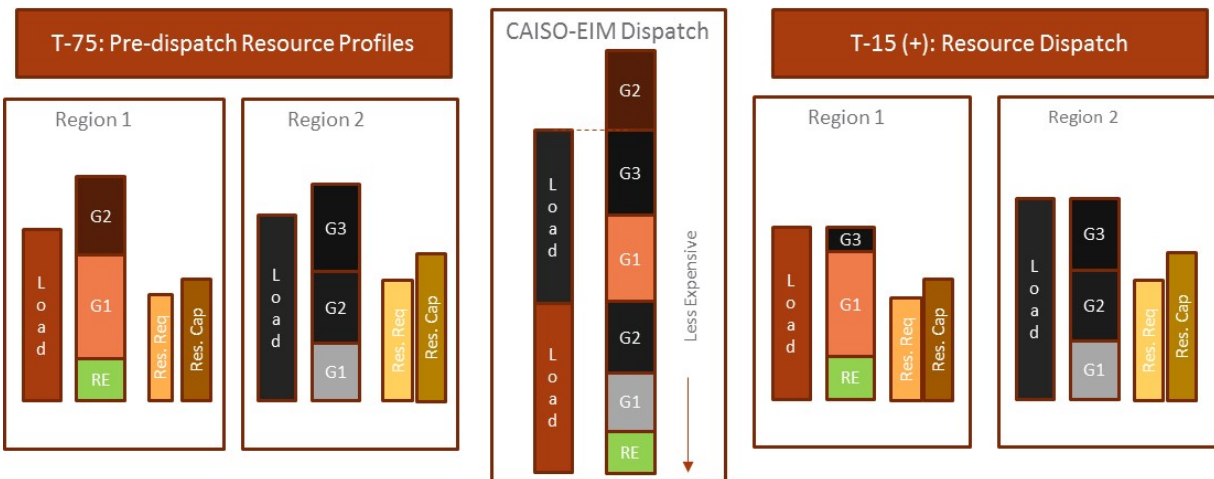


Figure 5.7. Energy Imbalance Market Operations

As noted in section 4.1.2, two scenarios were considered for bidding the BESS into the Western EIM. Under one scenario, EIM and Mid-C prices were developed on an hourly basis with the lowest hourly value among the two serving to charge the SSPC and the highest used when discharging the SSPC. The assumption under this scenario is that PGE would bid the SSPC into either market on an hourly basis. With an offer to sell previously stored energy at a bid price lower than the market price, the resource would be dispatched to discharge until the stored energy was depleted. In this scenario, it is assumed that its capacity would be fully dispatched in the 15-minute intervals and nothing would be left for 5-minute dispatch. The result of this scenario would have generated \$27,674 in 2016 after accounting for energy costs and RTE losses. EIM price data were obtained from the PacifiCorp West load aggregation point nearest to the PGE service territory (ELAP_PACW_APND).

An alternative scenario was also run in which PGE would bid the SSPC into the EIM on an hourly basis but it would be dispatched by CAISO subject to 5-minute real-time market (RTM) prices. This scenario takes advantage of BESS flexibility in providing energy more rapidly throughout each hour. When bid into the 5-minute RTM, EIM benefits for the SSPC were \$152,619 annually or \$2.1 million in PV terms over 20 years. EIM benefits expand to \$214,109 annually or \$2.9 million in PV terms over 20 years if the BESS energy capacity expands to 5 MWh. A scenario was run in which the battery only provided primary frequency response, demand response, and Western EIM services. The results slightly exceeded the base case registering \$5.9 million in benefits over 20 years.

5.4 Evaluation of Alternative Scenarios and Sensitivity Analysis

To explore the sensitivity of the results to varying a number of key assumptions, the research team conducted a series of sensitivity analyses. The various scenarios are outlined below and their impacts were measured in comparison to the base case. Sensitivity analysis was performed by making the following adjustments to the assumptions:

- SA 1: Battery energy was limited to 750 kWh of capacity to keep SOC between 20 percent and 80 percent
- SA 2: No ability to predict demand response events
- SA 3: BESS RTE varied between 80 percent and 90 percent
- SA 4: Discount rate varied by 1 percentage point
- SA 5: BESS used only for primary frequency response, demand response, and Western EIM participation
- SA 6: EIM prices for 2015 used
- SA 7: The high-year Mid-C prices are used (2016 was the low year)
- SA 8: The primary frequency response value set based on CAISO contract with SCL
- SA 9: Assume perfect foreknowledge of primary frequency response events
- SA 10: Energy capacity set at 5 MWh
- SA 11: Energy capacity set at 10 MWh
- SA 12: Energy capacity set at 15 MWh
- SA 13: Energy capacity set at 20 MWh
- SA 14: Lower capital costs presented in Lahiri 2017 used.

The results of each sensitivity analysis are presented in Figure 5.8. Note the table that appears below the figure. The sensitivity analysis results suggest that changes in the energy capacity and use of current-day price figures would profoundly change the results of the economic assessment, reaching up to \$20.5 million (with low capital cost assumption). Note that the changes in energy capacities (SA 10 to SA 13) account for impact on both costs and benefits. All other scenarios evaluate changes in only one side of the investment equation.

As shown, most sensitivity analyses result in improvements to the economic results, suggesting that the base case used in this case was somewhat conservative. The most negative impact is revealed in SA1 when the battery capacity is limited to 750 kWh by setting strict SOC range parameters (20–80 percent) within which the BESS must operate at all times. On the positive side, using the higher value for primary frequency response tied to the CAISO contract with SCL would increase benefits by \$1.9 million over 20 years. Perfect foreknowledge of frequency response events would free up 300 kWh of energy capacity in the BESS for other applications, resulting in an increase of nearly \$600,000 in total benefits. Most other sensitivity analyses (e.g., adjusted RTE for battery, modified discount rate, use of alternative price years) had a negligible impact on economic returns.

Figure 5.9 presents the various ROI ratios for the various scenarios defined as part of the sensitivity analysis. The ROI ratio is defined as present value benefits divided by present value revenue requirements under each defined scenario. Note that cells shaded in red have ROI ratios under 0.5, cells shaded yellow have ROI ratios between 0.5 and 1.0, and cells shaded green represent scenarios with ROI ratios in excess of 1.0. When the cost estimates presented by PGE are used in the denominator of the ROI calculations, all fall short of 1.0, meaning that benefits fall short of revenue requirements. When estimates based on current-day prices presented in Lahiri (2017) are used as the cost basis, the base case ROI ratio is roughly 1.0 and several scenarios generate positive net benefits. When the energy capacity is scaled up to 5 MWh, 10 MWh, and 15 MWh, ROI ratios reach 1.15, 1.24, and 1.08, respectively. With 20 MWh, the ROI ratio falls below unity.

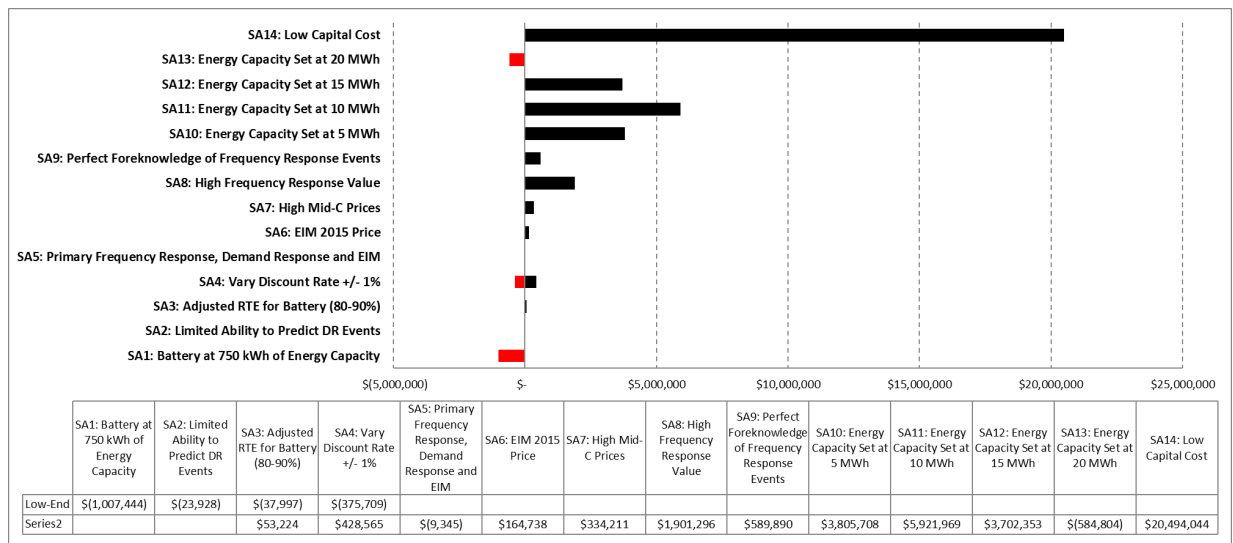


Figure 5.8. Sensitivity Analysis Results

	Base Case	Batt-750 kW of Capacity	Demand Response Alternative Constraint	Batt-80% RTE	Batt-90% RTE	Primary Requency Response, Demand Response and EIM	EIM 2015 Price
PGE Actuals	0.21	0.17	0.21	0.21	0.21	0.21	0.21
PGE Today	0.40	0.33	0.40	0.40	0.41	0.40	0.41
Lahiri 2017 Basis	0.74	0.62	0.74	0.74	0.75	0.74	0.76
Lahiri 2017 Basis - 5 MWh							
Lahiri 2017 Basis - 10 MWh							
Lahiri 2017 Basis - 15 MWh							
Lahiri 2017 Basis - 20 MWh							
	High Mid-C Prices	Perfect Foreknowledge of Frequency Response Event	High Frequency Response	Batt-5 MWh	Batt-10 MWh	Batt-15 MWh	Batt-20 MWh
PGE Actuals	0.22	0.23	0.27				
PGE Today	0.42	0.44	0.53				
Lahiri 2017 Basis	0.79	0.82	0.98				
Lahiri 2017 Basis - 5 MWh							
Lahiri 2017 Basis - 10 MWh				1.24			
Lahiri 2017 Basis - 15 MWh				1.08			
Lahiri 2017 Basis - 20 MWh				0.90			

Figure 5.9. Return on Investment Ratios for Alternative Scenarios

6.0 Conclusions

This assessment examined the financial feasibility of the SSPC by monetizing the values derived from nine services it could provide to PGE and the customers it serves. The BESS and the grid conditions in which it operates were modeled and an optimization tool was employed to explore tradeoffs between services and to develop optimal control strategies.

The results provide crucial insights into the practical application of the SSPC. The following lessons were drawn from this analysis.

1. The SSPC was originally conceived as a groundbreaking R&D project that would advance PGE's understanding of, and technical capacity around, the integration of energy storage, smart grid technologies, and microgrid resources. As a result of the focus of the SSPC and the more nascent stage of development the technology was in when the facilities were originally designed, system costs were high at \$20.4 million. Based on current-day prices present in deals being completed across the U.S., evidence suggests that a 5 MW / 1.25 MWh BESS could be designed and built today for approximately \$5.4 million.
2. In terms of economic operation, the SSPC is currently underutilized, operating an average of 14 hours per month, or 1.9 percent of available hours. With that noted, PGE is using the BESS for the highest value application (primary frequency response), the value of which is estimated at \$264,000 annually or \$3.6 million in PV terms over 20 years. Modeling completed for this study indicates that optimal operation of the BESS could generate an additional \$170,000 in value annually or \$2.3 million over 20 years.
3. SSPC benefits for the base case (\$5.8 million) fall far short of the revenue requirements for the SSPC as originally designed and built. However, results indicate that co-optimized benefits equal 74 percent of system revenue requirements when current prices are used. As mentioned previously, primary frequency response was deemed the highest value benefit. All other use cases or services yielded an additional \$2.3 million in currently unrealized benefits over 20 years. Of those services, arbitrage when also bidding into the Western EIM held the most revenue potential at \$0.7 million, followed by regulation down (\$0.7 million), demand response (\$0.4 million), and Volt-VAR/CVR (\$0.4 million). Note that PNNL relied on its own production cost model in developing all ancillary service values.
4. The SSPC possesses a small energy capacity (1.25 MWh in relation to its power capacity of 5 MW). With an energy to power ratio of only 0.25, it is not well suited to engage in most energy-intensive applications such as arbitrage or ancillary services. While expanding the energy capacity would increase costs, modeling results indicate that doing so would generate much more value. By upsizing the energy storage capacity to 5 MWh and 10MWh, the additional value allows the benefits (\$13.3 million and \$20.3 million, respectively) to exceed the system's revenue requirements (\$11.5 and \$16.4 million, respectively). The ROI ratios of the scenarios that include these higher energy capacities reach 1.24. The value would be much higher yet if the BESS was sited in a manner that generated locational benefits associated with outage mitigation, distribution deferral, or PV integration.
5. The BESS energy to power ratio impacts the costs, benefits, and hence ROI of the project. The ROI ratio exceeds 1.0 with energy to power ratios falling between 0.5 and 3.5, peaking at 1.24 for a system with an energy to power ratio of 2.0.

6. Primary frequency response and demand response provide tremendous value despite the fact that those services are concentrated in a very small number of hours each year—17 and 19, respectively. While the SSPC would be optimally engaged in arbitrage and ancillary services 78 percent of the time, those services only generate 27 percent of the total value.
7. The Western EIM represents an interesting opportunity for PGE. A scenario was run in which PGE would bid the SSPC into the EIM on an hourly basis but it would be dispatched by CAISO subject to 5-minute RTM prices. This scenario takes advantage of BESS flexibility in providing energy more rapidly throughout each hour. When bid into the 5-minute RTM, EIM benefits were estimated at \$152,619 annually or \$2.1 million in PV terms over 20 years.
8. Energy capacity tests indicate that the RTE without counting auxiliary power for the BESS ranged from 78–85 percent, the RTE peaked at a 3,000 kW discharge, and the RTE decreased with increasing charge power demonstrating that the lithium-ion BESS prefers moderate (C/2 to C rate) charging.
9. The AC power delivered by all BESS blocks was quite uniform. This was supported by uniform per cell internal resistance among the BESS vaults, racks, and blocks. Interesting linear relationships with R^2 of >0.98 were found for deviations in SOC versus deviations in voltage for vaults with racks, vaults within blocks, and vaults across all blocks. Weaker relationships were found for the deviations in Δ SOC versus Δ current, Δ voltage versus Δ current, Δ SOC versus Δ temperature, Δ voltage versus Δ temperature, and Δ current versus Δ temperature pairs, with some demonstrating negative slope. This provided insight into the inner workings of the BESS.
10. When operated in a normal manner, the BESS took 12–13 seconds to reach rated power. Three blocks experienced similar ramp rates, while the other blocks registered 68 and 50 percent of the rate measured for the first three blocks. During discharge, the ramp rate for the blocks with lower rates decrease with decreasing SOC, while the stronger blocks have a stable ramp rate across the SOC range investigated. The charge ramp rate is stable for all blocks across all SOCs, with the slower blocks registering similar ramp rate percentages to those of the faster blocks.
11. The BESS ramp rate was in the range of 67 to 100 percent of rated power in one second when the BESS was set in the special ramp mode. This indicates that the ramp rate limitation is not due to the BESS hardware, but due to the nature of the commands it receives.

This report represents the output of the first of a two-phase effort under the GMLC. Phase II will involve the development of enhanced control strategies to assist PGE in realizing the benefits of energy storage in real-time.

7.0 References

- Anderson P. 2016. *Conservation Voltage Reduction (CVR)*. Accessed on January 10, 2017 at <https://www.idahopower.com/pdfs/AboutUs/PlanningForFuture/irp/2013/DecMtgMaterials/ConservationVoltageReduction.pdf>
- Balducci PJ, C Jin, D Wu, MCW Kintner-Meyer, P Leslie, and C Daitch. 2013. *Assessment of Energy Storage Alternatives in the Puget Sound Energy System*. PNNL-23040, Pacific Northwest National Laboratory, Richland, WA.
- CAISO-California Independent System Operator. 2016a. *California Independent System Operator Corporation Filing of Rate Schedule No. 86, Transferred Frequency Response Agreement between the CAISO and the City of Seattle*. Accessed September 5th at http://www.caiso.com/Documents/Nov22_2016_TransferredFrequencyResponseServiceAgreement_CitySeattle_ER17-411.pdf. Sacramento, CA.
- CAISO-California Independent System Operator. 2016b. *California Independent System Operator Corporation Filing of Rate Schedule No. 86, Transferred Frequency Response Agreement between the CAISO and the Bonneville Power Administration*. Accessed September 5th, 2017 at http://www.caiso.com/Documents/Nov22_2016_TransferredFrequencyResponseServiceAgreement_BonnevillePowerAdministration_ER17-408.pdf. Sacramento, CA.
- CAISO-California Independent System Operator. 2017. *Western Energy Imbalance Market Frequently Asked Questions*. Folsom, CA.
- Dominion Voltage Inc. 2012. *Utility Case Study: Volt/VAR Control at Dominion*. Accessed on December 22, 2016 at https://www.michigan.gov/documents/energy/Powell_418130_7.pdf
- Enerdel Media. 2013. *Enerdel's 5 Megawatt Energy Storage System Comes Online as Part of Portland General Electric's Salem Smart Power Project*. Accessed June 6th 2017 at <http://www.enerdel.com/wp-content/uploads/2013/04/PGEESSCommissioningRelease.pdf>.
- Lahiri S. 2017. *Assessing CAPEX for Storage Projects. Presentation at Storage Week*. Oakland, CA.
- Navigant-Navigant Consulting, Inc. 2017. *Energy Storage Potential Evaluation*. Prepared for Portland General Electric. Boulder, CO.
- Osborn M, J Heimensen, J Lovinger, E Lovro, and C Reis. 2013. *Opportunities and Challenges for Portland General Electric's Salem Smart Power Project (SSPP): an evaluation of the SSPP's potential system benefits, cost-effectiveness, and market participation*. June
- Pinney D, T Lovas, and C Miller. 2014. *Costs and Benefits of Conservation Voltage Reduction: CVR Warrants Careful Examination* (pp. 45-73). Accessed on December 21, 2016 at https://www.smartgrid.gov/files/NRECA_DOE_Costs_Benefits_of_CVR_0.pdf
- Portland General Electric. 2016. *Salem Smart Power Center (SSPC) Use and Valuation Test Cases: Testing, Optimization and Next Steps - Briefing Paper*. Portland, OR.

Samaan N, R Bayless, M Symonds, TB Nguyen, C Jin, and D Wu. 2013. *Analysis of Benefits of an Energy Imbalance Market in the NWPP*. PNNL-22877, Pacific Northwest National Laboratory, Richland, WA.

Schweiger H, O Obeidi, O Komesker, A Raschke, M Schiemann, C Zehner, M Gehner, M Keller, and P Birke. 2010. Comparison of Several Methods for Determining the Internal Resistance of Lithium Ion Cells. *Sensors* 2010, 10, 5604-5625. Accessed July 3, 2017 at <http://www.mdpi.com/1424-8220/10/6/5604>

Sergici S, S Sunderhauf, and B Allison. 2016. *Conservation Voltage Reduction Econometric Impact Analysis*. Accessed on January 10, 2017 at http://www.brattle.com/system/publications/pdfs/000/005/289/original/AESP_2016_Pepco_MD_CVR_Presentation_5-9-16.pdf

Solar City Grid Engineering. 2016. *Energy Efficiency Enabled by Distributed Solar PV via Conservation Voltage Reduction: A methodology to calculate the benefits of distributed PV with smart inverters in providing conservation voltage reduction*. Technical Brief (pp. 6-7). Accessed on January 5, 2017 at http://www.solarcity.com/sites/default/files/SolarCity-CVR_Benefits_Methodology-2016-06-28_v2.pdf

Uluski B. 2011. *Volt/VAR Control and Optimization Concepts and Issues*. Accessed at: <http://cialab.ee.washington.edu/nwess/2012/talks/uluski.pdf>

Viswanathan VV, DR Conover, M Kintner-Meyer, S Ferreira, D Rose, and D Schoenwald. 2012. *Protocol for Uniformly Measuring and Expressing the Performance of Energy Storage Systems*. PNNL-22010, Pacific Northwest National Laboratory, Richland, WA

Viswanathan VV, DR Conover, AJ Crawford, S Ferreira, and D Schoenwald. 2014. *Protocol for Uniformly Measuring and Expressing the Performance of Energy Storage Systems*. PNNL-22010 Rev. 1, Pacific Northwest National Laboratory, Richland, WA.

Whitener K, C Eustis, and W Lei. 2014. *Salem Smart Power Center (SSPC) Use and Valuation Test Cases: Testing, Optimization and Next Steps*. SSPC Project Advisory Committee Briefing Paper.

Wilson T. 2012. *Volt/VAR Optimization – Special Case Studies*. Accessed on December 22, 2016 at <http://cialab.ee.washington.edu/nwess/2012/talks/tom.pdf>

Appendix A
Supplemental Data Tables

Appendix A

Supplemental Data Tables

Table A.1. SSPC Tag List

Variable Name	PGE Tag?	Short Description
Bank1_1.CellTempAvg	Yes	
Bank1_1.CellTempMax	Yes	
Bank1_1.CellTempMin	Yes	
Bank1_1.CellVoltAvg	Yes	
Bank1_1.CellVoltDelta	Yes	
Bank1_1.PackAdjSOC	Yes	
Bank1_1.TotalAmps	Yes	
Bank1_2.CellTempAvg	Yes	
Bank1_2.CellTempMax	Yes	
Bank1_2.CellTempMin	Yes	
Bank1_2.CellVoltAvg	Yes	
Bank1_2.CellVoltDelta	Yes	
Bank1_2.PackAdjSOC	Yes	
Bank1_2.TotalAmps	Yes	
Bank1_3.CellTempAvg	Yes	
Bank1_3.CellTempMax	Yes	
Bank1_3.CellTempMin	Yes	
Bank1_3.CellVoltAvg	Yes	
Bank1_3.CellVoltDelta	Yes	
Bank1_3.PackAdjSOC	Yes	
Bank1_3.TotalAmps	Yes	
Bank1_4.CellTempAvg	Yes	
Bank1_4.CellTempMax	Yes	
Bank1_4.CellTempMin	Yes	
Bank1_4.CellVoltAvg	Yes	
Bank1_4.CellVoltDelta	Yes	
Bank1_4.PackAdjSOC	Yes	
Bank1_4.TotalAmps	Yes	
Bank1_5.CellTempAvg	Yes	
Bank1_5.CellTempMax	Yes	
Bank1_5.CellTempMin	Yes	
Bank1_5.CellVoltAvg	Yes	
Bank1_5.CellVoltDelta	Yes	
Bank1_5.PackAdjSOC	Yes	
Bank1_5.TotalAmps	Yes	

Variable Name	PGE Tag?	Short Description
Bank1_6.CellTempAvg	Yes	
Bank1_6.CellTempMax	Yes	
Bank1_6.CellTempMin	Yes	
Bank1_6.CellVoltAvg	Yes	
Bank1_6.CellVoltDelta	Yes	
Bank1_6.PackAdjSOC	Yes	
Bank1_6.TotalAmps	Yes	
Bank1_7.CellTempAvg	Yes	
Bank1_7.CellTempMax	Yes	
Bank1_7.CellTempMin	Yes	
Bank1_7.CellVoltAvg	Yes	
Bank1_7.CellVoltDelta	Yes	
Bank1_7.PackAdjSOC	Yes	
Bank1_7.TotalAmps	Yes	
Bank1_8.CellTempAvg	Yes	
Bank1_8.CellTempMax	Yes	
Bank1_8.CellTempMin	Yes	
Bank1_8.CellVoltAvg	Yes	
Bank1_8.CellVoltDelta	Yes	
Bank1_8.PackAdjSOC	Yes	
Bank1_8.TotalAmps	Yes	
Bank2_1.CellTempAvg	Yes	
Bank2_1.CellTempMax	Yes	
Bank2_1.CellTempMin	Yes	
Bank2_1.CellVoltAvg	Yes	
Bank2_1.CellVoltDelta	Yes	
Bank2_1.PackAdjSOC	Yes	
Bank2_1.TotalAmps	Yes	
Bank2_2.CellTempAvg	Yes	
Bank2_2.CellTempMax	Yes	
Bank2_2.CellTempMin	Yes	
Bank2_2.CellVoltAvg	Yes	
Bank2_2.CellVoltDelta	Yes	
Bank2_2.PackAdjSOC	Yes	
Bank2_2.TotalAmps	Yes	
Bank2_3.CellTempAvg	Yes	
Bank2_3.CellTempMax	Yes	
Bank2_3.CellTempMin	Yes	
Bank2_3.CellVoltAvg	Yes	
Bank2_3.CellVoltDelta	Yes	
Bank2_3.PackAdjSOC	Yes	
Bank2_3.TotalAmps	Yes	

Variable Name	PGE Tag?	Short Description
Bank2_4.CellTempAvg	Yes	
Bank2_4.CellTempMax	Yes	
Bank2_4.CellTempMin	Yes	
Bank2_4.CellVoltAvg	Yes	
Bank2_4.CellVoltDelta	Yes	
Bank2_4.PackAdjSOC	Yes	
Bank2_4.TotalAmps	Yes	
Bank2_5.CellTempAvg	Yes	
Bank2_5.CellTempMax	Yes	
Bank2_5.CellTempMin	Yes	
Bank2_5.CellVoltAvg	Yes	
Bank2_5.CellVoltDelta	Yes	
Bank2_5.PackAdjSOC	Yes	
Bank2_5.TotalAmps	Yes	
Bank2_6.CellTempAvg	Yes	
Bank2_6.CellTempMax	Yes	
Bank2_6.CellTempMin	Yes	
Bank2_6.CellVoltAvg	Yes	
Bank2_6.CellVoltDelta	Yes	
Bank2_6.PackAdjSOC	Yes	
Bank2_6.TotalAmps	Yes	
Bank2_7.CellTempAvg	Yes	
Bank2_7.CellTempMax	Yes	
Bank2_7.CellTempMin	Yes	
Bank2_7.CellVoltAvg	Yes	
Bank2_7.CellVoltDelta	Yes	
Bank2_7.PackAdjSOC	Yes	
Bank2_7.TotalAmps	Yes	
Bank2_8.CellTempAvg	Yes	
Bank2_8.CellTempMax	Yes	
Bank2_8.CellTempMin	Yes	
Bank2_8.CellVoltAvg	Yes	
Bank2_8.CellVoltDelta	Yes	
Bank2_8.PackAdjSOC	Yes	
Bank2_8.TotalAmps	Yes	
Bank3_1.CellTempAvg	Yes	
Bank3_1.CellTempMax	Yes	
Bank3_1.CellTempMin	Yes	
Bank3_1.CellVoltAvg	Yes	
Bank3_1.CellVoltDelta	Yes	
Bank3_1.PackAdjSOC	Yes	
Bank3_1.TotalAmps	Yes	

Variable Name	PGE Tag?	Short Description
Bank3_2.CellTempAvg	Yes	
Bank3_2.CellTempMax	Yes	
Bank3_2.CellTempMin	Yes	
Bank3_2.CellVoltAvg	Yes	
Bank3_2.CellVoltDelta	Yes	
Bank3_2.PackAdjSOC	Yes	
Bank3_2.TotalAmps	Yes	
Bank3_3.CellTempAvg	Yes	
Bank3_3.CellTempMax	Yes	
Bank3_3.CellTempMin	Yes	
Bank3_3.CellVoltAvg	Yes	
Bank3_3.CellVoltDelta	Yes	
Bank3_3.PackAdjSOC	Yes	
Bank3_3.TotalAmps	Yes	
Bank3_4.CellTempAvg	Yes	
Bank3_4.CellTempMax	Yes	
Bank3_4.CellTempMin	Yes	
Bank3_4.CellVoltAvg	Yes	
Bank3_4.CellVoltDelta	Yes	
Bank3_4.PackAdjSOC	Yes	
Bank3_4.TotalAmps	Yes	
Bank3_5.CellTempAvg	Yes	
Bank3_5.CellTempMax	Yes	
Bank3_5.CellTempMin	Yes	
Bank3_5.CellVoltAvg	Yes	
Bank3_5.CellVoltDelta	Yes	
Bank3_5.PackAdjSOC	Yes	
Bank3_5.TotalAmps	Yes	
Bank3_6.CellTempAvg	Yes	
Bank3_6.CellTempMax	Yes	
Bank3_6.CellTempMin	Yes	
Bank3_6.CellVoltAvg	Yes	
Bank3_6.CellVoltDelta	Yes	
Bank3_6.PackAdjSOC	Yes	
Bank3_6.TotalAmps	Yes	
Bank3_7.CellTempAvg	Yes	
Bank3_7.CellTempMax	Yes	
Bank3_7.CellTempMin	Yes	
Bank3_7.CellVoltAvg	Yes	
Bank3_7.CellVoltDelta	Yes	
Bank3_7.PackAdjSOC	Yes	
Bank3_7.TotalAmps	Yes	

Variable Name	PGE Tag?	Short Description
Bank3_8.CellTempAvg	Yes	
Bank3_8.CellTempMax	Yes	
Bank3_8.CellTempMin	Yes	
Bank3_8.CellVoltAvg	Yes	
Bank3_8.CellVoltDelta	Yes	
Bank3_8.PackAdjSOC	Yes	
Bank3_8.TotalAmps	Yes	
Bank4_1.CellTempAvg	Yes	
Bank4_1.CellTempMax	Yes	
Bank4_1.CellTempMin	Yes	
Bank4_1.CellVoltAvg	Yes	
Bank4_1.CellVoltDelta	Yes	
Bank4_1.PackAdjSOC	Yes	
Bank4_1.TotalAmps	Yes	
Bank4_2.CellTempAvg	Yes	
Bank4_2.CellTempMax	Yes	
Bank4_2.CellTempMin	Yes	
Bank4_2.CellVoltAvg	Yes	
Bank4_2.CellVoltDelta	Yes	
Bank4_2.PackAdjSOC	Yes	
Bank4_2.TotalAmps	Yes	
Bank4_3.CellTempAvg	Yes	
Bank4_3.CellTempMax	Yes	
Bank4_3.CellTempMin	Yes	
Bank4_3.CellVoltAvg	Yes	
Bank4_3.CellVoltDelta	Yes	
Bank4_3.PackAdjSOC	Yes	
Bank4_3.TotalAmps	Yes	
Bank4_4.CellTempAvg	Yes	
Bank4_4.CellTempMax	Yes	
Bank4_4.CellTempMin	Yes	
Bank4_4.CellVoltAvg	Yes	
Bank4_4.CellVoltDelta	Yes	
Bank4_4.PackAdjSOC	Yes	
Bank4_4.TotalAmps	Yes	
Bank4_5.CellTempAvg	Yes	
Bank4_5.CellTempMax	Yes	
Bank4_5.CellTempMin	Yes	
Bank4_5.CellVoltAvg	Yes	
Bank4_5.CellVoltDelta	Yes	
Bank4_5.PackAdjSOC	Yes	
Bank4_5.TotalAmps	Yes	

Variable Name	PGE Tag?	Short Description
Bank4_6.CellTempAvg	Yes	
Bank4_6.CellTempMax	Yes	
Bank4_6.CellTempMin	Yes	
Bank4_6.CellVoltAvg	Yes	
Bank4_6.CellVoltDelta	Yes	
Bank4_6.PackAdjSOC	Yes	
Bank4_6.TotalAmps	Yes	
Bank4_7.CellTempAvg	Yes	
Bank4_7.CellTempMax	Yes	
Bank4_7.CellTempMin	Yes	
Bank4_7.CellVoltAvg	Yes	
Bank4_7.CellVoltDelta	Yes	
Bank4_7.PackAdjSOC	Yes	
Bank4_7.TotalAmps	Yes	
Bank4_8.CellTempAvg	Yes	
Bank4_8.CellTempMax	Yes	
Bank4_8.CellTempMin	Yes	
Bank4_8.CellVoltAvg	Yes	
Bank4_8.CellVoltDelta	Yes	
Bank4_8.PackAdjSOC	Yes	
Bank4_8.TotalAmps	Yes	
Bank5_1.CellTempAvg	Yes	
Bank5_1.CellTempMax	Yes	
Bank5_1.CellTempMin	Yes	
Bank5_1.CellVoltAvg	Yes	
Bank5_1.CellVoltDelta	Yes	
Bank5_1.PackAdjSOC	Yes	
Bank5_1.TotalAmps	Yes	
Bank5_2.CellTempAvg	Yes	
Bank5_2.CellTempMax	Yes	
Bank5_2.CellTempMin	Yes	
Bank5_2.CellVoltAvg	Yes	
Bank5_2.CellVoltDelta	Yes	
Bank5_2.PackAdjSOC	Yes	
Bank5_2.TotalAmps	Yes	
Bank5_3.CellTempAvg	Yes	
Bank5_3.CellTempMax	Yes	
Bank5_3.CellTempMin	Yes	
Bank5_3.CellVoltAvg	Yes	
Bank5_3.CellVoltDelta	Yes	
Bank5_3.PackAdjSOC	Yes	
Bank5_3.TotalAmps	Yes	

Variable Name	PGE Tag?	Short Description
Bank5_4.CellTempAvg	Yes	
Bank5_4.CellTempMax	Yes	
Bank5_4.CellTempMin	Yes	
Bank5_4.CellVoltAvg	Yes	
Bank5_4.CellVoltDelta	Yes	
Bank5_4.PackAdjSOC	Yes	
Bank5_4.TotalAmps	Yes	
Bank5_5.CellTempAvg	Yes	
Bank5_5.CellTempMax	Yes	
Bank5_5.CellTempMin	Yes	
Bank5_5.CellVoltAvg	Yes	
Bank5_5.CellVoltDelta	Yes	
Bank5_5.PackAdjSOC	Yes	
Bank5_5.TotalAmps	Yes	
Bank5_6.CellTempAvg	Yes	
Bank5_6.CellTempMax	Yes	
Bank5_6.CellTempMin	Yes	
Bank5_6.CellVoltAvg	Yes	
Bank5_6.CellVoltDelta	Yes	
Bank5_6.PackAdjSOC	Yes	
Bank5_6.TotalAmps	Yes	
Bank5_7.CellTempAvg	Yes	
Bank5_7.CellTempMax	Yes	
Bank5_7.CellTempMin	Yes	
Bank5_7.CellVoltAvg	Yes	
Bank5_7.CellVoltDelta	Yes	
Bank5_7.PackAdjSOC	Yes	
Bank5_7.TotalAmps	Yes	
Bank5_8.CellTempAvg	Yes	
Bank5_8.CellTempMax	Yes	
Bank5_8.CellTempMin	Yes	
Bank5_8.CellVoltAvg	Yes	
Bank5_8.CellVoltDelta	Yes	
Bank5_8.PackAdjSOC	Yes	
Bank5_8.TotalAmps	Yes	
Battery Inverter System (BIS)_4006.Avg_Amps	Yes	
BIS_4006.Avg_Volts	Yes	
BIS_4006.kVar	Yes	
BIS_4006.kWatt	Yes	
BIS_4006.Power_Factor	Yes	
LV1_Breaker.Amps	Yes	

Variable Name	PGE Tag?	Short Description
LV1_Breaker.kVAR	Yes	
LV1_Breaker.kWatt	Yes	
LV1_Breaker.Volts	Yes	
LV2_Breaker.Amps	Yes	
LV2_Breaker.kVAR	Yes	
LV2_Breaker.kWatt	Yes	
LV2_Breaker.Volts	Yes	
LV3_Breaker.Amps	Yes	
LV3_Breaker.kVAR	Yes	
LV3_Breaker.kWatt	Yes	
LV3_Breaker.Volts	Yes	
LV4_Breaker.Amps	Yes	
LV4_Breaker.kVAR	Yes	
LV4_Breaker.kWatt	Yes	
LV4_Breaker.Volts	Yes	
LV5_Breaker.Amps	Yes	
LV5_Breaker.kVAR	Yes	
LV5_Breaker.kWatt	Yes	
LV5_Breaker.Volts	Yes	
IndexChg	No	
Index	No	
BIS_4006.kVA	No	Calculated from BIS_4006.kWatt and BIS_4006.kVar
LV1.5.kWatt	No	Add together the LVX_Breaker.kWatt tags
LVBIS.Diff.kWatt	No	Difference between BIS_4006.kWatt and LV1.5.kWatt
LVBIS.Diff.kVAR	No	Difference between BIS_4006.kVAR and the LVX_Breaker.kVAR tags
Bank1_1&2CurrentDiff	No	Difference in current between two vaults in same rack
Bank1_3&4CurrentDiff	No	Difference in current between two vaults in same rack
Bank1_5&6CurrentDiff	No	Difference in current between two vaults in same rack
Bank1_7&8CurrentDiff	No	Difference in current between two vaults in same rack
Bank2_1&2CurrentDiff	No	Difference in current between two vaults in same rack
Bank2_3&4CurrentDiff	No	Difference in current between two vaults in same rack
Bank2_5&6CurrentDiff	No	Difference in current between two vaults in same rack
Bank2_7&8CurrentDiff	No	Difference in current between two vaults in same rack

Variable Name	PGE Tag?	Short Description
Bank3_1&2CurrentDiff	No	Difference in current between two vaults in same rack
Bank3_3&4CurrentDiff	No	Difference in current between two vaults in same rack
Bank3_5&6CurrentDiff	No	Difference in current between two vaults in same rack
Bank3_7&8CurrentDiff	No	Difference in current between two vaults in same rack
Bank4_1&2CurrentDiff	No	Difference in current between two vaults in same rack
Bank4_3&4CurrentDiff	No	Difference in current between two vaults in same rack
Bank4_5&6CurrentDiff	No	Difference in current between two vaults in same rack
Bank4_7&8CurrentDiff	No	Difference in current between two vaults in same rack
Bank5_1&2CurrentDiff	No	Difference in current between two vaults in same rack
Bank5_3&4CurrentDiff	No	Difference in current between two vaults in same rack
Bank5_5&6CurrentDiff	No	Difference in current between two vaults in same rack
Bank5_7&8CurrentDiff	No	Difference in current between two vaults in same rack
Bank1_1TempDiff	No	Difference between max and min temp
Bank1_2TempDiff	No	Difference between max and min temp
Bank1_3TempDiff	No	Difference between max and min temp
Bank1_4TempDiff	No	Difference between max and min temp
Bank1_5TempDiff	No	Difference between max and min temp
Bank1_6TempDiff	No	Difference between max and min temp
Bank1_7TempDiff	No	Difference between max and min temp
Bank1_8TempDiff	No	Difference between max and min temp
Bank2_1TempDiff	No	Difference between max and min temp
Bank2_2TempDiff	No	Difference between max and min temp
Bank2_3TempDiff	No	Difference between max and min temp
Bank2_4TempDiff	No	Difference between max and min temp
Bank2_5TempDiff	No	Difference between max and min temp
Bank2_6TempDiff	No	Difference between max and min temp
Bank2_7TempDiff	No	Difference between max and min temp

Variable Name	PGE Tag?	Short Description
Bank2_8TempDiff	No	Difference between max and min temp
Bank3_1TempDiff	No	Difference between max and min temp
Bank3_2TempDiff	No	Difference between max and min temp
Bank3_3TempDiff	No	Difference between max and min temp
Bank3_4TempDiff	No	Difference between max and min temp
Bank3_5TempDiff	No	Difference between max and min temp
Bank3_6TempDiff	No	Difference between max and min temp
Bank3_7TempDiff	No	Difference between max and min temp
Bank3_8TempDiff	No	Difference between max and min temp
Bank4_1TempDiff	No	Difference between max and min temp
Bank4_2TempDiff	No	Difference between max and min temp
Bank4_3TempDiff	No	Difference between max and min temp
Bank4_4TempDiff	No	Difference between max and min temp
Bank4_5TempDiff	No	Difference between max and min temp
Bank4_6TempDiff	No	Difference between max and min temp
Bank4_7TempDiff	No	Difference between max and min temp
Bank4_8TempDiff	No	Difference between max and min temp
Bank5_1TempDiff	No	Difference between max and min temp
Bank5_2TempDiff	No	Difference between max and min temp
Bank5_3TempDiff	No	Difference between max and min temp
Bank5_4TempDiff	No	Difference between max and min temp
Bank5_5TempDiff	No	Difference between max and min temp
Bank5_6TempDiff	No	Difference between max and min temp
Bank5_7TempDiff	No	Difference between max and min temp
Bank5_8TempDiff	No	Difference between max and min temp

Table A.2. Benefits Estimates by Use Case for Base Scenario, High Frequency Response Scenario, Perfect Foreknowledge of Frequency Response Scenario and High Mid-C Prices Scenario

Use Cases	Base Case	High Frequency Response	Perfect Foreknowledge of Frequency Response Event	High Mid-C Prices
Charging Costs	\$(449,115)	\$(449,115)	\$(598,924)	\$(672,824)
Arbitrage	\$746,299	\$746,299	\$992,393	\$1,334,032
Demand Response	\$428,155	\$428,155	\$540,259	\$428,155
Regulation Up	\$374,609	\$374,609	\$530,485	\$348,361
Regulation Down	\$656,706	\$656,706	\$839,130	\$645,459
Primary Frequency Response	\$3,568,826	\$5,470,122	\$3,568,826	\$3,568,826
Spin Reserve	\$100,622	\$100,622	\$131,139	\$108,473
Non-Spin Reserve	\$46,124	\$46,124	\$58,809	\$45,956
Volt-VAR - CVR	\$393,619	\$393,619	\$393,619	\$393,619
Net Value	\$5,865,846	\$7,767,142	\$6,455,736	\$6,200,058

Table A.3. Benefits Estimates by EIM 2015 Price Scenario, Demand Response Alternative Constraint Scenario, and Varying Battery RTE Scenarios

Use Cases	EIM 2015 Price	Demand Response Alternative Constraint		
		Demand Response Alternative Constraint	Batt-80% RTE	Batt-90% RTE
Charging Costs	\$(562,486)	\$(396,344)	\$(382,345)	\$(533,373)
Arbitrage	\$1,037,417	\$667,807	\$644,960	\$874,981
Demand Response	\$428,155	\$428,155	\$428,155	\$428,155
Regulation Up	\$372,471	\$377,862	\$349,182	\$436,900
Regulation Down	\$646,765	\$653,760	\$698,263	\$598,195
Primary Frequency Response	\$3,568,826	\$3,568,826	\$3,568,826	\$3,568,826
Spin Reserve	\$101,730	\$101,352	\$88,163	\$102,098
Non-Spin Reserve	\$44,087	\$46,882	\$39,025	\$49,669
Volt-VAR - CVR	\$393,619	\$393,619	\$393,619	\$393,619
Net Value	\$6,030,585	\$5,841,919	\$5,827,849	\$5,919,070

Table A.4. Benefits Estimate by Use Case for 750 kWh Battery Capacity Case; Primary Frequency Response, Demand Response and EIM Case; and Varying Battery Energy Capacity Cases

Use Cases	Batt-750 kWh of Capacity	Primary Frequency Response, Demand Response and EIM	Batt-5 MWh	Batt-10 MWh
Charging Costs	\$(212,845)		\$(2,077,274)	\$(3,178,747)
Arbitrage	\$353,178	\$1,859,520	\$3,475,764	\$4,912,154
Demand Response	\$202,597	\$428,155	\$2,161,036	\$4,322,072
Regulation Up	\$165,760		\$2,120,632	\$5,785,926
Regulation Down	\$319,621		\$3,086,546	\$4,117,315
Primary Frequency Response	\$3,568,826	\$3,568,826	\$3,568,826	\$3,568,826
Spin Reserve	\$46,619		\$399,202	\$255,858
Non-Spin Reserve	\$21,027		\$193,180	\$127,407
Volt-VAR - CVR	\$393,619		\$393,619	\$393,619
Net Value	\$4,858,402	\$5,856,502	\$13,321,531	\$20,304,430

Table A.5. Benefits Estimates by Use Case for 15 MWh and 20 MWh Scenarios

Use Cases	Batt-15 MWh	Batt-20 MWh
Charging Costs	\$(3,611,276)	\$(3,823,382)
Arbitrage	\$5,592,677	\$5,996,841
Demand Response	\$6,618,173	\$6,753,237
Regulation Up	\$6,089,986	\$6,333,661
Regulation Down	\$3,786,252	\$3,721,061
Primary Frequency Response	\$2,971,424	\$2,971,424
Spin Reserve	\$760,402	\$777,126
Non-Spin Reserve	\$350,192	\$407,340
Volt-VAR - CVR	\$393,619	\$393,619
Net Value	\$22,951,449	\$23,530,929



Pacific Northwest
NATIONAL LABORATORY

*Proudly Operated by **Battelle** Since 1965*

902 Battelle Boulevard
P.O. Box 999
Richland, WA 99352
1-888-375-PNNL (7665)

U.S. DEPARTMENT OF
ENERGY

www.pnnl.gov